November 2023

Detection and control of environmentally transmissible viruses

Anand R. Soorneedi
University of Massachusetts Amherst

Detection and control of environmentally transmissible viruses

A Dissertation Presented

by

Anand R. Soorneedi

Submitted to the Graduate School of the
University of Massachusetts Amherst in partial fulfillment
of the requirements for the degree of

DOCTOR OF PHILOSOPHY

September 2023

Department of Food Science

Detection and control of environmentally transmissible viruses

A Dissertation Presented

by

Anand R. Soorneedi

Approved as to style and content by:

Matthew Moore

_____
Matthew D. Moore, Chair

Lynne McLandsborough

_____
Lynne A. McLandsborough, Member

JG

_____
John Gibbons, Member

Jiakai Lu

_____
Jiakai Lu, Member

Mandy Muller

_____
Mandy Muller, Member (External)

Lynne McLandsborough

_____
Lynne A. McLandsborough, Food Science
Department Head

DEDICATION

To mom and dad

“Good Mom and Dad hardly parent. They let their kids learn, fail, and grow without interference.” ― Trevor Carss

Acknowledgements

I would like to begin by thanking my advisor Dr. Matthew Moore for his unwavering support and the immense trust he placed in me when recruiting me as his first PhD student. He has been very instrumental in building my research career and I have learned a lot from him as I embark on my journey into the world of academic research. I look up to him not just as a mentor but as an amazing scientist who is very passionate about the work he does. He has been very supportive of my ideas in research, and I couldn't have asked for a better mentor. I respect him a lot for his conviction to do good science and penchant to support his mentees and help them succeed in their careers. While I will miss the funny lab meetings and jokes, I would share with him, I am hopeful that our paths will cross in the future (this is in no way an invitation to keep me on the lab mailing list after I graduate). Thanks, are also due to my committee members, who despite their busy schedules have taken the time to not only serve on my committee but also provide their valuable feedback on my research. It was an honor to have you all on my committee. I would also like to thank my fellow lab members (not in any order) Minji, Sloane, Nikhita, Brittany, Cassie, Tianyuan, Vrinda, Andy, Miyu, Louisa, Christina, Nathaneal, Randy, Pragathi, Bozhong, Julia and Lily for their camaraderie, stimulating discussions, and continuous support. Your collaboration has made this research both enjoyable and intellectually stimulating. I will miss working with you all and I am sure you will go on to do great things in the careers of your choosing. I would like to acknowledge the assistance and cooperation provided by the Food Science department staff (Moriah, Stacy, Deby and Dave). Their prompt and efficient support in several different aspects of my PhD journey has been crucial in various aspects of my academic journey. Special thanks to Cindy for putting up with me when I had to order supplies at the last minute. You are the best and I will miss working with you. I would like to thank my dear friends (both in and outside the food science department). Thank you for standing by my side, understanding the pressures of academia, and providing unwavering support, laughter, and encouragement during both the highs and lows of my PhD journey. Special thanks to Dr. Asha Rani from the Sela lab for the witty banter and words of wisdom you'd share with me during our snack breaks. I am deeply grateful to my family for their unconditional love, understanding, and encouragement during the

past 5 years. Thanks for putting up with my shenanigans. Their belief in me has been a constant source of motivation. Additionally, I would like to extend my appreciation to all my well-wishers (Ali, Orca, Mary Moore, Betsy, Marian Hazzard and others) who have supported me from near and afar.

Completing this dissertation has been a challenging yet fulfilling experience, and I am grateful to every one of you for being a part of this journey. Your contributions, whether big or small, have left an indelible mark on my academic and personal growth.

ABSTRACT

Detection and control of environmentally transmissible viruses

SEPTEMBER 2023

Anand R. Soorneedi, B.Sc., Andhra University

M.Sc., Bangalore University

M.S., Florida Institute of Technology

Directed by: Professor Matthew D. Moore

Viruses, owing to their ubiquitous nature and ability to infect almost every other species, have long been a subject of interest for scientists. Some of the virus species can be very deadly to humans and animals alike and can impose a huge economic and health burden across the world. The recent CoVID-19 pandemic underscores the importance of timely detection for developing effective intervention strategies. Unfortunately, some of the virus species that cause significant health and economic impacts do not have robust and reliable detection methods due to several reasons. In some cases, despite having gold standard methods for detection of viruses, lack of effective upstream sample preparation steps could result in underestimating the viral loads. Sample preparation prior to detection is an often-overlooked aspect of foodborne virus detection. The sample preparation step is very crucial especially when food and environmental samples are involved due to the small number of infectious virus particles in a large volume of sample (eg. Fresh produce and sewage). Earlier studies have shown that representative gut bacteria strains can capture human norovirus from environmental samples. But the capture efficiency is largely dependent on the culture media conditions. The current study

focuses on this aspect of sample concentration prior to detection using engineered bacterial strains. We have demonstrated that using engineered bacterial strains could effectively improve the capture efficiency of human norovirus particles from stool samples. We noticed an upwards of 65% capture efficiency with all the engineered clones we tested. This is much higher compared to that of conventional PEG or magnetic bead-based methods wherein the capture efficiencies are <30%. Moreover, the engineered *E. coli*-based capture method can be scaled up to accommodate larger sample volumes. The engineered *E. coli*-based capture and concentration technique is also not susceptible to change in media conditions as the inducible expression of norovirus specific peptides expressed on the surface can be fine-tuned. This is the first time ever someone has used engineered E. coli for capture and concentration of human norovirus from environment samples. Moreover, the ease with which the engineered bacteria can be cultured and utilized for capture of norovirus makes it an ideal method for sample concentration prior to detection in resource limited settings.

Control of environmentally transmissible viruses is an important aspect from a public health standpoint. To achieve this, conventional disinfection strategies employ a wide variety of chemical compounds which can often be detrimental to human health. To circumvent this issue, we propose the use of novel disinfection strategies that employ engineered water nanostructures for neutralizing both foodborne and environmental viruses. The residue-free disinfection methods proposed can be employed in a food industry setting without any problem. The EWNS cocktails used in this study showed more efficacy against a coronavirus surrogate and vegetative bacteria than MS2.

Miniscule amounts of active ingredients were required to achieve inactivation of pathogens on high touch surfaces. Targeted and precise delivery of active ingredients is superior to conventional “wet” treatments. With the EWNS system, we were able to achieve complete inactivation of the SARS-CoV-2 surrogate HCoV229E after just 1 minute exposure. This demonstrates the potential of the EWNS system as an effective method for inactivating viruses on surface. The potential of EWNS for air disinfection is currently being tested.

We also highlight the importance of using UV-C based disinfection methods for combating environmentally significant viruses. We tested the efficacy of 4 different commercially available UV-C light-based systems for their disinfection capacity. The two handheld devices we tested lived up to their claims of disinfecting viruses on surfaces. The airborne inactivation results show promise for occupational deployment of ceiling-based UVC 222 nm technology for a high level of SARS-CoV-2 inactivation in the air within a short time. But the potential for UV-C based disinfection techniques requires further scrutiny.

Table of Contents

Acknowledgements---------- 6

Abstract---------- 8

List of Tables---------- 15

List of Figures---------- 16

Chapter 1: A survey of norovirus concentration methods and the potential for use of bacteria as an effective concentration agent.---------- 17

1.1 Abstract ---------- 17

1.2 Introduction ---------- 18

1.3 Concentration conundrum: ---------- 20

1.4 Overview of conventional virus sample preparation methods: ---------- 21

1.4.1 Nonspecific Norovirus Concentration Methods: ---------- 21

1.4.1.1 Polyethylene Glycol (PEG) precipitation: ---------- 22

1.4.1.2 Ultracentrifugation:---------- 23

1.4.1.3 Ultrafiltration: ---- 23
1.4.1.4 Charge based concentration methods: ---- 24
1.4.1.4.1 Cationic separation: ---- 24
1.4.1.4.2 Anionic separation: ---- 25
1.4.1.5 Adsorption/elution: ---- 25
1.4.1.5.1 Membrane/filter-based concentration: ---- 25
1.4.1.5.2 Glass wool-based concentration: ---- 27
1.4.1.5.3 Glass powder: ---- 27
1.4.1.6 Other adsorption-based concentration methods: ---- 28
1.4.2 Specific Norovirus Concentration Methods ---- 28
1.4.2.1 Immunoconcentration: ---- 28
1.4.2.2 Ligand based concentration techniques for norovirus: ---- 29
1.4.2.2.1 Histo blood group antigen based concentration: ---- 29
1.5 Foundational work demonstrating norovirus binding to enteric bacteria: ---- 31
1.6 Conclusion: ---- 32
1.7 References: ---- 32
Chapter 2: Capture and concentration of human noroviruses in foods and environmental samples by engineered bacterial strains ---- 39
2.1 Abstract: ---- 39
2.2 Introduction: ---- 40
2.3 Materials and methods: ---- 43
2.3.1 Virus strains: ---- 43
2.3.2 Bacterial isolates and engineered *E. coli*: ---- 44
2.3.3 Engineered *E. coli* expressing norovirus specific peptides: ---- 44
2.3.3.1 Cloning and Expression of INP-Peptide Fusion Protein in an Expression Vector: ---- 44
2.3.4 Bacteria-virus binding and pull-down assay: ---- 45
2.3.5 Chloroform purification of norovirus containing stool sample: ---- 46
2.3.6 Nucleic acid extraction and viral RNA detection: ---- 46
2.3.7 RT-qPCR data analysis: ---- 47

2.3.8 Statistical analysis: ----------47

2.3.9 TEM image analysis of GII.4 VLP binding to engineered E. coli strains: ---------- 48

2.4 Preliminary results and discussion:----------48

2.4.1 Wild type bacteria were able to capture norovirus GII.4:----------48

2.4.2 Chloroform purification of the norovirus containing stool sample: ----------49

2.4.3 Engineered *E. coli* strains expressing GII.4 norovirus binding peptides captured norovirus in stool sample display higher efficiency than native binder *E. cloacae*: ----------50

2.4.4 Binding efficiency of human norovirus GII.4 to engineered *E. coli* strains and *E. cloacae*: ----------51

2.4.5 Stool sample degradation:----------51

2.4.6 GII.4 VLP's were able to bind to pGrogu (scaffold): ---------- 54

2.4.7 Engineered *E. coli* strains did not capture norovirus GI.1 in stool sample: ----------55

2.5 Discussion:----------56

2.6 Plan for future work:----------57

2.7 References:----------57

Chapter 3: Evaluation of Caenorhabditis elegans for enrichment of and as an in vivo infectivity model for noroviruses ----------61

3.1 Abstract: ----------61

3.2 Introduction: ----------62

3.3 Meet the worms: ----------64

3.4 *C. elegans* expresses fucosylated carbohydrates on its intestinal cells and is an emerging model for nonenveloped viral infection in the intestine:----------65

3.5 Materials and methods:----------66

3.5.1 Generation of CD300lf-expressing *C. elegans* mutants:----------66

3.5.2 Generation and culture of murine norovirus (MNV)-1:----------66

3.5.3 Enumeration of murine norovirus using RT-qPCR:----------67

3.5.4 Evaluation of the ability of MNV-1 to infect *C. elegans* mutant: ----------67

3.5.5 Evaluation of MNV-1 to infect C. elegans using fluorescent labeled antibody:----------67

3.6 Preliminary results:----------68

3.6.1 *C. elegans* captures human noroviruses:----------68

3.6.2 *C. elegans* promotes murine norovirus replication: ---- 68

3.6.3 Noroviruses are ingested and bound in the intestinal cells of *C. elegans*: ---- 70

3.7 Discussion and future experiments: ---- 72

3.8 References: ---- 72

Chapter 4: Inactivating SARS-CoV-2 and human norovirus Surrogates on Surfaces Using Engineered Water Nanostructures Incorporated with Nature Derived Antimicrobials ---- 77

4.1. Abstract: ---- 77

4.2. Introduction: ---- 78

4.3. Materials and Methods: ---- 80

4.3.1. Generation of EWNS: ---- 80

4.3.2. Selection of Antimicrobial Active Ingredients: ---- 81

4.3.3. Physicochemical Characterization of EWNS: ---- 82

4.3.4. Viral Inoculation, Exposure, and Recovery: ---- 82

4.3.5 MS2 Plaque Assay: ---- 84

4.3.6 HCoV-229E Plaque Assay: ---- 84

4.3.7 Statistical Analysis: ---- 85

4.4 Results and Discussion: ---- 85

4.4.1Generation and Physicochemical Characterization of EWNS Nanoaerosol: ---- 85

4.4.2 EWNS-based nano-sanitizer inactivation of foodborne pathogen surrogates on spinach and stainless-steel coupons: ---- 89

4.5 Conclusions: ---- 94

4.6 References: ---- 95

Chapter 5: Assessment of SARS-CoV-2 surrogate inactivation on surfaces and in air using UV and blue light-based intervention technologies ---- 99

5.1 Abstract: ---- 99

5.2 Introduction: ---- 100

5.3 Materials and Methods: ---- 103

5.3.1 Description of Devices Tested: ---- 103

5.3.2 Viral Strain: ---- 104

5.3.3 HCoV-229E Plaque Assay: ---- 104

5.3.4 Experimental Setup for Inactivation of HCoV-229E on Surface:---------- 105
5.3.5 Surface Inoculation and Recovery of HCoV-229E: ---------- 106
5.3.6 Experimental Setup for Inactivation of HCoV-229E in Air:---------- 106
5.3.7 Generation of HCoV-229E Bioaerosols:---------- 107
5.3.7.1 Bioaerosol Sampling: ---------- 108
5.3.7.2 Environmental Parameters:---------- 108
5.3.8 Statistical Analysis:---------- 108
5.4 Results and Discussion:---------- 109
5.5 Figures and Tables: ---------- 117
5.6 References:---------- 121
Conclusion: ---------- 127

List of Tables

Table Page

1. The sequences of peptides in the engineered *E. coli* strains ……..... 45

2. List of primers and probes used in current study……... 46

3. Mitigation strategies to prevent virus degradation in stool sample…….. 51

4. C. elegans captures human norovirus…… 68

5. Active Ingredients (AIs) utilized to generate various EWNS…… 85

6. Details of devices tested in this study……..……117

List of Figures

Figure		Page
1	Binding efficiency of human norovirus GII.4 to representative bacterial strains	49
2	Binding efficiency of human norovirus GII.4 to engineered *E. coli* strains.	50
3	TEM images of GII.4 VLP's bound to pGrogu (* scaffold).	55
4	Binding of norovirus capsid protein (P domain) to the intestinal track of C.elegans.	68
5	Wild type worms displayed a 1.5-fold increase in log genome copies after 72 hr. incubation.	69
6	Mutant worms displayed a 1.5-fold increase in log genome copies after 72 hr. incubation	69
7	Microscopy visualizing ingestion and binding of MNV in the intestinal cells of *C. elegans.*	70
8	Microscopy visualizing ingestion and binding of MNV in *C. elegans.*	71
9	Detailed schematic to represent the generation of EWNS and the treatment of HCoV-229E inoculated surface (a).	81
10	Inactivation of HCoV-229E on surface, after treatment with EWNS.	88
11	Inactivation of MS2 on spinach from EWNS-based nano-sanitizer.	89
12	Inactivation of bacteriophage MS2.	90
13	Inactivation of HCoV-229E on surface, after treatment with EWNS.	92
14	Schematic of the surface inactivation efficacy testing of chosen UV/light-based intervention technologies against an inoculated SARS-CoV-2 surrogate.	118
15	Schematic of the air disinfection efficacy testing of UV based device C.	119
16	Summary of the surface inactivation efficacy testing of UV/light-based devices.	120
17	Inactivation of aerosolized HCoV-229E by device C as a function of UV exposure dose (uJ/cm2).	121

Chapter 1

A survey of norovirus concentration methods and the potential for use of bacteria as an effective concentration agent.

1.1 Abstract

Foodborne viruses are the leading cause of foodborne illness globally[1]. Norovirus is a highly contagious foodborne virus that causes stomach and intestinal inflammation, leading to symptoms such as nausea, vomiting, diarrhea, and stomach cramps[2]. It is particularly challenging to control because it can survive for long periods of time on a variety of surfaces, such as countertops, door handles, and even clothing[3]. This makes it easy for the virus to spread from person to person and from surface to surface. The concentration of virus in a sample is important for detection because it determines the sensitivity of the diagnostic test being used. If the concentration of the virus is too low, it may not be detected by the test, resulting in a false negative result. To obtain accurate results, it is important to have an adequate concentration of the virus in the sample being tested. Because norovirus contamination of foods occurs at low levels, concentration of viruses from foods is often required prior to detection[4]. In general, norovirus concentration techniques can be grouped into nonspecific and specific concentration techniques[5]. Nonspecific concentration techniques, like polyethylene glycol precipitation or filtration, exploit the common physiochemical properties of the viruses[6,7]. Specific techniques utilize recognition elements, like antibodies, to capture and concentrate noroviruses from food samples more specifically. Numerous nonspecific and specific

techniques for norovirus concentration have been reported with varying degrees of efficiencies and limitations observed. In general, nonspecific concentration methods can often achieve optimal concentration efficiencies, however these methods often can co-concentrate inhibitory substances from foods that can interfere with downstream detection[7–9]. Conversely, many specific techniques often enable removal of potential inhibitory substances but can often lack ideal concentration efficiency[10]. The purpose of this review is to survey the different norovirus concentration techniques relevant to food and environmental samples. Additionally, this review will survey recent work investigating norovirus binding to bacteria considering the potential of bacteria to be used as a concentration reagent for noroviruses from foods.

1.2 Introduction

Human norovirus is the leading cause of non-bacterial gastroenteritis and is associated with a significant public health and economic burden. Noroviruses belong to the *Caliciviridae* family of viruses, are non-enveloped, and contain a single stranded, positive sense RNA genome. The global norovirus disease burden is estimated to be around 685 million cases and around 200,000 deaths annually[11]. Norovirus is highly transmissible and most commonly causes vomiting and diarrhea in infected individuals. While it primarily spreads through the fecal-oral route when individuals encounter other infected individuals or surfaces that carry the infectious virus particles, transmission through inhalation and swallowing of vomitus droplets is also suspected to be possible.

Noroviruses are the leading cause of foodborne illness, and there are several properties that these viruses have that contribute to their high estimated level of foodborne transmission. Some of them include: the generally low levels of norovirus contamination

that occur in foods and the environment, lack of a reliable capture and concentration method prior to detection, the very low infectious dose of norovirus, asymptomatic infections that go unreported, and varying willingness among doctors to recommend appropriate laboratory tests when patients with gastrointestinal symptoms are presented. Further, routine testing of foods for viruses is often not performed because of several difficulties in efficiently detecting viruses from these foods. One of the primary limitations is the lack of an efficient, rapid, and inexpensive method to concentrate/enrich viruses from food and environmental samples.

Since norovirus has a low infectious titer (18-100 particles) and contamination of norovirus in foods tends to occur at low levels, the potential for foodborne transmission of viruses below the limits of detection exists. Given that culture-based enrichment of viruses from food and environmental samples is not feasible, concentration of noroviruses from foods prior to detection is often required prior to detection. Although numerous promising downstream norovirus detection techniques have been reported, comparatively less attention has been focused on improving and developing enhanced upstream norovirus concentration techniques[5].

The purpose of this review is to survey and present techniques used for concentration of human noroviruses from food and environmental samples prior to detection, as well as to discuss recent developments in binding of noroviruses to bacteria in the context of the potential for bacteria to be used as novel foodborne virus concentration reagents.

1.3 Concentration conundrum:

Foodborne viruses like the human norovirus (HuNoV) and hepatitis A virus (HAV) have been implicated in many recorded foodborne outbreaks. Human norovirus is the leading cause of foodborne illnesses in the US and globally[12–15], while HAV is responsible for viral hepatitis. The human rotavirus is another foodborne virus of concern that causes childhood gastroenteritis. Viral foodborne outbreak cases are predominantly attributed to consuming contaminated shellfish, vegetables, and fruits. In the US and Canada alone during the period from 2017-2021, more than 20 recalls due to foodborne viruses were issued, specifically for shellfish and frozen berries. Some infections are also caused by consuming contaminated water like hepatitis E virus (HEV). Owing to the significant human health and economic impact caused by foodborne viruses, their detection becomes extremely important in curbing major outbreaks. Despite this seemingly high number of foodborne outbreaks of viruses, most foodborne virus outbreaks tend to go undetected.

Detection of foodborne pathogens requires a multipronged approach especially when foodborne viruses are involved. Unlike their bacterial counterparts, viruses cannot grow in the environment and hence require a specific host for their replication thus rendering the use of traditional media-based enrichment techniques used for bacteria from foods inapplicable. Most foodborne viruses are generally resistant to several environmental stressors such as heat, pH, light and certain commonly used disinfectants. This property allows many foodborne viruses to persist in foods and the environment for extended periods of time. The infectious dose of most food-borne viruses is low. Similarly, viral contamination of foods often occurs at low levels, thus requiring concentration of a low number of viruses from foods prior to detection. In the case of bacterial and fungal

pathogens, the problem of detecting low levels of contamination in foods can often be mitigated by the inclusion of enrichment (culture) steps prior to utilization of detection technology. These enrichment steps can add a significant amount of time to the detection process and often require specialized equipment to carry out. However, such culture-based enrichment steps are not realistically feasible when viral, toxin, and small molecule contaminants that may be present in foods or the environment. Food-borne virus detection involves (i) concentration of virus from different matrices (ii) viral genome extraction and purification and (iii) molecular detection.

1.4 Overview of conventional virus sample preparation methods:

Norovirus is estimated to require only a handful of particles to cause illness in individuals and can persist in foods and the environment for weeks. Further, this virus is highly transmissible and can be rapidly spread, making rapid detection of viruses in foods and the environment important for reducing illness. The area of sample processing and concentration prior to downstream detection has been of increasing interest and focus in the past decade, and exciting work on novel sample processing techniques is continuing to be conducted. The lack of a novel rapid, cost-effective, scalable, and consistent sample processing technique for noroviruses remains the major hurdle in routine sampling and detection of noroviruses from food and environmental samples. Norovirus concentration methods can be broadly grouped into nonspecific and specific concentration methods. Nonspecific methods tend to exploit the generally homogeneous physiochemical properties of noroviruses, whereas specific methods focus on specifically capturing and separating noroviruses from samples.

1.4.1 Nonspecific Norovirus Concentration Methods:

1.4.1.1 Polyethylene Glycol (PEG) precipitation:

PEG precipitation has been shown to be an effective concentration method for norovirus from a wide variety of matrices. PEG precipitation is often preceded by an elution step at an alkaline or neutral pH. Varying concentrations of PEG (ranging from 8-16%) are used depending on the sample from which norovirus needs to be concentrated[16–18]. Combining the PEG precipitation method with acid adsorption and alkaline elution upstream can result in virus recoveries ranging from 5-90% depending on the matrix involved[19–21]. PEG concentration in conjunction with alkalic elution was used to confirm a norovirus outbreak involving raspberries[22]. PEG precipitation for norovirus concentration from fat/protein-based foods like hamburgers resulted in the successful recovery of 10^4 RT-PCRU (Real-time PCR units). Similarly, around 24% recovery of norovirus was observed when whipped cream was used as a food matrix[23]. Compared to other concentration methods which were used in conjunction with the elution recovery method, PEG precipitation exhibited better recovery efficiencies when different matrices were involved. Despite its importance in the successful confirmation of norovirus outbreaks from different food and environmental samples, PEG precipitation for norovirus concentration suffers from a few drawbacks like varying consistencies when complex samples like shellfish are involved[24,25]. Also, PEG precipitation is not effective as a standalone concentration method and has to be used in conjunction with upstream acid adsorption and alkaline elution strategies[26,27]. When used as a standalone concentration method, PEG precipitation can co-concentrate inhibitory substances and also the amount of time required for the precipitation step could be an issue[28]. Moreover, pH

neutralization of virus eluate needs to be performed before using PEG precipitation to concentrate the virus particles in a given sample.

1.4.1.2 Ultracentrifugation:

The process of concentrating norovirus from food and environmental samples using ultracentrifugation involves precipitation of viral particles by centrifugal forces ranging from 120,000 X g to 235,000 X g. This method of concentration has displayed generally less efficiency compared to PEG precipitation when different food matrices are involved. For fresh produce, ultracentrifugation was able to recover only 0.1% of NoV GI.1 compared to 13% by PEG precipitation[29]. A recent study has shown that ultracentrifugation for concentration of human norovirus GII from raw sewage samples was effective when compared to a novel elution and skimmed-milk flocculation procedure, the size of sample analyzed, and the rotors used for centrifugation could be factors that limit their utilization for broader routine testing of foods for virus. Ultracentrifugation can usually be used for processing larger sample volumes but requires the use of specialized equipment. Moreover, the inconsistency in the concentration efficiencies obtained with this method could pose a potential threat of false negatives in some samples.

1.4.1.3 Ultrafiltration:

Ultrafiltration makes use of filters that are equipped with membrane pores that can permit the passage of low molecular mass particles (less than 50-100kDa) and liquids. Virus particles are usually trapped on the membrane and can be eluted in subsequent steps. One of the major advantages of using ultrafiltration for concentration is that this method while

allowing for the processing of larger sample volumes can also help remove many potential PCR inhibitors. This becomes very important when downstream molecular methods for virus detection are used. The recovery rates of different virus particles can be increased by pretreatment of the membrane filters with bovine serum albumin (BSA) or sonication of the purified virus eluate[30]. Using a tangential flow ultrafiltration method, high virus recovery rates (~78%) were obtained with NoV GII spiked deionized water samples[31]. Compared to other concentration methods (like PEG precipitation), ultrafiltration suffers from low concentration rates. A few major disadvantages of using ultrafiltration for concentration include lower levels of virus recovery compared to other concentration techniques, potential fouling of the filters used for the procedure. The recovery rates using this method are not consistent and differ from one research group to another[32]. Finally, an upstream additional purification step should be included to ensure higher recovery rates of viruses using this method.

1.4.1.4 Charge based concentration methods:

1.4.1.4.1 Cationic separation:

Cationic separation relies on the use of positively charged magnetic particles to capture and concentrate virus particles, whose capsid proteins often carry a net negative charge at neutral pH. The magnetic particles with virus particles bound are captured using a magnetic bead recovery system[33].. Automated magnetic cationic based concentration platforms are currently available which have varying capture and concentration capacities depending on the matrix and virus being targeted. Cationic coated filter method was successfully used for the detection of noroviruses 64 surface water samples collected from the Tamagawa River in Japan. In that study, norovirus concentration was carried out

using 900-mm-diameter HA filter coated with a cation Al(3+), followed by a rinsing step to remove aluminum ions and subsequent elution of virus particles in 1mM NaOH. The filtrate was then centrifuged, and the final supernatant obtained was used for PCR detection of the specific viruses. Using this method, noroviruses belonging to genotype 1 and genotype 2 were detected in a high positive ratio 34(54%) and 28(44%) respectively out of 64 samples tested[34].

Cationic separation is like ultracentrifugation in that they both require specialized equipment and trained personnel to carry out the concentration of virus particles from different samples.

1.4.1.4.2 Anionic separation:

Virus recovery rates when using negatively charged membranes or filters varied across different samples and research groups making it difficult to adopt this as a standard method for virus concentration. Moreover, clogging of filters and membranes when turbid samples were used poses a problem when adsorption-based methods are used for enteric virus concentration[35].

1.4.1.5 Adsorption/elution:

1.4.1.5.1 Membrane/filter-based concentration:

Enteric viruses like norovirus, poliovirus and others can be concentrated using membranes made up of cellulose acetate or nitrate[36]. The electrostatic forces drive the binding of the virus to the membranes. Appreciable recovery rates of different enteric viruses were possible by using adsorption-based concentration methods also based upon charge-based binding because of the buffer in which the sample is suspended. Earlier

adsorption-based concentration methods had to include a preconditioning step of the sample to allow for electrostatic binding of negatively charged virus particles to the negatively charged filter materials. This can be achieved by adjusting the pH of the sample and by adding positively charged ions (Al or Mg) to the solution[4]. Another variation of the adsorption-based concentration method for enteric viruses involves the use of negatively charged filters. These were originally used for concentrating virus particles from river water and other water sources. The recovery rates are like that when membranes were used.

Since positively charged filters can eliminate the preconditioning step mentioned above, they have been used for absorbing different foodborne viruses from water samples. The virus recovery rates of positively charged filters is similar to that of negatively charged ones[37].

Charge-modified nylon membranes carrying a positive charge have been reported to be effective in the concentration of a variety of enteric viruses prior to RT-PCR detection. The low cost, ease of use and the lack of needing a preconditioning step make this an attractive choice for virus concentration prior to detection. Several advances have been made in developing membranes that have varying concentration efficiencies depending on the matrix involved. Polyvinylidene Fluoride (PVDF) membranes and cartridges are an excellent example of such modified membranes that can be used for removal of influenza (enveloped) and poliovirus (nonenveloped) particles from pharmaceutical products[38].

While the above mentioned membrane/filter based concentration methods are effective in handling larger sample volumes, they suffer from some severe shortcomings such as (i)

requirement of a preconditioning step to ensure adsorption when negatively charged membranes/filters are used (ii) elution steps following virus binding to membrane/filters can be tricky and involves use of buffers that could often inhibit downstream detection methods like RT-PCR and (iii) virus concentration rates and recovery rates across different classes of the membranes/filters is not consistent and repeatable results are not observed for some of the membranes/filters used.

1.4.1.5.2 Glass wool-based concentration:

In this method, glass wool is packed into a column evenly at an adequate density and the sample is allowed to flow through the column. The virus particles will be adsorbed to the filter matrix and can be eluted by increasing the pH. Poliovirus at 10^2 pfu was recovered from 400 liters of drinking water using this method[39]. Other viruses like adenovirus and reovirus were also concentrated using this method. Norovirus from spiked sewage and polluted water samples was also concentrated using this method. While this method does not require a preconditioning of the sample, it still requires that the columns be pre-washed with HCL, water, NaOH and finally again with water to a neutral pH. The efficiency of this method in removing inhibitors that can interfere with downstream detection techniques is not well documented.

1.4.1.5.3 Glass powder:

This method of concentration uses glass beads instead of glass fibers as filter matrix. This helps the system from getting clogged, which often is the case with glass fibers. The apparatus used for glass powder concentration is very complex and hence is not the first choice for virus particle concentration from larger volumes of sample[40].

1.4.1.6 Other adsorption-based concentration methods:

Adsorbents like magnesium silicate, silicon dioxide (SiO2) and powdered coal have been used to concentrate a wide range of viruses from different water samples[41]. While these are effective in concentrating enteric viruses from the samples, some of these must be followed up with a secondary concentration method to remove any impurities associated that might potentially inhibit downstream detection methods like RT-PCR which is currently the gold standard for norovirus detection.

1.4.2 Specific Norovirus Concentration Methods

1.4.2.1 Immunoconcentration:

Immunoconcentration (IMC) utilizes paramagnetic beads coupled to a virus-specific antibody (IgG) allowing for (i) separation of virus particles from contaminating substances in the sample of interest and (ii) virus concentration in a single step. The capture/concentration step is followed by a RT-PCR step for detection of noroviruses in stool samples. In a study to compare the concentration efficacy of paramagnetic beads with a direct heat release method, IMC demonstrated a 2000-fold increase in concentration of norovirus. The direct heat release method utilizes expensive and environmentally unsafe freon reagents while immunoconcentration relies on inexpensive paramagnetic beads that can be prepared in mass quantities. Moreover, the use of affinity selection in IMC ensures that the subsequent PCR amplification signal is a true reflection of the intact virus particles[42]. While immunoconcentration addresses some of the issues associated with concentrating norovirus from different samples like keeping the PCR inhibitor concentrations to a minimum, its long term usage especially the antibody

mediated concentration is under question due to the antigenic drift associated with several foodborne viruses[43].

1.4.2.2 Ligand based concentration techniques for norovirus:

1.4.2.2.1 Histo blood group antigen-based concentration:

Application of ligands for human norovirus detection was first demonstrated by Marionneau et al., in 2002[44]. Histoblood group antigens (HBGAs) are the putative human cellular receptors for norovirus. HBGAs are complex terminal carbohydrates present on red blood cells, mucosal cells etc. The HBGAs are generated from disaccharide precursors that then undergo monosaccharide addition mediated by different glycosyltransferases. The ABH and Lewis antigen systems are often implicated in human norovirus binding. HBGA like moieties have been identified on certain foods and microflora too.

The norovirus binding capabilities of HBGAs came into light when epidemiological studies concluded that patients with O blood group were more susceptible to norovirus infection (subsequently known as secretors due to the presence of fucosyltransferase enzyme that catalyzes monosaccharide addition to disaccharide precursors of HBGAs and aid in their maturation)[45]. On the other hand, challenge studies identified non-secretors with two non-functional FUT2 alleles which leads to the absence of HBGAs in their saliva, making them resistant to norovirus infection. Molluscan shellfish (particularly oysters) which have been implicated in norovirus outbreaks have been shown to carry type-A and type-O HBGA-like residue in their tissues. Viral persistence studies on leafy

greens have shown that sugars found in HBGAs are also found in the leafy greens and can aid in norovirus binding.

While these studies have implicated the role of HBGAs in human norovirus infection, additional factors have been identified that can promote infection in different norovirus strains. Technical and ethical issues preclude the use of human HBGAs for norovirus concentration from complex food matrices. To circumvent this issue, porcine gastric mucin (PGM) has been shown to be effective in capturing genogroup I and II strains of human norovirus from food and environmental samples[46]. Immunoconcentration of human norovirus exploits the property of PGM for norovirus concentration from samples. Magnetic beads coated with PGM are used for initial concentration followed by elution of bound norovirus into an appropriate buffer.

While this could be an effective way of concentrating norovirus from a wide variety of matrices with little to no inhibitory substances (that could potentially interfere with downstream detection techniques), not all strains of norovirus can be concentrated using HBGAs or HBGA like moieties. There are ongoing studies to determine the role of additional co-factors/attachment factors that could potentially bind to norovirus and help in their concentration from different matrices. Understanding the role of the additional factors can help us develop effective concentration strategies targeting human norovirus in various samples.

While several of the methods described above for concentration of foodborne viruses from different matrices may sound promising, nearly all have inherent limitations in terms of the volume of sample that can be processed, high cost, and/or tendency to co-concentrate inhibitory substances. Generally, the nonspecific methods discussed display

ideal capture efficiency, but often have limitations in scalability and tendency to co-concentrate substances from foods that can inhibit downstream detection. Specific methods allow for effective washing and removal of potential inhibitory substances from the sample matrix, but often have not displayed optimal capture efficiency, are costly, and have limitations in scale. While bacteria have not been traditionally used for capture and concentration of noroviruses from difficult to isolate matrices, they have been shown to bind noroviruses mediated by histo-blood group like antigens expressed on their surface.

1.5 Foundational work demonstrating norovirus binding to enteric bacteria:

Histo-blood group antigens (HBGAs) have been implicated as cofactors for at least some strains of human norovirus. HBGA expression is not limited to humans, as similar carbohydrates have also been observed in bacteria, including foundational work by Miura et al.[47] that observed strain-dependent human norovirus binding to Enterobacter cloacae isolated from feces. Subsequent work by numerous other groups has also demonstrated direct binding of both GI and GII noroviruses to a variety of Gram-positive and Gram-negative bacteria, however, further work to specifically identify the bacterial components responsible for the binding has yet to be reported[48]. This is important, as one suspected mechanism by which bacteria are thought to enhance noroviral infection is this interaction facilitating virus binding to host cells. A recent study by Almand et al. characterized the binding between HBGA-like molecules expressed by seven bacterial strains (four Gram-negative and three Gram-positive) isolated from stool that were previously demonstrated to bind noroviruses[49]. Each bacterial species displayed observable and differential HBGA profiles when assayed with different anti-HBGA

antibodies. Further, use of viral-particle overlays with six different human norovirus strains suggested a broad level of viral interaction with the bacteria, often with multiple potential bacterial components implicated in binding. Interestingly, a 35 kDa bacterial component was observed to display both HBGA activity and exhibited viral binding across a broad range of norovirus strains, but was not identified[49].

1.6 Conclusion:

More work to characterize the interactions of specific bacterial components with viable bacteria and knockouts is needed. Further, the observed capture efficiency of noroviruses by a number of these bacteria exceeds 60%, an efficiency notably higher than the specific concentration methods discussed above, suggesting that bacteria may show promise as novel capture and concentration reagents. Further, bacterial strain, culture conditions, and binding assay used are also major considerations that vary across these reports and likely influence the results observed.

1.7 References:

1. CDC. Foodborne Illnesses and Germs. *Centers for Disease Control and Prevention* https://www.cdc.gov/foodsafety/foodborne-germs.html (2022).
2. Capece, G. & Gignac, E. Norovirus. in *StatPearls* (StatPearls Publishing, 2022).
3. CDC. CDC VitalSigns - Preventing Norovirus Outbreaks. *Centers for Disease Control and Prevention* https://www.cdc.gov/vitalsigns/norovirus/index.html (2019).
4. Katayama, H., Shimasaki, A. & Ohgaki, S. Development of a Virus Concentration Method and Its Application to Detection of Enterovirus and Norwalk Virus from Coastal Seawater. *Appl. Environ. Microbiol.* **68**, 1033–1039 (2002).

5. Liu, L. & Moore, M. D. A Survey of Analytical Techniques for Noroviruses. *Foods* **9**, 318 (2020).
6. Bartsch, C. *et al.* Comparison and optimization of detection methods for noroviruses in frozen strawberries containing different amounts of RT-PCR inhibitors. *Food Microbiol.* **60**, 124–130 (2016).
7. Stals, A., Baert, L., Van Coillie, E. & Uyttendaele, M. Extraction of food-borne viruses from food samples: A review. *Int. J. Food Microbiol.* **153**, 1–9 (2012).
8. Bosch, A., Guix, S., Sano, D. & Pintó, R. M. New tools for the study and direct surveillance of viral pathogens in water. *Energy Biotechnol. Environ. Biotechnol.* **19**, 295–301 (2008).
9. Croci, L. *et al.* Current Methods for Extraction and Concentration of Enteric Viruses from Fresh Fruit and Vegetables: Towards International Standards. *Food Anal. Methods* **1**, 73–84 (2008).
10. Moore, M. D., Goulter, R. M. & Jaykus, L.-A. Human norovirus as a foodborne pathogen: challenges and developments. *Annu. Rev. Food Sci. Technol.* **6**, 411–433 (2015).
11. Stegmaier, T., Oellingrath, E., Himmel, M. & Fraas, S. Differences in epidemic spread patterns of norovirus and influenza seasons of Germany: an application of optical flow analysis in epidemiology. *Sci. Rep.* **10**, 14125 (2020).
12. Scallan, E. *et al.* Foodborne Illness Acquired in the United States—Major Pathogens. *Emerg. Infect. Dis.* **17**, 7 (2011).

13. Kirk, M. D. *et al.* World Health Organization Estimates of the Global and Regional Disease Burden of 22 Foodborne Bacterial, Protozoal, and Viral Diseases, 2010: A Data Synthesis. *PLOS Med.* **12**, e1001921 (2015).
14. Lopman, B. A., Steele, D., Kirkwood, C. D. & Parashar, U. D. The Vast and Varied Global Burden of Norovirus: Prospects for Prevention and Control. *PLOS Med.* **13**, e1001999 (2016).
15. Bartsch, S. M., Lopman, B. A., Ozawa, S., Hall, A. J. & Lee, B. Y. Global Economic Burden of Norovirus Gastroenteritis. *PLOS ONE* **11**, e0151219 (2016).
16. Park, H., Kim, M. & Ko, G. Evaluation of Various Methods for Recovering Human Norovirus and Murine Norovirus from Vegetables and Ham. *J. Food Prot.* **73**, 1651–1657 (2010).
17. Desk, N. Researcher presents method to detect norovirus in food. *Food Safety News* https://www.foodsafetynews.com/2019/09/researcher-presents-method-to-detect-norovirus-in-food/ (2019).
18. Mäde, D., Trübner, K., Neubert, E., Höhne, M. & Johne, R. Detection and Typing of Norovirus from Frozen Strawberries Involved in a Large-Scale Gastroenteritis Outbreak in Germany. *Food Environ. Virol.* **5**, 162–168 (2013).
19. Gyawali, P., Kc, S., Beale, D. J. & Hewitt, J. Current and Emerging Technologies for the Detection of Norovirus from Shellfish. *Foods* **8**, 187 (2019).
20. Cashdollar, J. l. & Wymer, L. Methods for primary concentration of viruses from water samples: a review and meta-analysis of recent studies. *J. Appl. Microbiol.* **115**, 1–11 (2013).

21. McLellan, N. L., Weir, S. C., Lee, H. & Habash, M. B. Polyethylene glycol (PEG) methods are superior to acidification for secondary concentration of Adenovirus and MS2 in water. 2021.11.19.469352 Preprint at https://doi.org/10.1101/2021.11.19.469352 (2021).
22. Le Guyader, F. S. *et al.* Detection of noroviruses in raspberries associated with a gastroenteritis outbreak. *Int. J. Food Microbiol.* **97**, 179–186 (2004).
23. Leggitt, P. R. & Jaykus, L. A. Detection methods for human enteric viruses in representative foods. *J. Food Prot.* **63**, 1738–1744 (2000).
24. Atmar, R. L. *et al.* Detection of Norwalk virus and hepatitis A virus in shellfish tissues with the PCR. *Appl. Environ. Microbiol.* **61**, 3014–3018 (1995).
25. Häfliger, D., Gilgen, M., Lüthy, J. & Hübner, P. Seminested RT-PCR systems for small round structured viruses and detection of enteric viruses in seafood. *Int. J. Food Microbiol.* **37**, 27–36 (1997).
26. Kingsley, D. H. An RNA extraction protocol for shellfish-borne viruses. *J. Virol. Methods* **141**, 58–62 (2007).
27. Calder, L. *et al.* An outbreak of hepatitis A associated with consumption of raw blueberries. *Epidemiol. Infect.* **131**, 745–751 (2003).
28. Raymond, P., Paul, S., Perron, A. & Deschênes, L. Norovirus Extraction from Frozen Raspberries Using Magnetic Silica Beads. *Food Environ. Virol.* **13**, 248–258 (2021).
29. Dubois, E. *et al.* Modified concentration method for the detection of enteric viruses on fruits and vegetables by reverse transcriptase-polymerase chain reaction or cell culture. *J. Food Prot.* **65**, 1962–1969 (2002).

30. Jones, T. H., Brassard, J., Johns, M. W. & Gagné, M.-J. The effect of pre-treatment and sonication of centrifugal ultrafiltration devices on virus recovery. *J. Virol. Methods* **161**, 199–204 (2009).

31. Farkas, K., McDonald, J. E., Malham, S. K. & Jones, D. L. Two-Step Concentration of Complex Water Samples for the Detection of Viruses. *Methods Protoc.* **1**, 35 (2018).

32. Rutjes, S. A., Lodder-Verschoor, F., van der Poel, W. H. M., van Duijnhoven, Y. T. H. P. & de Roda Husman, A. M. Detection of noroviruses in foods: a study on virus extraction procedures in foods implicated in outbreaks of human gastroenteritis. *J. Food Prot.* **69**, 1949–1956 (2006).

33. Fumian, T. M., Leite, J. P. G., Marin, V. A. & Miagostovich, M. P. A rapid procedure for detecting noroviruses from cheese and fresh lettuce. *J. Virol. Methods* **155**, 39–43 (2009).

34. Application of Cation-Coated Filter Method to Detection of Noroviruses, Enteroviruses, Adenoviruses, and Torque Teno Viruses in the Tamagawa River in Japan | Applied and Environmental Microbiology. https://journals.asm.org/doi/10.1128/AEM.71.5.2403-2411.2005.

35. Norling, L. *et al.* Impact of multiple re-use of anion-exchange chromatography media on virus removal. *J. Chromatogr. A* **1069**, 79–89 (2005).

36. Hata, A., Matsumori, K., Kitajima, M. & Katayama, H. Concentration of enteric viruses in large volumes of water using a cartridge-type mixed cellulose ester membrane. *Food Environ. Virol.* **7**, 7–13 (2015).

37. Junter, G.-A. & Lebrun, L. Cellulose-based virus-retentive filters: a review. *Rev. Environ. Sci. Biotechnol.* **16**, 455–489 (2017).

38. Oshima, K. H., Evans-Strickfaden, T. T., Highsmith, A. K. & Ades, E. W. The use of a microporous polyvinylidene fluoride (PVDF) membrane filter to separate contaminating viral particles from biologically important proteins. *Biol. J. Int. Assoc. Biol. Stand.* **24**, 137–145 (1996).

39. Lambertini, E. *et al.* Concentration of Enteroviruses, Adenoviruses, and Noroviruses from Drinking Water by Use of Glass Wool Filters. *Appl. Environ. Microbiol.* **74**, 2990–2996 (2008).

40. Joret, J. C. *et al.* Virus concentration from secondary wastewater: Comparative study between epoxy fiberglass and glass powder adsorbents. *Eur. J. Appl. Microbiol. Biotechnol.* **10**, 245–252 (1980).

41. Shi, H., Pasco, E. V. & Tarabara, V. V. Membrane-based methods of virus concentration from water: a review of process parameters and their effects on virus recovery. *Environ. Sci. Water Res. Technol.* **3**, 778–792 (2017).

42. Gilpatrick, S. G., Schwab, K. J., Estes, M. K. & Atmar, R. L. Development of an immunomagnetic capture reverse transcription-PCR assay for the detection of Norwalk virus. *J. Virol. Methods* **90**, 69–78 (2000).

43. Kobayashi, S., Natori, K., Takeda, N. & Sakae, K. Immunomagnetic capture rt-PCR for detection of norovirus from foods implicated in a foodborne outbreak. *Microbiol. Immunol.* **48**, 201–204 (2004).

44. Marionneau, S. *et al.* Norwalk virus binds to histo-blood group antigens present on gastroduodenal epithelial cells of secretor individuals. *Gastroenterology* **122**, 1967–1977 (2002).

45. Nordgren, J. & Svensson, L. Genetic Susceptibility to Human Norovirus Infection: An Update. *Viruses* **11**, (2019).

46. Tian, P., Engelbrektson, A. & Mandrell, R. Two-Log Increase in Sensitivity for Detection of Norovirus in Complex Samples by Concentration with Porcine Gastric Mucin Conjugated to Magnetic Beads. *Appl. Environ. Microbiol.* **74**, 4271–4276 (2008).

47. Miura, T. *et al.* Histo-Blood Group Antigen-Like Substances of Human Enteric Bacteria as Specific Adsorbents for Human Noroviruses. *J. Virol.* **87**, 9441–9451 (2013).

48. Almand, E. A., Moore, M. D., Outlaw, J. & Jaykus, L. A. Human norovirus binding to select bacteria representative of the human gut microbiota. *PLOS ONE* **12**, e0173124 (2017).

49. Almand, E. A., Moore, M. D. & Jaykus, L.-A. Characterization of human norovirus binding to gut-associated bacterial ligands. *BMC Res. Notes* **12**, 607 (2019).

Chapter 2: Capture and concentration of human noroviruses in foods and environmental samples by engineered bacterial strains.

2.1 Abstract:

Human noroviruses are the leading cause of non-bacterial gastroenteritis across the world and the fourth leading cause of foodborne death in the United States[1]. One of the major challenges in control of human noroviruses is the lack of an efficient enrichment strategy for viruses from food and environmental samples prior to detection. Existing norovirus concentration methods have several limitations, such as higher cost, lack of scalability, and generally low capture efficiency (<30%)[2]. The purpose of the current study was to evaluate the use of nonpathogenic *Escherichia coli (E. coli)* mutants engineered to express norovirus-specific peptides on their surface for concentration of human norovirus (GII.4) prior to detection. *E. coli* strains were engineered to present norovirus-specific peptides by cloning them to the C-terminus of the ice nucleation protein after introduction of a serine-glycine spacer (SGGGGSGGGGSGGGGS). Norovirus GII.4 Sydney capture efficiency by engineered *E. coli* was determined by suspension assay-RT-qPCR by calculating removal of input virus from suspension. Capture efficiencies ranged from 66% (SD ±4.0) to 81% (SD ±0.24) among the 7 different engineered *E. coli* strains and *E. cloacae*, a native-binding norovirus bacterium. The highest capture efficiencies observed with the engineered *E. coli* strains, 81.34 % (SD ±0.2) and 76.55% (SD ±1.0) were higher than that observed with *E. cloacae* (76%, SD ±3.0), as well as the no-peptide scaffold control. The engineered *E. coli* strains were also tested for their capture efficiency of human norovirus GI.1 using removal from supernatant. We did not observe any capture of the norovirus GI.1 from stool sample after 2hrs of incubation with the

engineered *E. coli*. Using engineered *E. coli* had the added benefit of being inducible, potentially making the mutants less prone to media/growth conditions as has been reported for *E. cloacae*. We were able to demonstrate the potential of engineered *E. coli* strains expressing norovirus specific peptides for concentration of noroviruses prior to detection. Owing to the ease of deployment, cost-effectiveness, and potential to be scaled up for handling larger volumes, we envision this method can be easily adopted for concentration of norovirus from foods, patient, and environmental samples.

2.2 Introduction:

Human noroviruses are the leading cause of foodborne illness and fourth leading cause of foodborne death in the United States[1]. Rapid concentration and detection of human norovirus from food and environmental samples is essential for their prevention and control; however, it remains one of the leading challenges in control of human norovirus[3]. Human norovirus is present in food and environmental samples at low levels but cannot realistically be cultivated *in vitro* for routine food and environmental testing; thus, sample concentration prior to detection is required[4].

For decades, concentration of norovirus from samples effectively and efficiently at low cost has been a major challenge. There are many reasons for this, reviewed elsewhere. Historically, nonspecific methods exploiting the physical and electrostatic properties of the human norovirus capsid have been utilized for concentration purposes[3]. These methods include elution-concentration, ultrafiltration, cationic bead concentration, flocculation, immunomagnetic separation, and ultracentrifugation. Unfortunately, these methods are cumbersome, can have poor recovery efficiencies (3-25% recovery though some have been shown to be higher), and detection inhibitors remain.

The non-specific concentration methods have the major drawback of concentrating multiple inhibitors of downstream detection, which is especially problematic in the case of human noroviruses. Specifically, reverse transcriptase quantitative polymerase chain reaction (RT-qPCR) has been the gold standard downstream detection method for human noroviruses in food and environmental samples[5]; however, it is very sensitive to inhibition from food matrices. The concept of using binding ligands to specifically concentrate human norovirus from complex sample matrices has gained traction because it allows for washing away sample matrix inhibitors. The approach commonly involves the use of paramagnetic nanoparticles (beads) to which target-specific ligands are tethered. Such ligands include monoclonal antibodies, single chain antibodies, peptides, HBGAs, porcine gastric mucin (which contains HBGAs), and nucleic acid aptamers[6,7]. The use of ligands for specific capture and separation of viral particles from food samples allows for removal of sample matrix-associated inhibitors through washing in addition to concentration. The specificity of these ligands for norovirus allows for removal of other organisms and components that might complicate detection. However, all these ligands have some negatives. Unfortunately, these ligand-bead based methods have a low recovery/capture efficiency (typically <30%)[8]. Overall, the use of ligands with paramagnetic beads limits the degree to which assays can be scaled up. Even with the use of ideal ligands, magnetic bead-based concentration, and detection—in addition to the cost of functionally modifying the ligands to be able to be presented on the beads—would pose too much a cost and too low a capture efficiency (sensitivity) to be effectively used for routine concentration of human noroviruses from food and environmental samples.

Evidence has recently been presented that some intestinal bacteria containing HBGA-like moieties can bind human norovirus with high avidity[9]. A recent study has demonstrated the successful use of three different strains of bacteria for successful removal of human norovirus VLPs from water solution when used in conjunction with membrane filtration[10]. Additional studies focused on the human gut bacteria have reported the presence of a variety of bacterial species that can effectively bind several human norovirus strains with capture efficiencies sometimes exceeding 90%[11]. The binding efficiencies of these representative gut bacteria have been shown to be highly dependent on the bacterial propagation media used. While the exact mechanism behind the binding of norovirus to bacteria and the factors involved warrants further investigation, the possibility of employing bacteria for human norovirus concentration from a wide variety of complex sample matrices cannot be ignored.

One of the potential drawbacks to using bacteria that natively bind noroviruses is the fact that norovirus capture with these bacteria has been demonstrated to significantly differ based upon culture conditions[11]. Genetic engineering and surface display of ligands with affinity for human norovirus that can be inducibly expressed may provide more consistent capture. Previous studies on *Pseudomonas syringae* have identified the presence of an ice nucleation protein that can nucleate ice crystals at a higher temperature than would normally occur[12]. The ice nucleation protein has been instrumental in facilitating the expression of engineered proteins on the surfaces of bacteria. Abbaszadegan et al. have demonstrated that by fusing the human poliovirus receptor hPVR, to the C-terminal end of a truncated ice nucleation protein, allows it to be presented on the surface of an engineered *E. coli*[2]. The engineered *E. coli* was then able

to recover poliovirus from 1-liter samples with recovery efficiencies ranging from 70-99%. Cloning a chimeric INP-viral ligand construct into a plasmid expression vector can allow for inducible overexpression of the viral ligands on the surface of bacteria. While successful attempts to express the norovirus P domain on the surface of *E. coli* for studying viral capsid binding characteristics have been reported, no binding has been reported[13]. The current study is aimed at the development and efficacy testing of a novel engineered *E. coli*-based capture and concentration method targeting human norovirus. By developing a bacterial construct that can express a high affinity norovirus binding peptide, we aim to achieve significantly higher norovirus capture efficiencies than may be observed by conventional bead-based assays (typically around <30%).

The key to developing such an inducible norovirus binding *E. coli* construct would be to find the appropriate peptides. Production and identification of 12mer peptides targeting human norovirus have been reported elsewhere[14,15]. Given the short length, the norovirus binding peptides can be cloned to the C-terminus of a truncated INP as outlined in Abbaszadegan et al. along with a spacer sequence to reduce steric hindrance during surface expression of the norovirus ligands.

2.3 Materials and methods:

2.3.1 Virus strains:

Human fecal specimens derived from outbreaks and confirmed positive (by RT-PCR) for GII.4, and GI.1 norovirus were obtained courtesy of Dr. Lee Ann Jaykus, North Carolina State University and Dr. Juan Leon, Emory University, Atlanta, GA respectively.

Norovirus GII.4 and GI.1 stool samples were diluted to 20% and 10% (v/v) in 1X PBS, pH 7.2, aliquoted into single use aliquots, and stored at -80°C until use.

2.3.2 Bacterial isolates and engineered *E. coli*:

Reference strains of *Bacillus spp, Enterobacter cloacae, Staphylococcus aureus, Klebsiella spp, Citrobacter spp, Enterococcus faecium, Hafnia alvei* were grown in half strength TSB media (unless otherwise specified) overnight at 37C. Overnight cultures were centrifuged, and pellets resuspended in TSB+5% glycerol for preparing glycerol stocks. Glycerol stocks of the reference strains were stored at -80C and revived right before the pull-down assay.

2.3.3 Engineered *E. coli* expressing norovirus specific peptides:

2.3.3.1 Cloning and Expression of INP-Peptide Fusion Protein in an Expression Vector:

Plasmids containing a truncated INP protein along with a glycine-serine spacer (SGGGGSGGGGSGGGGS)[16] and different high affinity norovirus binding peptides were generated by Thermofisher Geneart. The plasmid (containing an Ampicillin resistant marker) was transformed into *E. coli* BL21(DE3) cells and successful transformants were isolated from LB-Amp plates. Five percent Glycerol stocks of engineered *E. coli* were prepared in TSB and stored at -80C. The sequences of peptides in the engineered *E. coli* strains are as follows.

Table.1: The sequences of peptides in the engineered *E. coli* strains.

	Name	Amino acid sequence	Affinity (nM)	Reference
Mando1	LDY	LDYRSWAPYATS	N/A	Rogers et al[5]
Mando2	IQY	IQYRSWIPFSYP	N/A	Rogers et al[5]
Mando3	LSI	LSIRSYTSPQWQ	N/A	Rogers et al[5]
Mando4	YRS	YRSFDPWYPPVH	N/A	Rogers et al[5]
Mando5	LPS	LPSWYLAYQKII	N/A	Rogers et al[5]
Mando6	QHK	QHKMHKPHKNTKGGGGSC	99.8	Hwang et al[56]
Mando7	QHI	QHIMHLPHINTL	185	Hwang et al[56]

*Along with the above 7 clones expressing different norovirus specific peptides, a scaffold expressing just the ice nucleation protein along with the spacer was included in the study as a control.

2.3.4 Bacteria-virus binding and pull-down assay:

All strains of bacteria were grown as described above. Starting concentrations (input) of bacteria for the different strains were enumerated via growth curves to ensure that the amounts of bacteria used were comparable between different strains.

Prior to the binding and pull-down assay, bacterial cultures were grown for 12hr at 37°C in 10ml of select medium. The cells were pelleted, washed, and resuspended in 10ml PBS, pH 7.2. The cells are diluted to a final concentration of $1x10^7$ cfu/ml. For the pull-down assay 100ul of 10% human norovirus GII.2 or GI.1, 100ul of the resuspended bacteria and 300ul of PBS were added to a 2ml Eppendorf tube. The mixture was incubated for 2hr at room temperature on a rotating platform. To ensure even mixing of the bacteria+virus suspension, 0.5ul of Tween-20 was added to each tube. Following the

2hr incubation, the suspension was pelleted at 8000rpm for 5 mins at room temperature. The supernatant was removed for enumerating the unbound virus using RT-qPCR. Positive controls consisted of just the input virus suspension without any bacteria.

2.3.5 Chloroform purification of norovirus containing stool sample:

Chloroform purification of the 10% GII.4 stool samples was performed as mentioned elsewhere[17]. Briefly, to the GII.4 containing stool sample (10%) in PBS (pH 7.2), equal volume of chloroform was added in a microcentrifuge tube. The tube was centrifuged at 5000 X g for 15 mins at 4^{O}C. The supernatant was carefully removed and aliquoted (~ 100 ul/tube) into fresh labelled Eppendorf tubes and stored at -80^{O}C until further use.

2.3.6 Nucleic acid extraction and viral RNA detection:

Supernatant from the pull-down assay was used for RNA extraction using a QIAamp Viral RNA mini kit. The RNA was eluted in 20ul of nuclease free water and stored at -80ºC until further use. Viral RNA detection using RT-qPCR was performed using primers and probes as outlined in table 1. The PCR master mix was prepared according to the manufacturer's instructions using the NEB Luna one step universal probe RT-PCR kit. The BioRad CFX96 Real time PCR machine was used for running the PCR. The PCR cycling conditions are 30 mins at 50°C, 15 mins at 95°C, 45 cycles of 15s at 95°C, 30s at 60°.

Table 2: List of primers and probes used in current study[18,19]

Oligonucleotide	Sequence (5'-3')	Product Length	Assay	Reference
JJV2F	CAA GAG TCA ATG TTT AGG TGG ATG AG	98bp	One Step Real-Time	Jothikumar et al. 2005

			RT-PCR	
COG2R	TCG ACG CCA TCT TCA TTC ACA		One Step Real-Time RT-PCR	Kageyama et al. 2003
RING2-TP	FAM-TGG GAG GGC GAT CGC AAT CT-BHQ		One Step Real-Time RT-PCR	Kageyama et al. 2003

2.3.7 RT-qPCR data analysis:

Standard curves for RT-qPCR in triplicate were constructed as previously described using ten-fold serial dilutions of viral RNA in nuclease free water. The Cq value corresponding to each serial dilution was plotted and the data analyzed using a linear regression to establish the slope. The lowest dilution at which all three replicates of the PCR were positive for the viral RNA was established as the lower limit of detection and designated as 1 RT-qPCR unit (RT-qPCRU). The virus input concentration (in RT-qPCRUs) before exposure to bacteria and in the supernatants following exposure to the different bacterial strains were estimated based on the standard curve. Virus binding efficiency was calculated based on loss to supernatant, i.e., ((Total virus input- virus lost to supernatant)/total virus input)), expressed as log capture efficiency[11].

2.3.8 Statistical analysis:

The suspension assay was performed in triplicate, Binding efficiency data was expressed as described above. The error bars indicate ± standard deviation across the replicates.

Statistical comparison between binding efficiencies of the representative strain E. cloacae and the engineered bacterial clones was performed using OriginPro software. One-way ANOVA analysis was performed with a Tukey (HSD) and a p value <0.05 was considered significant.

2.3.9 TEM image analysis of GII.4 VLP binding to engineered *E. coli* strains:

Briefly, GII.4 VLP's (purchased from Native antigen company, catalog # REC32015-100) were used in the pull-down assay as mentioned above with pGrogu, pMando1, pMando3, pMando4, pMando5, *E. cloacae* and *E. coli* (C3000). The VLP's were used at a 1:1000 dilution in the respective media used for culturing the engineered *E. coli* and *E. cloacae.* Following incubation of the VLP's with the bacteria, the suspension was centrifuged at 8000rpm for 1min at RT to collect the bacterial pellets. The pellets were washed in PBS and resuspended in 1ml of PBS (pH 7.2). For TEM, a carbon grid was used, and the samples were stained using Nano-W® (Methylamine Tungstate) and allowed to airdry at RT overnight. The grids were images using FEI Tecnai-T12 TEM at the UMass electron microscopy core.

2.4 Preliminary results and discussion:

2.4.1 Wild type bacteria were able to capture norovirus GII.4:

Our preliminary results have indicated that the wild type of representative strains tested in the current study were able to bind human norovirus GII.4 from the 10% diluted stool sample following chloroform purification of the stool sample. The initial results with just 10% stool sample did not show any binding with any of the wild type strains tested.

2.4.2 Chloroform purification of the norovirus containing stool sample:

The GII.4 patient stool samples were chloroform purified (Moore lab protocol for chloroform purification of Norovirus from stool samples) and diluted 1/10000 before use in the suspension assay. This seemed to have resolved the issue of non-binding of norovirus to wild type bacteria observed before (Figure 1).

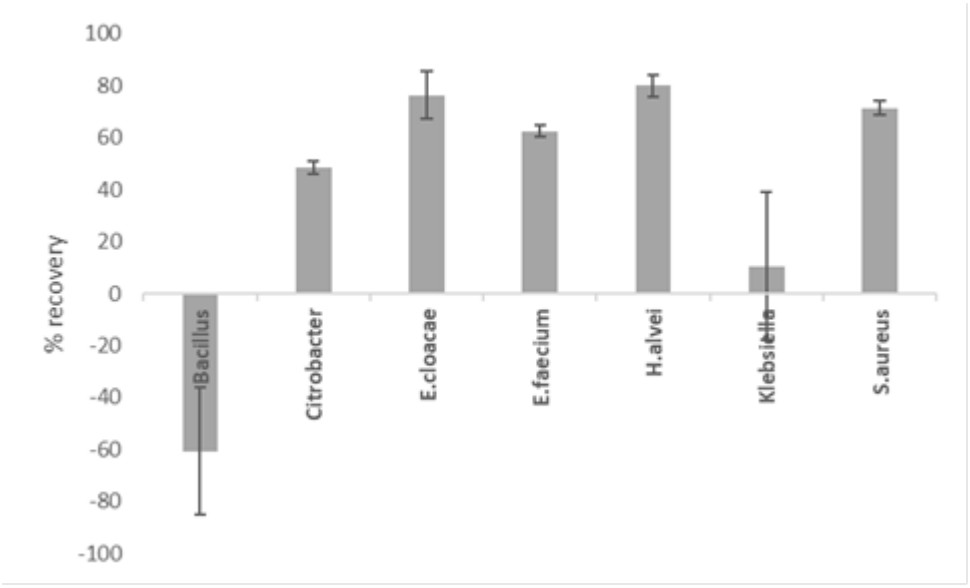

Fig 1. Binding efficiency of human norovirus GII.4 to representative bacterial strains. Data represents averages and standard deviations of the assays performed in triplicate. Percentage of binding efficiency was determined by loss-to-supernatant (total input virus-virus in supernatant)/total input virus. All bacterial strains were grown in half strength TSB medium under anaerobic conditions at 37ºC overnight.

2.4.3 Engineered *E. coli* strains expressing GII.4 norovirus binding peptides captured norovirus in stool sample display higher efficiency than native binder *E. cloacae*:

Previous studies have shown that *Enterobacter cloacae* was able to capture three different norovirus strains (GII.4 Sydney, GII.4 New Orleans & GI.6) with capture efficiencies of 89.6%, 89.2% and 67.9% for the three strains respectively[11]. We tested the norovirus capture efficiency of *E. cloacae* alongside the engineered strains. Some of the engineered strains were able to capture norovirus GII.4 at a higher concentration compared to *E. cloacae*.

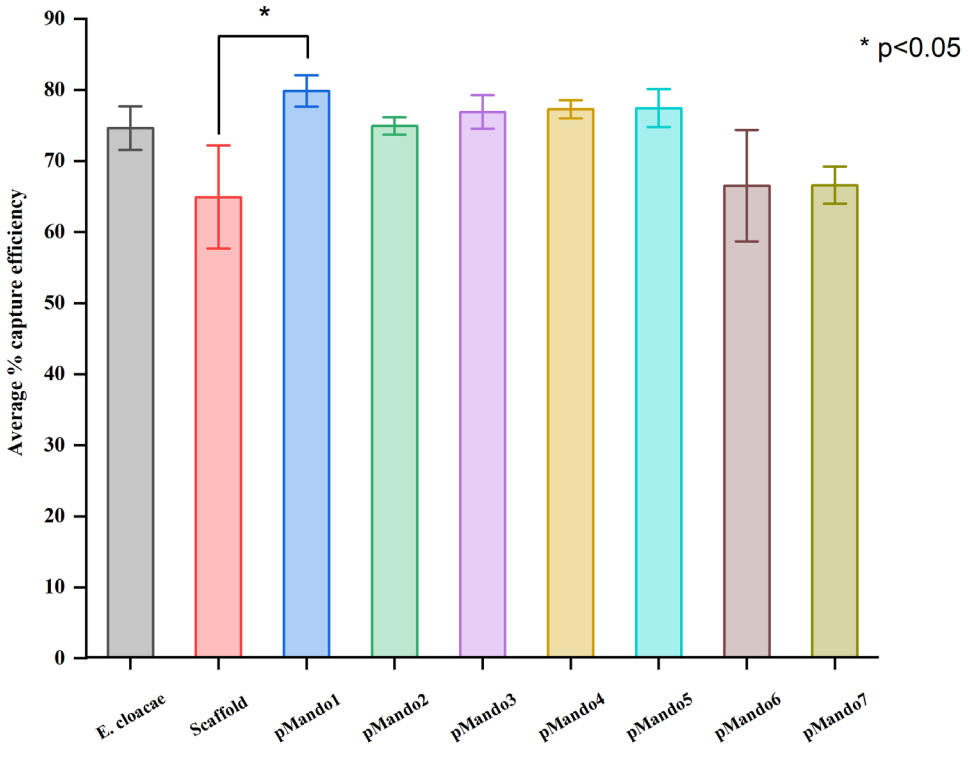

Fig 2. Binding efficiency of human norovirus GII.4 to engineered *E. coli* strains.

Data represents averages and standard deviations of the assays performed in triplicate. Percentage of binding efficiency was determined by loss-to-supernatant (total input virus-virus in supernatant)/total input virus. All bacterial strains were grown in half strength TSB medium under anaerobic conditions at 37ºC overnight. * Indicates a p value < 0.05

2.4.4 Binding efficiency of human norovirus GII.4 to engineered *E. coli* strains and *E. cloacae*:

The line indicates the total virus input during the pull-down assay. Data are expressed as mean log10 concentration of bacteria bound (in qRT-PCRU) (bars) and percent binding efficiency as determined by loss to supernatant (total virus input-virus in supernatant)/total virus input).

2.4.5 Stool sample degradation:

The GII.4 containing stool sample in our possession started degrading and we tested out a few different mitigation strategies to prevent the degradation (see table below). The Cq values of the GII.4 containing stool samples from the input virus sample dropped to around 34 after just 1hr of incubation, while the 0' time point gave us a Cq value of 29. This was more than a log difference in the Cq value between the 0' and 1hr time points. None of the mitigation strategies worked and so we switched to testing a new stool sample that has been tested positive for human norovirus GI.1

Table.3 Mitigation strategies to prevent virus degradation in stool sample:

Mitigation strategy	**Procedure**	**Notes**
Reduction in	The pull-down assay	While the reduction in incubation

incubation time	was reduced to 1hr instead of 2hrs.	time reduced the degradation, it still seems to be time dependent and even 1hr incubation showed an overall reduction in PCR signal compared to the 0' time point.
Chloroform purification	10% HuNoV GII.4 samples were purified using equal volume of chloroform prior to pull down assay	This did not resolve the issue of norovirus degradation.
Chloroform purification + filter sterilization	HuNoV GII.4 samples were chloroform purified as mentioned above and the purified samples were filter sterilized using a 0.2uM syringe filter unit	This did not resolve the issue of norovirus degradation.
FBS treatment	Prior to the pull-down assay, FBS was added to the virus stocks for a final concentration of 1%	The FBS treatment temporarily resolved the norovirus degradation issue, but the samples started degrading after 2hr incubation at room temperature.

3X Protease inhibitor treatment	The stool samples were treated with 3X Protease inhibitor to remove the effect of any proteases in the stool.	The virus recovery after protease treatment from the 0' and 2hr incubation samples was very different indicating virus degradation
0.1% Tween-80 treatment	Tween-80 was added to a final concentration of 0.1% during the pull-down assay	Tween-80 addition did not seem to resolve the virus degradation issue.
Protease inhibitor + Tween-80 treatment	The protease inhibitor cocktail and Tween-80 were used in combination during the pull-down assay	This did not resolve the issue of norovirus degradation in the stool sample.
RNAse treatment	To freshly prepared 10% Norovirus stool stocks, RNAse-A was added	RNAse treatment of sample did not successfully stop norovirus degradation in the stool.
Low retention tubes	The pull-down assay was performed in low retention 2ml	The use of low retention tubes did not resolve the issue and there was observable norovirus degradation in

	Eppendorf tubes to rule out the possibility of norovirus particles sticking to the sides of the tubes during incubation	the stool sample.

2.4.6 GII.4 VLP's were able to bind to pGrogu (scaffold):

To visualize the localization of norovirus particles to the surface of engineered and wild type *E. coli*, GII.4 VLP's were used as a substitute for human stool sample containing infectious GII.4. We observed that there is a heavy localization of GII.4 VLP's on the surface of pGrogu (the clone expressing just the INP and Serine spacer). This is expected as we observed similar capture efficiencies with the infectious norovirus from stool with pGrogu. The fucosylated carbohydrates on the surface of *E. coli* have been shown to bind human norovirus particles and the binding of GII.4 VLP particles to the pGrogu scaffold could be attributed to that. We had to switch to using ultrapure water for preparing suspensions of the virus particle bound bacteria as we noticed heavy salt crystal occlusion on the rest of the clones, we tested making it difficult to observe any potential binding of the VLP's to the surface of bacteria. To circumvent this issue, we plan on using ultrapure water for the capture and pulldown assays going forward.

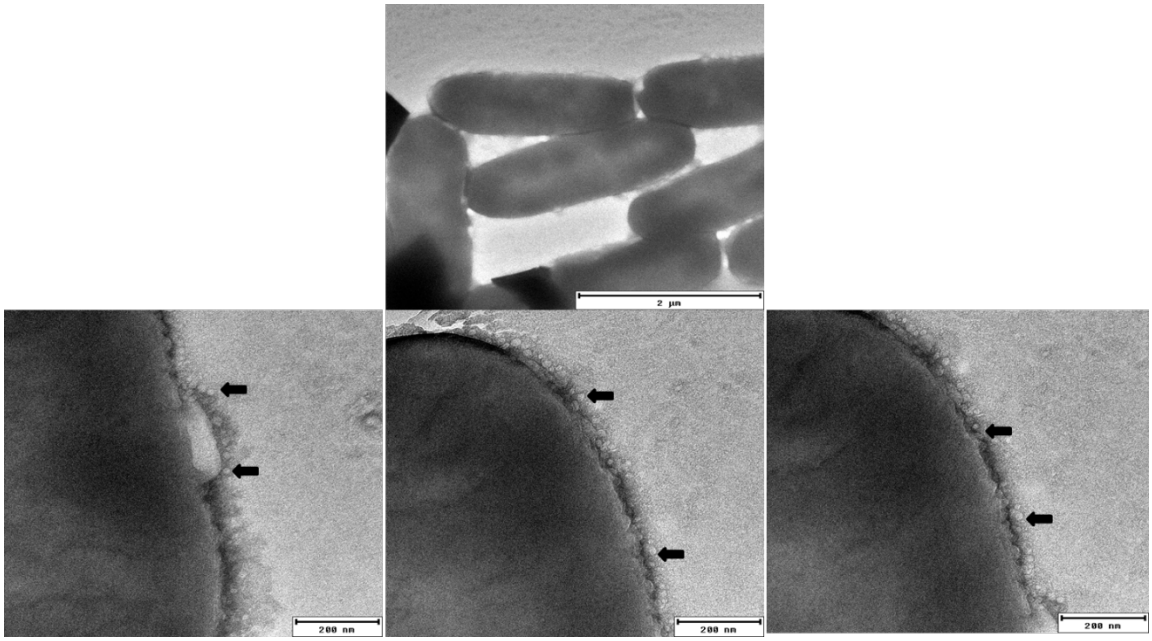

Fig 3. TEM images of GII.4 VLP's bound to pGrogu (* scaffold). The VLP particles are indicated by arrows. The image in the top panel shows pGrogu bacteria and the bottom panels indicate binding of the VLP's on the surface of pGrogu.

2.4.7 Engineered *E. coli* strains did not capture norovirus GI.1 in stool sample:

The efficiency of engineered *E. coli* strains in capturing GI.1 from stool sample was tested. The engineered *E. coli* strains were not able to capture GI.1 from 10% diluted stool samples. To eliminate the effects of any inhibitory substances in the stool sample that might interfere with the binding, chloroform purification of the stool samples was performed. This also did not improve the capture efficiency of GI.1 by the engineered strains.

2.5 Discussion:

While the engineered *E. coli* expressing just the scaffold was able to display binding of GII.4, this could possibly be attributed to the HBGA- like moieties that are present on *E. coli*. Since the binding efficiency of the scaffold strain did not exceed the other engineered strains, we are not concerned about it.

One of the reasons for the degradation of the GII.4 containing sample over a period can be attributed to the fact that we had several instances of the -80C freezer failing during the experiments and we had to move our samples to back up storage freezer. The capsid integrity may have been compromised but since PCR does not differentiate between infectious virus particles and plain RNA, we were able to observe a signal from the degraded samples too. But we did include an RNAse step to be able to differentiate between infectious virus particles and free RNA but that seems to still not have an effect. This could possibly be due to the residual RNAse that was not targeted by the inhibitor. In the future, we plan on incorporating a higher concentration of EDTA into the buffer during the pull-down step. EDTA is an efficient chelator of metal ion enzyme cofactors. By adding it to the buffer during the pull-down step, we hypothesize that the enzymatic activity of any enzymes presents in the stool sample that could compromise the capsid integrity of the virus could be prevented.

Since we were able to demonstrate the binding of the engineered strains to human norovirus GII.4, we tested the efficacy of these strains to capture GI.1 from stool samples. In our preliminary studies, we noticed that the engineered strains were not able to bind the GI.1 in the stool sample even after chloroform purification of the stool sample. It must be noted that some of the engineered strains in the current study

(Mando1, 2, 3, 4&5) express a peptide specific for GI.1. The reason for this is yet to be investigated.

2.6 Plan for future work:

We plan on continuing to test the new stool sample containing GI.1 as it currently seems to be stable without any degradation, though initial study (mentioned above) suggested little capture when calculated by removal from supernatant. However, we will also evaluate recovery efficiency with GI stool, which will involve incubation with bacteria, a wash step, then elution and recovery of remaining bound virus. We also plan to conduct fluorescent and microscopy using GII.4 P particles and virus-like particles (VLPs), as well as with GI.1 VLPs. Enzymatic activity by proteases could be one of the potential reasons for the virus capsid degradation we have been observing in our capture studies so far, though intact norovirus capsids have been demonstrated to be resistant to many intestinal proteases; suggesting that the capsid integrity could have been compromised.

2.7 References:

1. Scallan, E. *et al.* Foodborne Illness Acquired in the United States—Major Pathogens. *Emerg. Infect. Dis.* **17**, 7 (2011).
2. Abbaszadegan, M., Alum, A., Abbaszadegan, H. & Stout, V. Cell Surface Display of Poliovirus Receptor on Escherichia coli, a Novel Method for Concentrating Viral Particles in Water ▿ . *Appl. Environ. Microbiol.* **77**, 5141–5148 (2011).
3. Liu, L. & Moore, M. D. A Survey of Analytical Techniques for Noroviruses. *Foods* **9**, 318 (2020).

4. Zaczek-Moczydlowska, M. A., Beizaei, A., Dillon, M. & Campbell, K. Current state-of-the-art diagnostics for Norovirus detection: Model approaches for point-of-care analysis. *Trends Food Sci. Technol.* **114**, 684–695 (2021).
5. Pang, X., Lee, B., Chui, L., Preiksaitis, J. K. & Monroe, S. S. Evaluation and Validation of Real-Time Reverse Transcription-PCR Assay Using the LightCycler System for Detection and Quantitation of Norovirus. *J. Clin. Microbiol.* **42**, 4679–4685 (2004).
6. Tian, P., Engelbrektson, A. & Mandrell, R. Two-Log Increase in Sensitivity for Detection of Norovirus in Complex Samples by Concentration with Porcine Gastric Mucin Conjugated to Magnetic Beads. *Appl. Environ. Microbiol.* **74**, 4271–4276 (2008).
7. Giamberardino, A. *et al.* Ultrasensitive Norovirus Detection Using DNA Aptasensor Technology. *PLoS ONE* **8**, e79087 (2013).
8. Almand, E. A., Moore, M. D. & Jaykus, L.-A. Norovirus Binding to Ligands Beyond Histo-Blood Group Antigens. *Front. Microbiol.* **8**, (2017).
9. Almand, E. A., Moore, M. D. & Jaykus, L. A. Characterization of human norovirus binding to gut-Associated bacterial ligands. *BMC Res. Notes* **12**, 1–6 (2019).
10. Matsushita, T., Shirasaki, N., Tatsuki, Y. & Matsui, Y. Investigating norovirus removal by microfiltration, ultrafiltration, and precoagulation-microfiltration processes using recombinant norovirus virus-like particles and real-time immuno-PCR. *Water Res.* **47**, 5819–5827 (2013).

11. Almand, E. A., Moore, M. D., Outlaw, J. & Jaykus, L. A. Human norovirus binding to select bacteria representative of the human gut microbiota. *PLOS ONE* **12**, e0173124 (2017).
12. de Araujo, G. G., Rodrigues, F., Gonçalves, F. L. T. & Galante, D. Survival and ice nucleation activity of Pseudomonas syringae strains exposed to simulated high-altitude atmospheric conditions. *Sci. Rep.* **9**, 7768 (2019).
13. Niu, M. *et al.* Engineering Bacterial Surface Displayed Human Norovirus Capsid Proteins: A Novel System to Explore Interaction Between Norovirus and Ligands. *Front. Microbiol.* **6**, 1448 (2015).
14. Rogers, J. D. *et al.* Identification and characterization of a peptide affinity reagent for detection of noroviruses in clinical samples. *J. Clin. Microbiol.* **51**, 1803–1808 (2013).
15. Hwang, H. J. *et al.* High sensitive and selective electrochemical biosensor: Label-free detection of human norovirus using affinity peptide as molecular binder. *Biosens. Bioelectron.* **87**, 164–170 (2017).
16. Rodríguez-Martínez, L. M. *et al.* Antibody derived peptides for detection of Ebola virus glycoprotein. *PLoS ONE* **10**, 1–17 (2015).
17. Shin, G.-A. & Sobsey, M. D. Inactivation of norovirus by chlorine disinfection of water. *Water Res.* **42**, 4562–4568 (2008).
18. Jothikumar, N. *et al.* Rapid and Sensitive Detection of Noroviruses by Using TaqMan-Based One-Step Reverse Transcription-PCR Assays and Application to Naturally Contaminated Shellfish Samples. *Appl. Environ. Microbiol.* **71**, 1870–1875 (2005).

19. Kageyama, T. *et al.* Broadly Reactive and Highly Sensitive Assay for Norwalk-Like Viruses Based on Real-Time Quantitative Reverse Transcription-PCR. *J. Clin. Microbiol.* **41**, 1548–1557 (2003).

Chapter 3: Evaluation of *Caenorhabditis elegans* for enrichment of and as an *in vivo* infectivity model for noroviruses

3.1 Abstract:

Noroviruses are the leading cause of foodborne illness and fourth leading cause of foodborne death in the United States[1]. One of the biggest roadblocks to the detection and study of human noroviruses has been the historical lack of an effective concentration method for and infectivity model of noroviruses; the latter of which has taken over four decades to achieve[2]. While only two models for human norovirus infectivity have been reported in the past 7 years[3,4], challenges still remain due to lack of consistency, limited throughput, cost constraints and limitations on culture condition manipulations (inclusion of bacteria, bile acids and other conditions)[3,5]. Additionally, the lack of an effective means of specifically concentrating a small number of noroviruses from food samples has limited the ability to detect noroviruses from foods. Here we investigate the potential of *Caenorhabditis elegans* (*C. elegans*) to serve as both a model for *in vivo* norovirus infectivity as well as a reagent for the capture and concentration of infectious noroviruses prior to detection. Our preliminary results indicate that wild type *C. elegans* worms can support the internalization and replication of murine norovirus (a common surrogate for human norovirus). Upon treatment of wild type *C. elegans* worms with MNV, there was a 39-fold increase in the genome equivalent copies after 72 hrs. of incubation. Preliminary studies have also shown that wild type *C. elegans* was able to capture ~65.4% of human norovirus GII.4 after just 1hr of incubation indicating the affinity of *C. elegans* to human norovirus.

Future work to complete this chapter will include further evaluation of *C. elegans* as an infectivity model for noroviruses by evaluating potential factors that influence replication (input virus concentration, virus strain, bacterial microflora, and role of *C. elegans* egg formation in replication). Additional work will also continue evaluation of *C. elegans* to capture and discriminate infectious noroviruses from samples prior to detection.

3.2 Introduction:

Human noroviruses are the leading cause of foodborne illness and fourth leading cause of foodborne death in the U.S. and globally[1]. In addition to a severe public health burden, foodborne noroviruses are estimated to cause $2.7-3.9 billion in economic losses in the U.S. alone every year[6]. Several properties of human noroviruses make them extremely difficult to control, such as: low infectious dose (18-100 particles), ability to survive on environmental surfaces for over a month, high diversity, rapid mutation with the ability to escape long term host immunity, and general resistance to many common disinfectants[7]. In addition, the lack of a favorable infectivity model has hampered the study of human noroviruses, including identification of effective disinfectants, detection of only infectious viral particles, and study of norovirus pathogenesis (including virus-bacteria interactions)[8].

For over four decades, attempts to cultivate human noroviruses *in vitro* were unsuccessful. However, a number of genetically and/or structurally similar cultivable viruses in the *Caliciviridae* family were identified and are still widely used[9]. However, all these related surrogates have limitations including relative stability compared to human norovirus (affecting inactivation study) and the cultivation conditions can be manipulated

(i.e., inclusion of bacteria/foreign reagents or disinfectants because of cytotoxicity). One of the most closely related surrogates to human noroviruses is murine norovirus (MNV)[10]. Murine noroviruses comprise genogroup V of the *Norovirus* genus and had been the only noroviruses able to be cultivated in tissue culture[11]. Others use MNV infection of mice as the most widely and commonly used *in vivo* models. However, these all have significant limitations, such as differences in susceptibility, disease display, cost, throughput, time and expertise required that has limited application in food and agriculturally relevant study[8].

In 2014, Jones et al. published a major report demonstrating the ability to culture human norovirus GII.4 in a B-cell line with the inclusion of bacteria, suggesting enteric bacteria may promote norovirus infection, supporting other previous reports in mice[3]. However, this model has limitations with consistency and the required complexity of the incubation conditions that have limited its application. Subsequently, Ettayebi et al. reported replication of multiple human norovirus genotypes in stem cell-derived human intestinal organoids that did not require bacteria but was enhanced (and required by one genotype) by the inclusion of bile acids[12]. Of the two models, this has been more widely utilized subsequently, but still has limitations that restrict its ability for adoption. Although these two human norovirus tissue culture systems will continue to be extremely valuable for the study of norovirus biology, both have numerous limitations related to consistency, cost, time, manipulability, and ease of adoption[13]. The zebrafish larva model for human norovirus replication has potential limitations related to the amount of input virus required for infection and the output virus produced.[14] Moreover, the limitations in conclusions that can be drawn from host-virus interactions relative to mammalian models

makes this a less attractive model for human norovirus culture. Jones et al. reported the first *in vitro* B-cell based model for murine norovirus. While this B-cell based model for murine norovirus showed some promise, potential limitations like reproducibility, viral titers produced and requirement of coincubation with bacteria exist. Recent reports demonstrate that CD300lf acts as a proteinaceous receptor for murine norovirus[15]. Initially, terminal sialic acid was thought to be a receptor for MNV but when CD300lf was cloned into HeLa cells, MNV was able to jump the species barrier and infect human cells indicating the importance of CD300lf in murine norovirus infection[16].

3.3 Meet the worms:

C. elegans is a small animal with transparent body of ~1 mm with a short lifecycle of ~3 days with lifespan of 3 weeks at 20ºC. *C. elegans* is easy to cultivate, easy to manipulate genes, and many genetically identical progeny (~300 progenies/nematode) can be obtained via hermaphroditic self-fertilization in a short time[17]. Thus, *C. elegans* is an excellent *in vivo* model for high throughput assays with less concern for cytotoxicity seen in mammalian tissue culture cells[18]. Previous studies suggest that *C. elegans* can be easily used for microbiome research, as it has a characteristic microbiome[19–23]. Previous studies confirmed that bacteria fed can easily colonize and form gut microbiome, also known to influence host health[19,23]. Alternatively, the host genetics significantly contribute to microbiome in *C. elegans* as seen in other models. Further, bleach can be used to obtain defined gut microbiota, making *C. elegans* a great model system to investigate host-or norovirus-microbiota interactions.

C. elegans is an emerging model for studying viruses, and establishment of a *C. elegans* norovirus model will greatly enhance the ability to study numerous fundamental and applied aspects related to them. Numerous recent reports exist utilizing *C. elegans* as a model for virus infection: Flock House virus, vesicular stomatitis virus, and members of the *Nodaviridae*[24]. All these viruses are RNA viruses, and members of the *Nodaviridae* are (+) ssRNA viruses that naturally infect the *C. elegans* intestine and display similar capsid organization to noroviruses. Further, interactions and the effect of Orsay virus on the gut microbiome have been reported, further underscoring the potential of *C. elegans* as a model for enteric viral infection[25].

3.4 *C. elegans* expresses fucosylated carbohydrates on its intestinal cells and is an emerging model for nonenveloped viral infection in the intestine:

Human noroviruses have been well documented to bind fucosylated carbohydrates, a number of which have been identified as co-receptors required for infection by numerous norovirus strains[26]. Further, epidemiological and *in vitro* data suggest that the presence and state of fucosyltransferase genes are a major host factor for infection by numerous norovirus strains[27]. *C. elegans* has also been found to express and generate numerous (>15) homologous fucosyltransferases; in particular those associated with those strongly implicated in norovirus infection, α-2 and α-3[28].

One of the major challenges in the investigation of norovirus inactivation is the limitation related to current *in vitro* and *in vivo* models mentioned above. The ability to have an *in vivo* system with the throughput of tissue culture at a lower cost and less susceptibility to cytotoxicity would be of notable value for discovery and evaluation of

different disinfectants and antivirals. Moreover, RT-qPCR is considered the gold standard for norovirus detection in food and environmental samples because of its generally broad reactivity (genogroup-level detection), analytical sensitivity, and throughput[29]. However, RT-qPCR overestimates the presence of infectious virus, as signal is observed from all present genomic RNA—including free RNA and that associated with noninfectious particles[30]. Thus, one method used to better approximate signal from infectious virus is to precede RT-qPCR with a receptor/cell binding step. A rapid, robust, and scalable culture method using *C. elegans* would be an ideal step before RT-qPCR to estimate infectivity and to estimate the efficacy of viral disinfectants.

3.5 Materials and methods:

3.5.1 Generation of CD300lf-expressing *C. elegans* mutants:

The nematode was synchronized using bleach solution and cultured at standard protocol[31]. The EG6699 strain of *C. elegans* was cloned using a donor plasmid containing the pNU936 backbone that contains the CD300lf sequence for insertion into the ttTi5605 site on chromosome II40 using the MosSCI method[32]. This will result in display of CD300lf on the epithelial cell surface of the digestive tract of *C. elegans* and was verified with PCR per NIH standard.

3.5.2 Generation and culture of murine norovirus (MNV)-1:

Murine norovirus-1 was obtained from ATCC (Cat # VR-1937)generated and cultured in RAW 264.7 cells with high glucose DMEM with 10% low endotoxin fetal bovine serum (must be <10 EU/ml) and other components as previously reported[33]. Similarly, MNV was quantified by plaque assay under a previously published protocol paper[34].

3.5.3 Enumeration of murine norovirus using RT-qPCR:

For capture and infectivity assays, viral genomes were extracted using the Qiagen QIAamp Mini Kit for viral RNA extraction. Quantification of MNV by RT-qPCR in capture experiments was conducted using the Fw-ORF1/ORF2, Rv-ORF1/ORF2 primer set with MGB-ORF1/ORF2 probe as previously reported[35], and relative PCR Units were generated using a standard curve.

3.5.4 Evaluation of the ability of MNV-1 to infect *C. elegans* mutant and wildtype worms:

C. elegans wild type and mutants (YPA01 and YPA02) were cultured by Junhyo Cho as described above to a density of 1,000 worms/well in a 12-well plate. Infection with filtered MNV stock at an MOI of 0.1 in S-medium based upon a previously reported assay for infection of the intestine via ingestion of Orsay virus. MNV levels were calculated based on the RT-qPCR protocol mentioned above and Cq values were converted to $\log_{10}$ genome copies.

3.5.5 Evaluation of MNV-1 to infect C. elegans using fluorescent labeled antibody:

Briefly, MNV-1 was cultured as mentioned earlier. Anti MNV-1 antibody (clone 5C4.10 from Millipore Sigma) was labeled with Alexa Fluor 594 (Apex antibody labeling kit, Cat # A10474). The labeled antibody was incubated with MNV-1 for 1hr and then the antibody labeled MNV was incubated with *C. elegans* for 24hrs at room temperature. The *C. elegans* worms were washed with M9 media once before imaging using a fluorescent microscope.

3.6 Preliminary results:

3.6.1 *C. elegans* captures human noroviruses:

We incubated *C. elegans* with norovirus GII.4 Sydney to determine if human noroviruses are captured by *C. elegans*. Results showed promising capture efficiency of human noroviruses by *C. elegans* (Table 4). To follow up, a fluorescently labeled norovirus capsid protein (P domain) was incubated with the wild type worms and visualized under a fluorescent microscope. The worms were able to internalize the labeled P-domain indicating that they are indeed permissive to norovirus binding (Fig 4).

Table 1. C. elegans captures human norovirus

Input Virus Titer (Genomic Copies/Well)	Percent of norovirus captured (%)	
Worms/Well	**1000**	**2000**
10^3	65.4%	42.6%
10^2	57.2%	23.3%
10^1	48.1%	16.2%

Filtered stool samples containing human norovirus GII.4 Sydney were inoculated into C. elegans and incubated at room temperature for one hour with shaking. The supernatant were used for virus quantitation by RT-qPCR and the amount of virus captured were calculated.

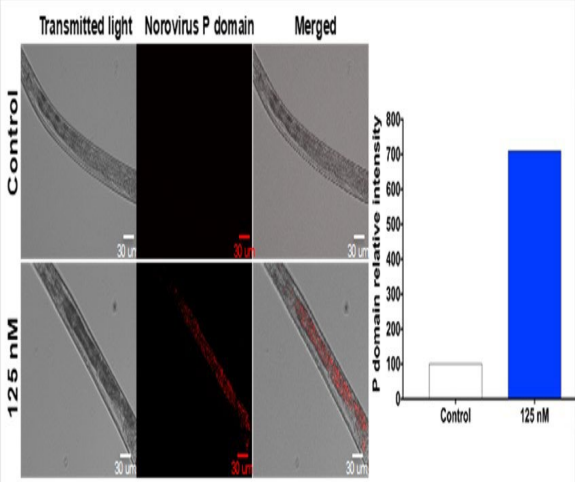

Fig.4. Binding of norovirus capsid protein (P domain) to the intestinal track of C. elegans. *Fluorescence tagged norovirus P domain was treated to C. elegans for 48 hours at 25 °C. After washing, nematodes were anesthetized with NaN_3 and observed with Fluorescent Cell Imager (ZOE, Bio-Rad), excitation at 556nm and emission at 615 nm.*

Junhyo Cho, Minji Kim & Sloane Stoufer 2021

3.6.2 *C. elegans* promotes murine norovirus replication: [4]

We treated murine norovirus with *C. elegans* (wild type and mutants) to determine if any murine norovirus can replicate in *C. elegans*. Our results surprisingly indicate that while the CD300If expressing mutant worms were able to promote MNV replication but also

the wild type worms displayed at least a 1.5-fold increase in log genome copies after 72 hr. incubation (Fig. 5&6)

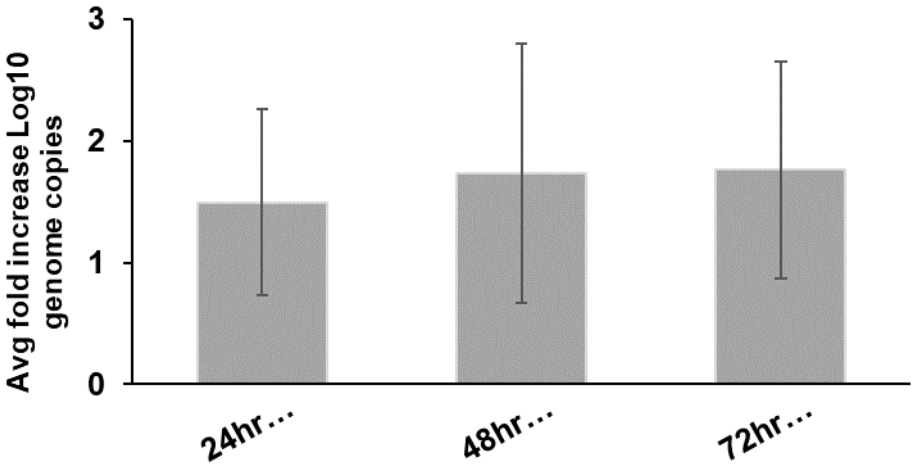

Wild type worms

Figure.5 RT-qPCR was performed following RNA extraction from both the supernatant and worms (following triple wash with distilled water) using MNV specific primers and probe. The Cq values were converted to log genome copies from the standard curve. Error bars indicate standard error from two independent replicates.

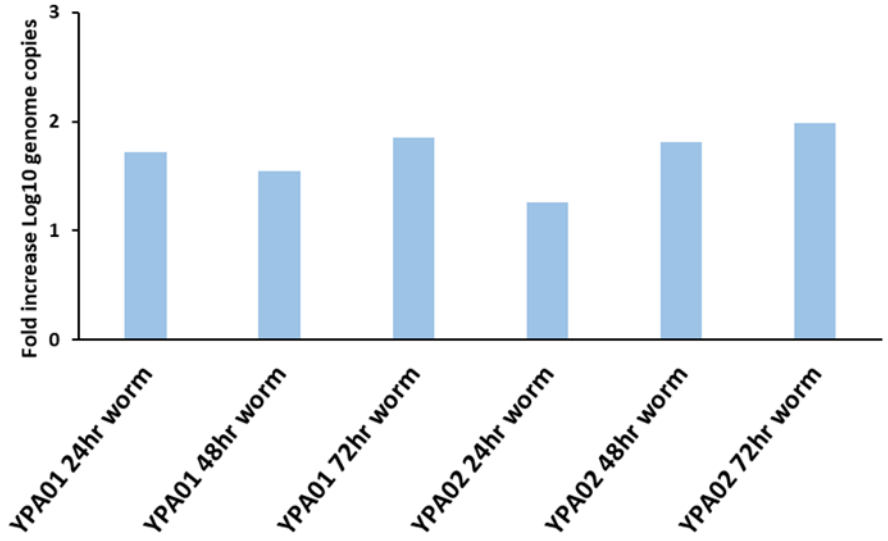

Mutant worms

Figure.6 RT-qPCR was performed following RNA extraction from both the supernatant and worms (following triple wash with distilled water) using MNV specific primers and probe. The Cq values were converted to log10 genome copies from the standard curve. Error bars are not included as this trial was only performed once.

3.6.3 Noroviruses are ingested and bound in the intestinal cells of *C. elegans*:

We were able to still detect RT-qPCR signal after worms were washed three times, suggesting that some virus may have been ingested and internalized. This was confirmed by detecting MNV-1 antibody clone 5C4.10 that was labeled with Alexa Fluor 594 (Ex/Em 590/617, red), in the intestinal cells of *C. elegans* (Fig. 7).

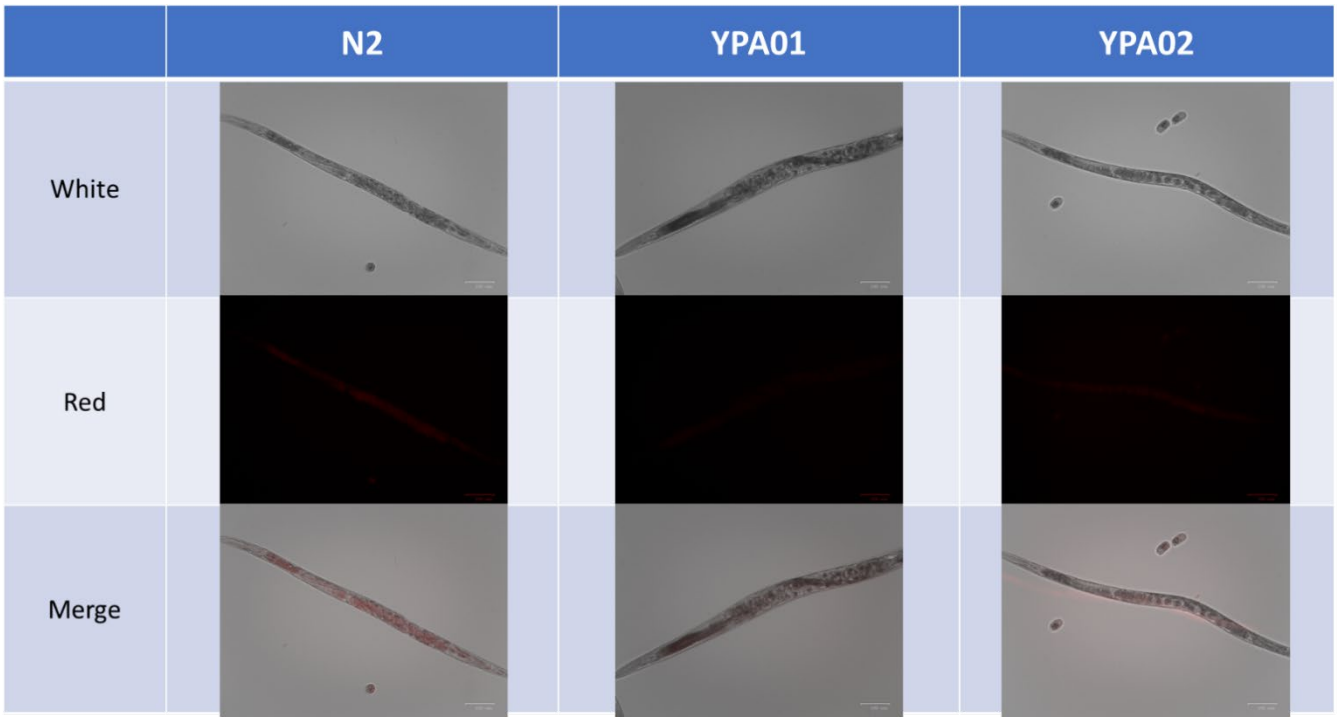

Image courtesy: Junhyo Cho & Minji Kim

Figure.7 Microscopy visualizing ingestion and binding of MNV in *C. elegans*. N2- wild type *C. elegans* worms and YPA01 and YPA02 (mutants expressing CD300If) were incubated with MNV for 24hr and imaged using a fluorescent microscope with light conditions Red: Gain-40, Exposure-1000, Intensity-20, Contrast-10

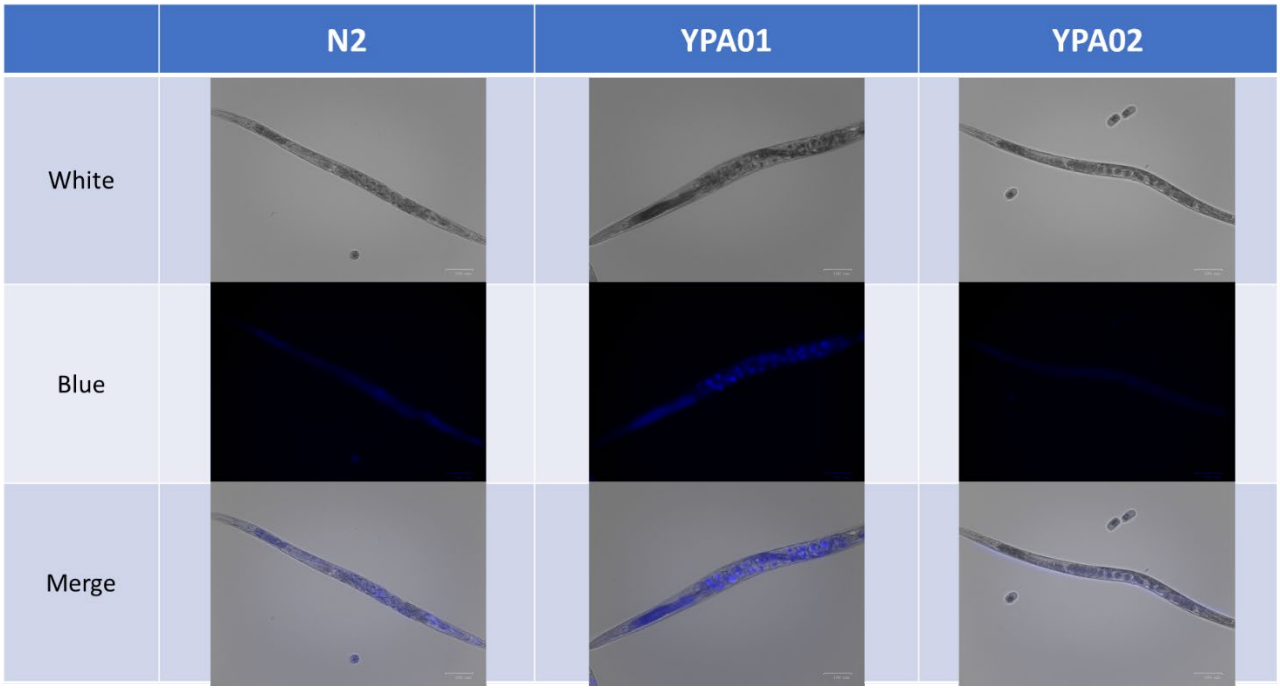

Image courtesy: Junhyo Cho & Minji Kim

Figure.8 Microscopy visualizing ingestion and binding of MNV in *C. elegans*. N2- wild type *C. elegans* worms and YPA01 and YPA02 (mutants expressing CD300If) were incubated with fluorescent antibody labeled MNV for 24hr and imaged using a fluorescent microscope with light conditions Blue: Gain-40, Exposure-300, Intensity-40, Contrast-20

3.7 Discussion and future experiments:

Earlier models of human norovirus replication including the zebrafish larva and human intestinal enteroid model showed 3 log and 1.5 log increase in input virus load after incubation with MNV respectively[13]. The zebrafish larva model had a very high initial virus input (3.4 x 10^6 viral RNA copies of HuNoV) and despite that, the output virus was significantly lower in comparison[14]d. Moreover, the reproducibility and consistency of human norovirus replication in the zebrafish larvae model is under scrutiny. We should also take into consideration that the zebrafish model is not a faithful replication of the human gut environment. On the other hand, the human intestinal enteroid model was able to promote human norovirus GII.4 replication but the cost associated with establishing and maintaining the enteroid model are a major roadblock for large scale adoption of this animal model for routine human norovirus studies. In our current study, we observed internalization and replication of MNV in wild type *C. elegans* as evident from the microscopic images and fold increase in log converted genome copies following RT-qPCR of supernatant and worms following a stringent wash step. While we are unsure of what could have contributed to the MNV capture and replication in wild type worms Given the notable degree of replication seen in the wild type worms, we are currently planning to test the influence of several factors on MNV replication in the wild type while troubleshooting expression of the CD300lf receptor. Specifically, we are interested in evaluating the influence of the following on viral replication: input viral titer, bacterial microflora, worm life stage (egg development), and MNV strain, and presence of bile acid. We also plan on testing the ability of the wild type *C. elegans* to serve as a capture reagent prior to RT-qPCR to better discriminate infectious particles of MNV, subjected to

representative physical (heat) and chemical (bleach) inactivation compared to conventional plaque assay. Lastly, we plan on evaluating the ability of a *C. elegans* to determine infectivity of human noroviruses subjected to inactivation.

3.8 References:

1. Scallan, E. *et al.* Foodborne Illness Acquired in the United States—Major Pathogens. *Emerg. Infect. Dis.* **17**, 7 (2011).
2. Moore, M. D., Goulter, R. M. & Jaykus, L.-A. Human norovirus as a foodborne pathogen: challenges and developments. *Annu. Rev. Food Sci. Technol.* **6**, 411–433 (2015).
3. Jones, M. K. *et al.* Enteric bacteria promote human and mouse norovirus infection of B cells. *Science* **346**, 755–759 (2014).
4. Ettayebi, K. *et al.* Replication of human noroviruses in stem cell-derived human enteroids. *Science* **353**, 1387–1393 (2016).
5. Estes, M. K. *et al.* Human Norovirus Cultivation in Nontransformed Stem Cell-Derived Human Intestinal Enteroid Cultures: Success and Challenges. *Viruses 2019 Vol 11 Page 638* **11**, 638 (2019).
6. Bartsch, S. M., Lopman, B. A., Ozawa, S., Hall, A. J. & Lee, B. Y. Global Economic Burden of Norovirus Gastroenteritis. *PLOS ONE* **11**, e0151219 (2016).
7. Facts about norovirus. *European Centre for Disease Prevention and Control* https://www.ecdc.europa.eu/en/norovirus-infection/facts.
8. Todd, K. V. & Tripp, R. A. Human Norovirus: Experimental Models of Infection. *Viruses* **11**, (2019).

9. Cromeans, T. *et al.* Comprehensive Comparison of Cultivable Norovirus Surrogates in Response to Different Inactivation and Disinfection Treatments. *Appl. Environ. Microbiol.* **80**, 5743–5751 (2014).
10. Hirneisen, K. A. & Kniel, K. E. Comparing Human Norovirus Surrogates: Murine Norovirus and Tulane Virus. *J. Food Prot.* **76**, 139–143 (2013).
11. Na, Z. *et al.* Isolation and Identification of a Murine Norovirus Persistent Infection Strain in China. *Front. Vet. Sci.* **7**, (2020).
12. Ettayebi, K. *et al.* New Insights and Enhanced Human Norovirus Cultivation in Human Intestinal Enteroids. *mSphere* **6**, (2021).
13. Costantini, V. *et al.* Human Norovirus Replication in Human Intestinal Enteroids as Model to Evaluate Virus Inactivation. *Emerg. Infect. Dis.* **24**, 1453–1464 (2018).
14. Van Dycke, J. *et al.* A robust human norovirus replication model in zebrafish larvae. *PLOS Pathog.* **15**, e1008009 (2019).
15. Graziano, V. R. *et al.* CD300lf is the primary physiologic receptor of murine norovirus but not human norovirus. *PLoS Pathog.* **16**, e1008242 (2020).
16. Orchard, R. C. *et al.* Discovery of a proteinaceous cellular receptor for a norovirus. *Science* **353**, 933–936 (2016).
17. From genes to function: the C. elegans genetic toolbox - Boulin - 2012 - WIREs Developmental Biology - Wiley Online Library. https://wires.onlinelibrary.wiley.com/doi/10.1002/wdev.1.
18. O'Reilly, L. P., Luke, C. J., Perlmutter, D. H., Silverman, G. A. & Pak, S. C. C. elegans in high-throughput drug discovery. *Adv. Drug Deliv. Rev.* **0**, 247–253 (2014).

19. Zhang, F. *et al.* Caenorhabditis elegans as a Model for Microbiome Research. *Front. Microbiol.* **8**, (2017).
20. Berg, M. *et al.* Assembly of the Caenorhabditis elegans gut microbiota from diverse soil microbial environments. *ISME J.* **10**, 1998–2009 (2016).
21. Dirksen, P. *et al.* The native microbiome of the nematode Caenorhabditis elegans: gateway to a new host-microbiome model. *BMC Biol.* **14**, 38 (2016).
22. Samuel, B. S., Rowedder, H., Braendle, C., Félix, M.-A. & Ruvkun, G. Caenorhabditis elegans responses to bacteria from its natural habitats. *Proc. Natl. Acad. Sci.* **113**, E3941–E3949 (2016).
23. Han, B. *et al.* Microbial Genetic Composition Tunes Host Longevity. *Cell* **169**, 1249-1262.e13 (2017).
24. Gammon, D. B. Caenorhabditis elegans as an Emerging Model for Virus-Host Interactions. *J. Virol.* **91**, e00509-17 (2017).
25. Casorla-Perez, L. A. *et al.* Orsay Virus Infection of Caenorhabditis elegans Is Modulated by Zinc and Dependent on Lipids. *J. Virol.* **96**, e0121122 (2022).
26. Tenge, V. R. *et al.* Glycan Recognition in Human Norovirus Infections. *Viruses* **13**, 2066 (2021).
27. Hong, X. *et al.* Association of fucosyltransferase 2 gene with norovirus infection: A systematic review and meta-analysis. *Infect. Genet. Evol. J. Mol. Epidemiol. Evol. Genet. Infect. Dis.* **96**, 105091 (2021).
28. Yan, S., Jin, C., Wilson, I. B. H. & Paschinger, K. Comparisons of Caenorhabditis Fucosyltransferase Mutants Reveal a Multiplicity of Isomeric N-Glycan Structures. *J. Proteome Res.* **14**, 5291–5305 (2015).

29. Real time RT-PCR is the gold standard for laboratory diagnosis. *Clinical Laboratory int.* https://clinlabint.com/real-time-rt-pcr-is-the-gold-standard-for-laboratory-diagnosis/ (2020).
30. Dreier, J., Störmer, M., Mäde, D., Burkhardt, S. & Kleesiek, K. Enhanced Reverse Transcription-PCR Assay for Detection of Norovirus Genogroup I. *J. Clin. Microbiol.* **44**, 2714–2720 (2006).
31. Porta-de-la-Riva, M., Fontrodona, L., Villanueva, A. & Cerón, J. Basic Caenorhabditis elegans Methods: Synchronization and Observation. *J. Vis. Exp. JoVE* 4019 (2012) doi:10.3791/4019.
32. About MosSCI. *Modifying the C. elegans genome.* https://wormbuilder.org/old/?page_id=523 (2013).
33. Kitamoto, T. *et al.* Viral Population Changes during Murine Norovirus Propagation in RAW 264.7 Cells. *Front. Microbiol.* **8**, (2017).
34. Gonzalez-Hernandez, M. B., Bragazzi Cunha, J. & Wobus, C. E. Plaque assay for murine norovirus. *J. Vis. Exp. JoVE* e4297 (2012) doi:10.3791/4297.
35. Baert, L. *et al.* Detection of Murine Norovirus 1 by Using Plaque Assay, Transfection Assay, and Real-Time Reverse Transcription-PCR before and after Heat Exposure. *Appl. Environ. Microbiol.* **74**, 543–546 (2008).

Chapter 4: Inactivating SARS-CoV-2 and human norovirus Surrogates on Surfaces Using Engineered Water Nanostructures Incorporated with Nature Derived Antimicrobials

Most of this text is excerpted/modified from:

Vaze, N., Soorneedi, A. R., Moore, M. D., & Demokritou, P. (2022). Inactivating SARS-CoV-2 Surrogates on Surfaces Using Engineered Water Nanostructures Incorporated with Nature Derived Antimicrobials. Nanomaterials, 12(10), 1735.

Huang, R., Vaze, N., Soorneedi, A., Moore, M. D., Luo, Y., Poverenov, E., & Demokritou, P. (2021). A novel antimicrobial technology to enhance food safety and quality of leafy vegetables using engineered water nanostructures. Environmental Science: Nano, 8(2), 514-526.

Huang, R., Vaze, N., Soorneedi, A., Moore, M. D., Xue, Y., Bello, D., & Demokritou, P. (2019). Inactivation of hand hygiene-related pathogens using engineered water nanostructures. ACS Sustainable Chemistry & Engineering, 7(24), 19761-19769.

4.1. Abstract:

Human noroviruses are highly transmissible and have been demonstrated to be transmitted by surfaces and foods[1]. However, many commonly used inactivation agents have been reported to demonstrate less than ideal efficacy against them. Bleach is one of the chemical compounds that has been shown to effectively inactivate human norovirus, but it has limitations in areas and surfaces where it can be applied at necessary concentrations[2]. SARS-CoV-2 has also been suggested to be transmitted through high

touch surfaces and respiratory droplets and continues to exact a significant public health burden in food production/service and community settings. Although many commercial inactivation agents have been demonstrated to be efficacious against coronaviruses, many have potential to leave residues that could be harmful to health and the environment, especially with over-application. Here we report the use of a residue-free, dry ionized spray system for inactivating viruses that effectively can deliver nature-derived compounds (like Lysozyme, Hydrogen peroxide, Citric acid, Lysozyme, Nisin and Triethylene Glycol) for inactivation of viruses deposited on surfaces and foods. Specifically, we evaluated several nature-derived cocktails with EWNS against bacteriophage MS2, a human norovirus surrogate, and human coronavirus 229E. Our results indicate that when the engineered water nanostructure (EWNS) approach was used, there was a 1.4 log reduction in MS2 following just 5 minutes of treatment on stainless-steel, and a reduction of 1.4 log after 15 min when MS2 was deposited on a spinach surface. We were also able to demonstrate inactivation rates of 3.8 logs of HCoV-229E following just 30s of treatment with a Hydrogen peroxide (10% w/v) + Citric acid (1% w/v) + Lysozyme (0.1% w/v) + Nisin (0.0025% w/v) + Triethylene glycol (3% w/v) cocktail with the EWNS system.

4.2. Introduction:

Human norovirus infections make up the bulk of nonbacterial gastroenteritis infections around the world and pose a significant threat to both human health and economy[2]. Fresh produce and surfaces have been implicated in the spread of norovirus infections in food and environmental settings. Hundreds of disinfectants are currently available with a wide array of active ingredients and formulations[3]. The most common among them are

chlorine, quaternary ammonia compounds, alcohols and peroxides[4–6]. Each of these ingredients has its own limitations. For example, while chlorine-based disinfectants are highly efficient against bacteria and viruses, they can damage surfaces following prolonged exposure due to their strong oxidizing properties[7]. QACs and alcohols while not causing significant damage to surfaces are not so efficacious against non-enveloped viruses like the human norovirus[8]. Peroxides on the other hand can denature viral proteins but the efficacy data from published studies is very limited.

Now more than ever, there is an urgent need to develop effective antiviral technologies that can be deployed safely and effectively in different settings. The recent CoVID-19 pandemic has shown us how several industrial sectors have been widely affected. The food industry has been one of the very many major industries that took a hit during the CoVID-19 pandemic. Everything from supply chain disruptions to food production, processing and distribution have suffered immeasurable losses due to the pandemic.

A crucial aspect of reducing transmission of the virus is through environmental disinfection. To this end, a nanotechnology-based antimicrobial platform utilizing engineered water nanostructures (EWNS) was utilized to challenge the bacteriophage MS2 (surrogate for human norovirus) and human coronavirus 229E (HCoV-229E), a surrogate of SARS-CoV-2, on surfaces. The EWNS were synthesized using electrospray and ionization of aqueous solutions of antimicrobials, had a size in the nanoscale, and contained both antimicrobial agents and reactive oxygen species (ROS). Various EWNS were synthesized using single active ingredients (AI) as well as their combinations. The results of EWNS treatment indicate that EWNS produced with a cocktail of active ingredients was able to inactivate 3.8 logs and 1.4 logs of HCoV-229E and MS2, in 30 s

and 5mins of treatment respectively. The delivered dose of antimicrobials to the surface was measured to be in pico to nanograms. These results indicate the efficacy of EWNS technology as a nano-carrier for delivering a minuscule dose of active ingredients while inactivating different viruses (enveloped and non-enveloped).

4.3. Materials and Methods:

4.3.1. Generation of EWNS:

The concept of EWNS generation is illustrated in Figure 9. The main process involved in the generation of EWNS is a combined electrospray-ionization process, detailed in an earlier publication by the group. To expound, a stainless-steel capillary (EWNS emitter) is held vertically, and a funnel-shaped ground electrode assembly is placed directly underneath. The EWNS emitter is connected, at the top, to a container containing the AI solution. This container is connected to an air compressor, which is used to push the liquid flow through the emitter. A high voltage power supply (Spraybase, Cambridge, MA, USA) is utilized to produce the −6.8 kV to be delivered to the emitter. The emitter is held at 4 cm from the ground electrode. The grounded electrode is a disk that sits atop a funnel that is connected to a sampling apparatus that can be used to draw in the EWNS nanodroplets for characterization. During the process of EWNS generation, the applied electric field causes, at the tip of the capillary, the generation of the so-called Taylor cone, and, from the tip of this cone, highly charged nanodroplets, of the aqueous suspension of various AIs, are emitted. This Taylor cone is monitored visually using a camera. The shape and stability of this Taylor cone are monitored with the camera. Once a stable cone is confirmed, the EWNS nanodroplets are then sampled with the apparatus described above, to confirm their generation.

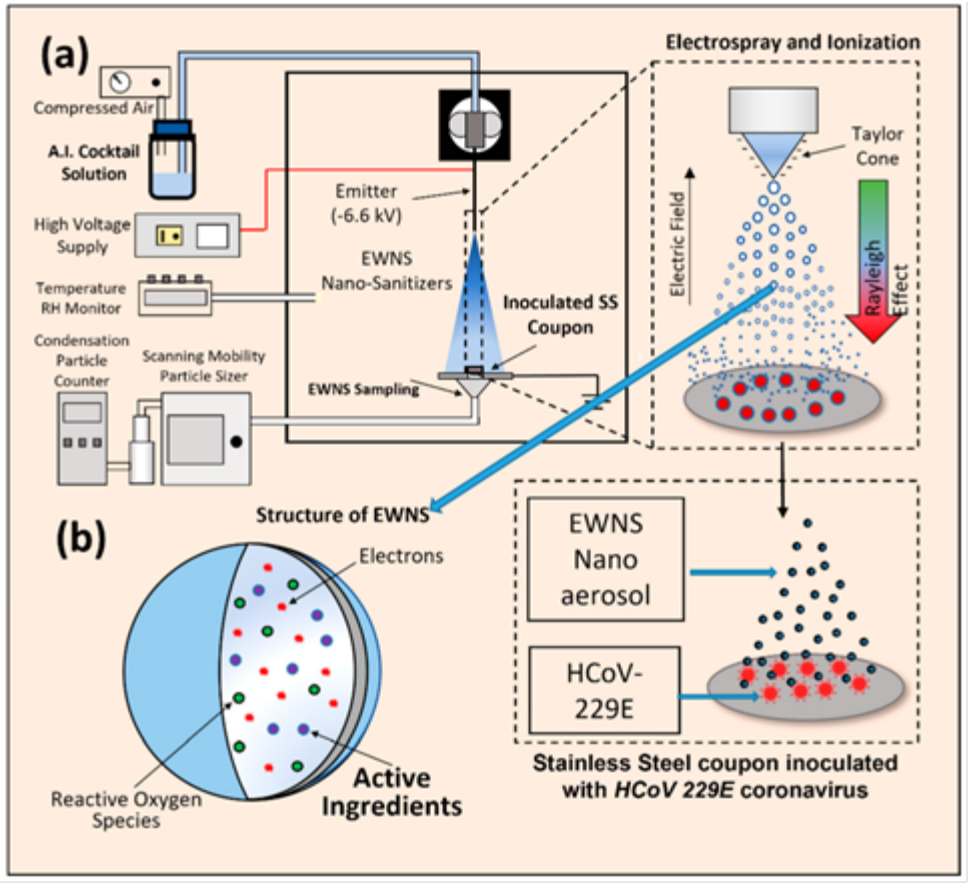

Figure 9. Detailed schematic to represent the generation of EWNS and the treatment of HCoV-229E inoculated surface (a). The structure of an individual EWNS (b) containing the A.I., ROS and charges is also shown[9].

4.3.2. Selection of Antimicrobial Active Ingredients:

From the peroxide class, hydrogen peroxide was chosen, as it is widely used in vapor form as a disinfectant in healthcare settings. An organic acid, citric acid (CA), was chosen as an antimicrobial from nature. CA is found in various citrus fruits and has antibacterial effects. Other natural substances explored were an enzyme (lysozyme) and a peptide (nisin), both currently being researched for their efficacy against bacteria. Lysozyme is found in bodily fluids such as tears, whereas nisin is used frequently in the

food preservation industry[10,11]. Surprisingly, although lysozyme would only primarily be thought to affect bacteria, some reports suggest heat denatured lysozyme may have efficacy against norovirus surrogates[12]. Although not expected to display inherently antiviral activity, nisin was included as it has previously been shown effective in EWNS against bacterial targets and would likely be included in a broader use antimicrobial product applied to combat viruses and bacteria. In addition to these agents that have previously been shown to be effective with EWNS, triethylene glycol (TREG) was evaluated for the first time with the EWNS system. A recent study has shown that atomized TREG is effective in inactivating common nosocomial pathogens[13]. This has made it an attractive AI candidate to be utilized in the EWNS system.

4.3.3. Physicochemical Characterization of EWNS:

The aerosol size and concentration of various EWNS produced was assessed with a Scanning Mobility Particle Sizer (SMPS) (TSI, Shoreview, MN, USA). The SMPS gives a size distribution of the nano-aerosol measured, and the arithmetic mean diameter of each EWNS formulation was obtained using the Aerosol Instrument Manager software (TSI, Shoreview, MN, USA). The nanodroplet concentration of the EWNS was also reported. Ten discreet measurements were performed, each for a duration of 120 s, and the average of the measurements was reported. The total dose of each EWNS treatment was obtained by calculating the mass of the nanodroplets produced during one minute of EWNS generation.

4.3.4. Viral Inoculation, Exposure, and Recovery:

In this study, bacteriophage MS2 (ATCC #15597-B1) and human coronavirus 229E (ATCC® VR-740™) were used. Bacteriophage MS2 stock was generated per ATCC

instructions and stored at −80°C. The bacteriophage MS2 stock (~10^{10} PFU/mL) was diluted 10,000 times with deionized water to a concentration of ~10^6 PFU/mL. HCoV229e was used at a stock concentration of 10^7 PFU/ml. 10 µL of the virus stock suspension (~10^5 PFU/ml) was inoculated as equally sized droplets on the surface of previously sterilized stainless-steel coupons. Spinach was used as a model of leafy vegetables in this study. Fresh spinach was bought from local supermarkets on the day of experiments. The spinach leaves were stored in their original container in a refrigerator at 4 °C with limited light exposure. Intact spinach leaves without obvious bruises were selected and cut into coupons (19 mm in diameter) using a sterile stainless-steel cork borer. The spinach coupons were then disinfected by exposure to ultraviolet light for 15 minutes for each side. The diameter of the stainless-steel coupons was 18.2 mm, and the thickness of the coupon was ~0.5 mm. It is worth noting that the stainless-steel coupon model was selected for the inoculation studies because it is used widely in previous EWNS studies, and its use allows comparison of inactivation data with this study. Furthermore, the stainless-steel coupon, as a model surface, is widely used in assessing antimicrobial efficacy in food safety and beyond. For MS2 study, 100 µL of the inoculum was added on the coupon in 10 droplets (10 µL/droplet). The final inoculation levels of bacteriophage MS2 was 10^5 PFU/coupon, respectively. The inoculated coupons were dried in a biosafety hood and then exposed to various EWNS-based nano sanitizers. To recover the inoculated virus from the coupons, each coupon was placed in a 50 mL centrifuge tube containing 5 mL of tryptic soy broth supplemented with 0.1% glucose, 2 mM CaCl2, and 10 µg/mL thiamine (for bacteriophage MS2) and for HCoV229e, post treatment, 100 µL of DMEM complete growth medium (10% FBS and 1% Penicillin-

Streptomycin) was gently added to the surface of the coupons. The surface was gently rinsed by pipetting the medium up and down. The rinsate was collected and used for preparing serial dilutions of the recovered virus in DMEM complete growth medium. The serially diluted virus suspension was used for setting up a viral plaque assay. Control coupons without EWNS treatment were also included in triplicate in this study.

4.3.5 MS2 Plaque Assay:

The protocol of MS2 plaque assay followed the method described by Su and D'Souza[14].

4.3.6 HCoV-229E Plaque Assay:

Briefly, Huh 7.5 cells were plated in 12-well plates and incubated overnight at 37ºC (5% CO2). The following day, virus suspension (10^7 PFU/mL) is serially diluted in DMEM complete growth medium (10% FBS and 1% Penicillin-Streptomycin). After aspirating the media from each well, 100 ul of virus dilutions were added to each well. The plates are incubated for 1 h at 37ºC with 5% CO2 with gentle rocking every 10 min. Following incubation, a mixture of 2X DMEM and 2.4% Avicel is overlayed on the cells avoiding any air bubbles. The cells along with the virus and Avicel overlay were incubated in a 37ºC incubator (5% CO2) for 4 days. For visualizing plaques after the 4-day incubation, cells were fixed with 5% formaldehyde for 1 h at room temperature. Formaldehyde was aspirated into an appropriate chemical waste container and the cell monolayer was gently rinsed with tap water or PBS. The cells were stained with 2% crystal violet solution for 30–60 min at RT on a shaking platform. The cells were then rinsed with tap water or PBS. We then let the monolayer air dry for 15–20 min inside the biosafety cabinet. The plaques were counted, and the pfu/mL was calculated using the following formula: Plaque count X virus dilution X 10 = PFU/mL sample.

4.3.7 Statistical Analysis:

Each EWNS treatment was performed in triplicate. Each data point represents the calculated arithmetic mean of three replicates. The error bars represent the standard deviation between the three replicates.

4.4 Results and Discussion:

4.4.1Generation and Physicochemical Characterization of EWNS Nano aerosol:

The EWNS were generated according to a well-established method, quoted in detail in the Materials and Methods section and illustrated in Figure 9. A detailed assessment of the incorporation of AIs across various antimicrobial classes into EWNS has been conducted in an earlier study[15]. AIs were chosen to cover a broad range of antimicrobials. The selection logic for these AIs is detailed in the Materials and Methods section. These AIs are detailed in Table 5.

Active Ingredients (AIs) utilized to generate various EWNS.

Active Ingredients (Concentrations)	Size (nm)	Nanodroplet Concentration (#/cc)	Dose Rate (pg/min)
Baseline (Water, No A.I. added)	18.28 ± 1.32	96,189 ± 16,720	NA
Hydrogen peroxide (10% *w/v*)	10.62 ± 2.15	2042 ± 779	0.06 ± 0.02
Citric acid (1% *w/v*)	35.6 ± 1.1	199,578 ± 49,343	23.56 ± 5.83
0.1% Lysozyme (0.1% *w/v*)	20.05 ± 0.61	79,006 ± 28,000	0.17 ± 0.06
0.0025% Nisin (0.0025 *w/v*)	14.3 ± 0.5	701,301 ± 55,276	0.01
3% Triethylene glycol (3% *w/v*)	56.58 ± 8.04	22,769 ± 7987	32.37 ± 11.36
Hydrogen peroxide (10% *w/v*) + Citric acid (1% *w/v*) + Lysozyme (0.1% *w/v*) + Nisin (0.0025% *w/v*) (Cocktail 1)	24.85 ± 3.75	75,409 ± 34,320	33.62 ± 15.30
Hydrogen peroxide (10% *w/v*) + Citric acid (1% *w/v*) + Lysozyme (0.1% *w/v*) + Nisin (0.0025% *w/v*) + Triethylene glycol (3% *w/v*) (Cocktail 2)	42.71 ± 3.36	43,364 ± 18,702	124.67 ± 53.77
Hydrogen peroxide (10% *w/v*) + Citric acid (1% *w/v*) + Nisin (0.0025% *w/v*) + Triethylene glycol (3% *w/v*) (Cocktail 3)	17.76 ± 0.41	63,463 ± 19,586	13.03 ± 4.02

Table 5 Active Ingredients (AIs) utilized to generate various EWNS.

The dose rate was calculated using a number of nanodroplets and is detailed as well[16]. The "baseline" EWNS were synthesized using only water (no antimicrobials) and had a diameter of 18.28 (±1.32) nm. This size is similar to what has been observed in earlier studies[17]. The 10% H_2O_2 produced EWNS with a size of 10.62 (±2.15) nm. Citric acid (CA) produced larger EWNS nanostructures with a diameter of 35.6 (±1.1) nm. This is consistent with earlier studies with EWNS, where CA nanodroplets have been shown to have a larger diameter. Lysozyme and nisin produced EWNS that were smaller in diameter with 20.05 (±0.61) and 14.3 (±0.5) nm, respectively. The largest EWNS created with a single AI was seen with the TREG. The diameter of the TREG EWNS nanodroplet was 56.58 (±8.04) nm. The efficacy of each EWNS in terms of inactivating the virus inoculated on coupons was assessed. For EWNS generated against HCoV-229E with single AIs, the results are summarized in Figure 10. The no exposure (control) shows no decay after 5 min of being inoculated onto the coupons. This is congruous with studies that have indicated the high survivability of HCoV-229E on surfaces over time. HCoV-229E has been shown to stay active on stainless-steel surfaces for up to 5 days. Because of this high survivability, there is a substantial risk of transmission through fomites and inactivating HCoV-229E on surfaces is a challenging task. For the treatment with baseline EWNS produced with water (baseline EWNS), 0.81 (±0.025) log reduction was observed after 1 min and 1 (±0.02) log after 5 min. The inactivation rate observed here is similar to the results obtained with the baseline EWNS against Influenza H1N1/PR/8[18]. For citric acid and lysozyme-produced EWNS nano-sanitizers, the inactivation showed a

linear inactivation curve, with 1.01 (±0.12) and 0.79 (±0.009) logs inactivation at 5 min, respectively. The calculated dose of the citric acid and lysozyme for the 5-min exposure was minuscule, 117.81 (±29.13) and 0.83 (±0.3) picogram, respectively. These results indicate that the incorporation of lysozyme into EWNS leads to efficacious inactivation with a picogram dose. For 1 min of nisin-EWNS treatment led to 0.73 (±0.02) log inactivation. For 5 min treatment, the inactivation was 1.11 (±0.11) logs with the calculated delivered dose of nisin being 0.07 (±0.01) picogram for the 5-min treatment. Nisin has been investigated for its ability to bind with the ACE2 receptor of the coronavirus and its potential to be an anti-coronavirus agent has been proposed. Evidence from this result suggests that EWNS is an effective nano-carrier for the potential use of nisin in this capacity[19]. For the case of EWNS nano-sanitizers produced with 10% H2O2, the inactivation at 1 and 5 min was 1.18 (±0.46) logs and 1.67 (±0.82) logs respectively, with the calculated dose being 0.32 (±0.12) picogram for 5 min treatment. Compared to other AIs evaluated, there is greater variability observed here between the three treatment runs. These results indicate the efficacy of the H_2O_2 EWNS treatment. Recent studies into the efficiency of H_2O_2 against HCoV-229E have shown that, although a bulk application of 0.5% H_2O_2 solution was effective against HCoV-229E, the potential cellular toxicity of the solution needed to be mitigated before *in vivo* application[20]. For skin disinfection, a 3% solution of hydrogen peroxide is commonly used, but it also can have deleterious effects on the skin leading to serious skin issues[21]. The picogram level dose delivered for effective inactivation suggests that the EWNS platform could make H_2O_2 applicable in these settings, where it cannot be applied due to toxicity and safety concerns. It is worth mentioning, however, that the observed large SD for the inactivation produced here is

because the inactivation depends on the dose of the active ingredient delivered to the viral inoculum. As the total dose of each EWNS treatment was obtained by calculating the mass of the nanodroplets produced during one minute of EWNS generation, a large deviation in nanodroplet size as compared to the mean would lead to a large deviation in volume, and thus, mass. Hence, for H_2O_2 as the active ingredient, the generated EWNS nano aerosol has a large deviation in the size distribution of the nanodroplets generated which results in a large deviation in the delivered dose and inactivation efficacy. For TREG, a similar trend of inactivation was observed as H_2O_2 and nisin, with 0.83 (±0.03) log in 1 min and 1.07 (±0.01) log in 5 min of treatment, with the dose of TREG for 5 min exposure being 161.87 (±56.78) picograms.

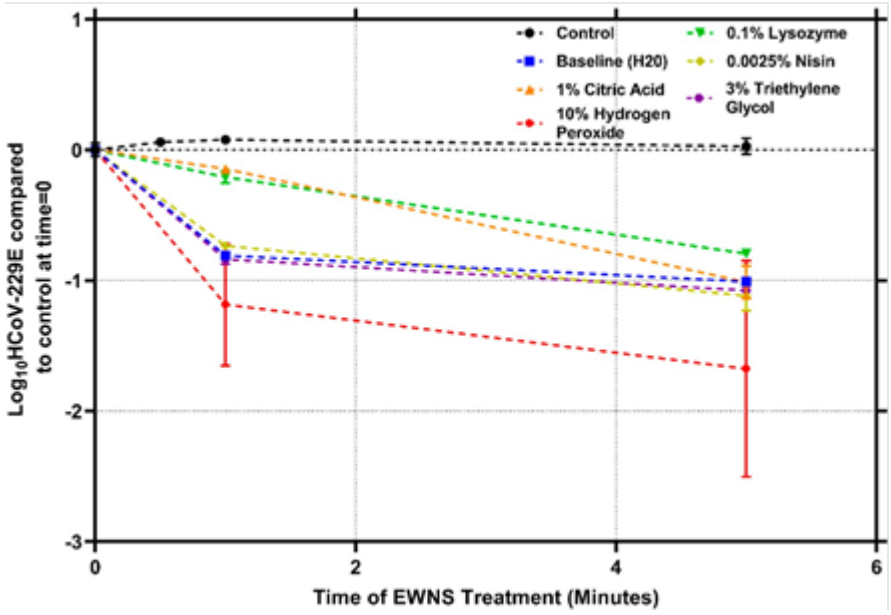

Figure 10. Inactivation of HCoV-229E on surface, after treatment with EWNS. The active ingredient utilized for producing each EWNS for treatment is indicated. Error bars represent standard deviation.

4.4.2 EWNS-based nano-sanitizer inactivation of foodborne pathogen surrogates on spinach and stainless-steel coupons:

EWNS-based nano-sanitizer inactivation of foodborne pathogen surrogates was carried out on spinach with optimal AI cocktail described above. With a 2-minute exposure, there was a 0.5 log reduction in MS2 and as the exposure time increased to 5 minutes, there was a 1.4 log reduction in MS2 compared to the input titer.

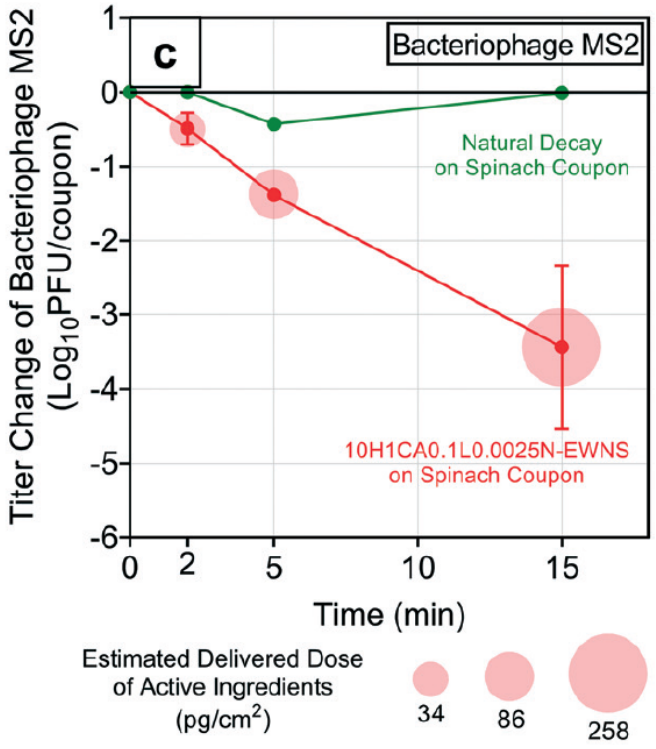

Figure 11 Inactivation of MS2 on spinach from EWNS-based nano-sanitizer synthesized with an AI cocktail (10% (w/v) hydrogen peroxide, 1% (w/v) citric acid, 0.1% (w/v) lysozyme and 0.0025% (w/v) nisin). The coupon was inoculated with ~10^6 PFU/coupon of bacteriophage MS2. The coupons were then exposed to the EWNS-based nano-sanitizers for 0–15 minutes as shown in Fig. 9A. The temperature and relative humidity were ~24°C and ~40%, respectively. The error bar represents 1 standard deviation.

Certain EWNS-based nano sanitizers synthesized with combined AIs that showed promising inactivation results with *E. coli* were chosen to challenge bacteriophage MS2 on a stainless-steel coupon[22]. Fig 12 summarizes the inactivation of bacteriophage MS2 with the EWNS-based nano sanitizer synthesized with a combination of 10% hydrogen peroxide, 1% citric acid, 0.1%, lysozyme, and 0.0025% nisin. Results show a 2.0 log reduction in 0.5 min, and the reduction was significantly higher ($P < 0.05$) than the natural decay. It is worth noting that all four AIs used in this EWNS-based nano sanitizers are FDA Generally Recognized as Safe (GRAS) substances.

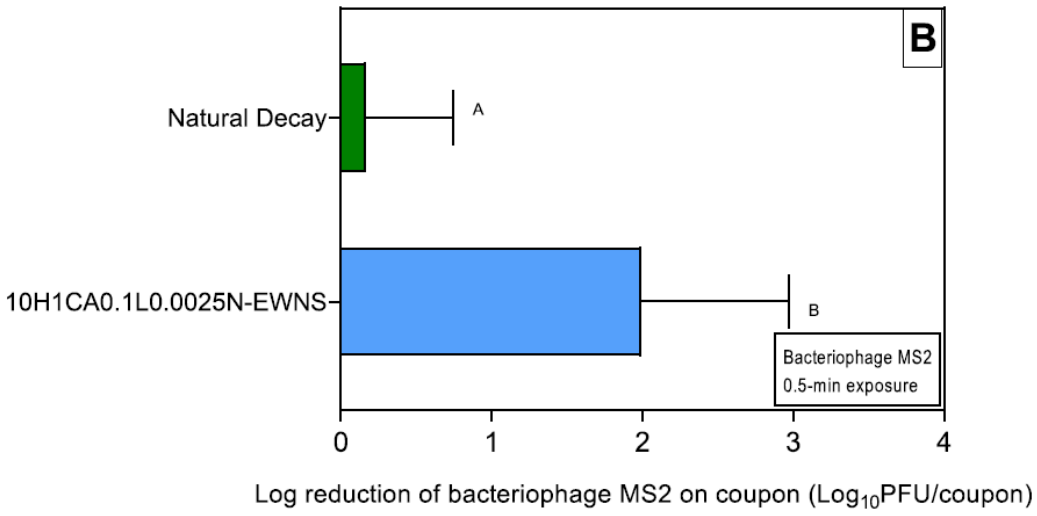

Figure 12. Inactivation of bacteriophage MS2. MS2 was inoculated on stainless-steel coupon and exposed to EWNS based nano sanitizers synthesized with various combined AIs. The coupon was inoculated with ~10^5 PFU/coupon of bacteriophage MS2 and exposed to different EWNS based nano sanitizers for 0.5 min in an exposure chamber as shown in Figure 9. The chamber temperature and relative humidity were ~24°C and ~40%, respectively. The error bar represents 1 standard deviation. Data labeled with the same uppercase letter are not significantly ($P > 0.05$) different from each other.

In summary, the EWNS nano-sanitizers produced with various AIs were able to significantly inactivate HCoV-229E and MS2 on a surface by delivering only minuscule levels of AIs. At 5 min of treatment, no significant difference was observed for all five AIs evaluated. H_2O_2 produced the highest inactivation level. H_2O_2, TREG, and nisin produced a biphasic inactivation, which has been observed in many earlier studies with antimicrobial efficacy testing[23]. When compared to the baseline EWNS, the results were not significantly improved after the addition of individual AIs. Another observation is the fact that dose values were higher for AIs that produced larger EWNS nanodroplets, namely citric acid, and TREG.

Earlier studies with AI-based EWNS have shown that these cocktail EWNS nanodroplets significantly increase the inactivation efficacy, as compared to single AIs due to synergistic effects. For example, EWNS produced with a cocktail of 1% H_2O_2 and 1% CA were utilized to inactivate *E. coli* on surfaces and the results of the study indicated that the efficacy rate of the cocktail was higher than that of the individual active ingredients combined[24]. In another study conducted by the authors for assessing the efficacy of EWNS against pathogens relevant to hand hygiene, this concept was further expanded with more AIs and their combinations were studied. A cocktail (cocktail 1) was developed, containing 10% H_2O_2, 1% CA, 0.1% lysozyme, and 0.0025% nisin, and it was found to have produced a significant reduction in the concentration of non-enveloped phage MS2[17].

The same cocktail used in the hand hygiene study was utilized in this study to produce EWNS nano-sanitizers and its efficacy against the HCoV-229E was assessed (cocktail 1). The results of the inactivation produced are shown in Figure 13. The EWNS produced by

this cocktail were found to have an average diameter size of 24.85 (±3.75) nm. Their inactivation observed for 30 s and 1 min was 0.78 (±0.017) and 0.92 (±0.012) logs. However, at 5 min treatment, complete inactivation, which corresponded to 3.8 logs reduction, was observed. The calculated dose delivered to the viral inoculum for 5 min exposure was 168.09 (±76.50) picograms. These results demonstrate the efficacy of the cocktail EWNS to inactivate HCoV-229E and MS2, with a minuscule dose of the antiviral active ingredients utilized. The picogram dosage also indicates the precisely targeted delivery of the active ingredients to the viral particles.

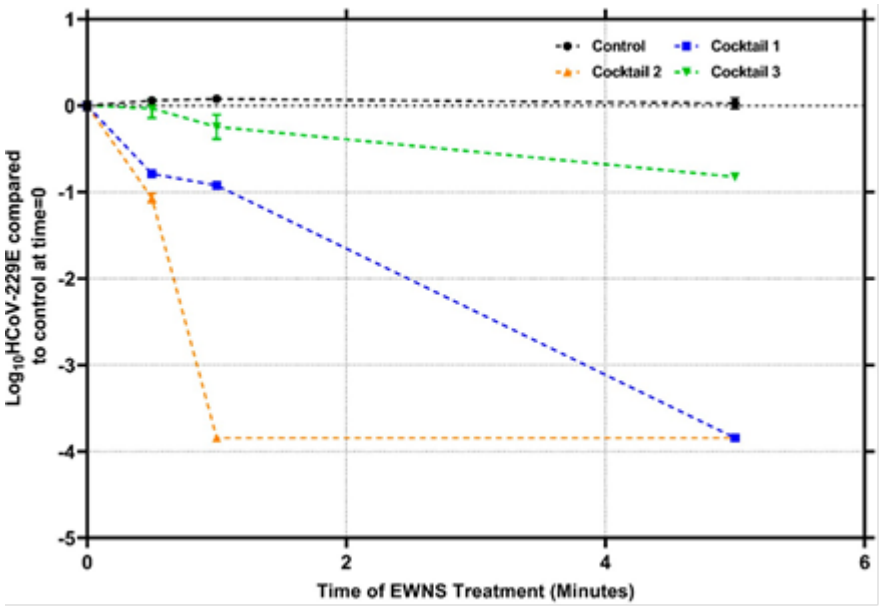

Figure 13. Inactivation of HCoV-229E on surface, after treatment with EWNS. The active ingredient cocktail utilized for producing each EWNS for treatment is indicated. Error bars represent standard deviation.

Furthermore, triethylene glycol (TREG), was added to the cocktail to further assess antiviral efficacy against HCoV-229E, the AI cocktail (cocktail 2) which contains 10% H_2O_2, 1% CA, 0.1% lysozyme, and 0.0025% nisin and 3% TREG was used to generate

EWNS nano-sanitizers. The size measurement shows that these nanodroplets were 42.71 (±3.36) nm in average size. This indicates that the addition of TREG led to an increase in the size of the EWNS produced. This would correspond with the observation that TREG as a single AI, produced the largest EWNS nanodroplet observed in this study at 56.58 (±8.04) nm. More interestingly, the addition to the AI cocktail of TREG resulted in an increase in the antiviral efficacy of the generated EWNS nano-sanitizers. Here, 30s of exposure led to a 1.06 (±0.05) logs reduction of HCoV-229E. For 1 min treatment, complete inactivation was observed, with a 3.8 logs reduction. Further timepoint was assessed at 5 min of treatment. The 3.8 logs reduction was also observed for 5 min. These results indicate an increase in the inactivation efficacy after the addition of TREG. The calculated dose delivered to the viral inoculum for complete inactivation in 1 min of exposure was 124.67 (±53.77) picograms. Another cocktail, containing only 10% H_2O_2, 1% CA, 0.0025% nisin, and 3% TREG was used, without any lysozyme added (cocktail 3). For this cocktail, the size characterization indicated the generation of a smaller nanodroplet than the other two cocktails utilized, with a 17.76 (±0.41) nm size. This is interesting as it shows the influence of lysozyme on the size of the nanodroplets produced. This new cocktail of EWNS nanodroplets was challenged with HCoV-229E. The results showed only a 0.24 (±0.14) logs reduction after 1 min treatment, which increased to 0.82 (±0.046) logs for 5 min of treatment. The total dose of the EWNS to the viral inoculum was 65.13 (±20.10) picogram.

The EWNS generation process involves only water and minuscule amounts of active ingredients utilized with no chemical residues or by-products left behind. Our previous publications address this issue in great detail[24]. It is worth emphasizing that the active

ingredients utilized and delivered using the EWNS nanocarrier platform are nontoxic and nature-derived, and only minuscule amounts are delivered (nanogram levels). It is also worth noting that although the EWNS technology has been shown to produce significant inactivation in the viral inoculum, there are, however, certain limitations of the methodology utilized. The HCoV-229E virus was inoculated onto the coupons in a salt-rich solution (4% FBS + DMEM). This makes it more challenging for the EWNS technology to reach the viral cells amidst the salt deposits, reducing its efficacy of inactivation. There is also a limitation to the recovery of exposed inoculum, however, the authors have attempted to maximize the recovery to obtain a more accurate picture of the EWNS' effect on the virus. In addition, the inactivation results are based on surface inoculation rather than the virus suspended in the air. Future studies will focus on the ability of the EWNS nano aerosol to interact with the virus in the air and provide efficient inactivation.

4.5 Conclusions:

In summary, in this study, we have evaluated the SARS-CoV-2 and human norovirus surrogate antiviral efficacy of the EWNS platform using antimicrobials and their mixtures. The results with the AI cocktails have indicated the efficacy of this platform to inactivate HCoV-229E and MS2 on different surfaces. Compared to conventional application practices for the AIs utilized in this study, the EWNS nano-carrier platform is advantageous, as it requires minuscule amounts of AIs for effective inactivation and the delivery is performed via aerosol. The targeted and precise delivery of the nanodroplets makes this technology an alternative to conventional (wet) treatments. Further research

into the application of EWNS for air disinfection is warranted given the promising data on surface inactivation.

4.6 References:

1. Karst, S. M. Pathogenesis of Noroviruses, Emerging RNA Viruses. *Viruses* **2**, 748–781 (2010).
2. Burden of Norovirus Illness in the U.S. | CDC. https://www.cdc.gov/norovirus/trends-outbreaks/burden-US.html.
3. Sato, J. *et al.* Effects of disinfectants against norovirus virus-like particles predict norovirus inactivation. *Microbiol. Immunol.* **60**, 609–616 (2016).
4. Gobeil, A., Maherani, B. & Lacroix, M. Norovirus elimination on the surface of fresh foods. *Crit. Rev. Food Sci. Nutr.* **62**, 1822–1837 (2022).
5. Soorneedi, A. R. & Moore, M. D. *Recent Developments in Norovirus Interactions with Bacteria*. *https://www.sciencedirect.com/science/article/pii/S221479932200128X* (Elsevier, 2022).
6. Faircloth, J. *et al.* The Efficacy of Commercial Surface Sanitizers against Norovirus on Formica Surfaces with and without Inclusion of a Wiping Step. *Appl. Environ. Microbiol.* **88**, e00807-22 (2022).
7. Gallandat, K., Wolfe, M. K. & Lantagne, D. Surface Cleaning and Disinfection: Efficacy Assessment of Four Chlorine Types Using Escherichia coli and the Ebola Surrogate Phi6. *Environ. Sci. Technol.* **51**, 4624–4631 (2017).
8. A critical review on the survival and elimination of norovirus in food and on food contact surfaces. *Food Standards Agency*

https://www.food.gov.uk/research/foodborne-disease/a-critical-review-on-the-survival-and-elimination-of-norovirus-in-food-and-on-food-contact-surfaces.

9. Vaze, N., Soorneedi, A. R., Moore, M. D. & Demokritou, P. Inactivating SARS-CoV-2 Surrogates on Surfaces Using Engineered Water Nanostructures Incorporated with Nature Derived Antimicrobials. *Nanomaterials* **12**, 1735 (2022).
10. Hughey, V. L., Wilger, P. A. & Johnson, E. A. Antibacterial activity of hen egg white lysozyme against Listeria monocytogenes Scott A in foods. *Appl. Environ. Microbiol.* **55**, 631–638 (1989).
11. Prince, A. *et al.* Lipid-II Independent Antimicrobial Mechanism of Nisin Depends On Its Crowding And Degree Of Oligomerization. *Sci. Rep.* **6**, 37908 (2016).
12. Takahashi, H. *et al.* Heat-Denatured Lysozyme Inactivates Murine Norovirus as a Surrogate Human Norovirus. *Sci. Rep.* **5**, 11819 (2015).
13. Kumaraswamy, M. *et al.* Decontaminating surfaces with atomized disinfectants generated by a novel thickness-mode lithium niobate device. *Appl. Microbiol. Biotechnol.* **102**, 6459–6467 (2018).
14. Su, X., Sangster, M. Y. & D'Souza, D. H. Time-dependent effects of pomegranate juice and pomegranate polyphenols on foodborne viral reduction. *Foodborne Pathog. Dis.* **8**, 1177–1183 (2011).
15. Vaze, N. *et al.* An integrated electrolysis – electrospray – ionization antimicrobial platform using Engineered Water Nanostructures (EWNS) for food safety applications. *Food Control* **85**, 151–160 (2018).

16. Pyrgiotakis, G. *et al.* Optimization of a nanotechnology based antimicrobial platform for food safety applications using Engineered Water Nanostructures (EWNS). *Sci. Rep.* **6**, 21073 (2016).
17. Huang, R. *et al.* Inactivation of Hand Hygiene-Related Pathogens Using Engineered Water Nanostructures. *ACS Sustain. Chem. Eng.* **7**, 19761–19769 (2019).
18. Vaze, N. *et al.* Inactivation of common hospital acquired pathogens on surfaces and in air utilizing engineered water nanostructures (EWNS) based nano-sanitizers. *Nanomedicine Nanotechnol. Biol. Med.* **18**, 234–242 (2019).
19. Bhattacharya, R., Gupta, A. M., Mitra, S., Mandal, S. & Biswas, S. R. A natural food preservative peptide nisin can interact with the SARS-CoV-2 spike protein receptor human ACE2. *Virology* **552**, 107–111 (2021).
20. Omidbakhsh, N. & Sattar, S. A. Broad-spectrum microbicidal activity, toxicologic assessment, and materials compatibility of a new generation of accelerated hydrogen peroxide-based environmental surface disinfectant. *Am. J. Infect. Control* **34**, 251–257 (2006).
21. Wilson, J. R., Mills, J. G., Prather, I. D. & Dimitrijevich, S. D. A toxicity index of skin and wound cleansers used on in vitro fibroblasts and keratinocytes. *Adv. Skin Wound Care* **18**, 373–378 (2005).
22. Huang, R. *et al.* A novel antimicrobial technology to enhance food safety and quality of leafy vegetables using engineered water nanostructures. *Environ. Sci. Nano* **8**, 514–526 (2021).

23. Vollenbroich, D., Ozel, M., Vater, J., Kamp, R. M. & Pauli, G. Mechanism of inactivation of enveloped viruses by the biosurfactant surfactin from Bacillus subtilis. *Biol. J. Int. Assoc. Biol. Stand.* **25**, 289–297 (1997).

24. Vaze, N. *et al.* A nano-carrier platform for the targeted delivery of nature-inspired antimicrobials using Engineered Water Nanostructures for food safety applications. *Food Control* **96**, 365–374 (2019).

Chapter 5: Assessment of SARS-CoV-2 surrogate inactivation on surfaces and in air using UV and blue light-based intervention technologies.

Most of this text is excerpted/modified from:

Singh, D., Soorneedi, A., Vaze, N., Domitrovic, R., Sharp, F., Lindsey, D., & Demokritou, P. (2022). Assessment of SARS-CoV-2 surrogate inactivation on surfaces and in air using UV and blue light-based intervention technologies. Journal of the Air & Waste Management Association, (just accepted).

5.1 Abstract:

The COVID-19 pandemic continues to disrupt food production and service operations and has created an urgent need to utilize existing and develop new intervention technologies for SARS-CoV-2 and other viruses' inactivation on surfaces and in the air. Ultraviolet (UV) technology has been shown to be an effective antimicrobial intervention. Here a study was conducted to determine the efficacy of commercially available UV and blue light-based devices for inactivating HCoV-229E, a surrogate of SARS-CoV-2. The results indicate that two UV devices designed for surface disinfection, with doses of 8.07 μJ/cm^2 for the 254 nm device and 20.61 μJ/cm^2 for the 275 nm device, were efficient in inactivating 4.94 logs of surface inoculated HCoV-229E. Additionally, a 222 nm UV device with intended ceiling-based operation was effective in inactivating 1.7 logs of the virus inoculated on surface, with a dose of 6 mJ/cm^2. A ceiling-based device designed to emit blue light at 405 nm was found to produce 89% reduction in HCoV-229E inoculated on a surface for a dose of 78 J/cm^2. Finally, the UV based 222 nm

device was found to produce a 90% reduction in the concentration of airborne HCoV-229E, at a 55 μJ/cm^2 dose. While noroviruses do not typically transmit through air, light-based interventions could still be potentially used for their inactivation on surfaces and in air. These results are indicative of the great potential of using UV based technology for the control of potential airborne and foodborne pathogens.

5.2 Introduction:

The recent coronavirus disease-19 (COVID-19) pandemic, caused by the sudden acute respiratory syndrome-coronavirus-2 (SARS-CoV-2) has highlighted the problem of rapid global spread of viral diseases. According to the CDC's COVID tracker, there have been more than 80 million people infected with SARS-CoV-2 in the United States, with more than one million deaths[1]. Susceptible people such as the elderly and even children can be infected and develop serious diseases[2]. The development of multiple vaccines has helped ease the disease burden on the U.S. economy and health care system, with restrictions being eased and case numbers reducing. However, the emergence of various mutant strains of SARS-CoV-2 and the lower-than-expected vaccination numbers due to vaccine hesitancy, have led to the recurrence of disease outbreaks. Moreover, recent reports from UK and China have also pointed to the possibility of underreporting of various other diseases during the pandemic. Significant among such diseases that went unchecked during the peak of the pandemic and subsequent easing of restrictions is human norovirus. The increase in norovirus outbreaks during the pandemic can be partially attributed to decreased surveillance and testing for possible endemic diseases as many nations were under strict lockdown that led to cases being underreported. Surprisingly, after the CoVID-19 restrictions were relaxed in the UK, there was a sustained increase in incidence of NoV

outbreaks in different parts of the country[3]. A similar pattern was also observed in China after the pandemic restrictions were relaxed[4]. As per the Public Health England's report, NoV outbreaks during and after the pandemic have exceeded the previous 5 seasons' average by 35%[5]. Among the outbreaks reported, 98% were norovirus related.

The current limitations of the vaccination approach for SARS-CoV-2 and limited treatment options available for norovirus infections underscore the need to approach the problem from another angle, by minimizing virus transmission using effective environmental intervention approaches including filtration and use of other emerging antimicrobial platforms[6,7,7–11].

To this effect, Ultraviolet (UV) light technology for disinfection purposes, also known as GUV (germicidal UV) has been utilized for sterilizing medical equipment, indoor microenvironments, as well as in the food and the water industry to inactivate microorganisms. UV acts primarily by producing DNA damage that the cell cannot overcome[12,13]. UV can also induce intracellular Reactive Oxygen Species[14], which have deleterious effects on the cell. The several types of UV utilized are Mercury-based lamps, light-emitting diodes (UV-C LED) and pulsed-xenon lamps that emit UV light across the entire UV spectrum with a peak emission near 230 nm[15]. These UV systems have been shown to be effective against pathogens both on surfaces and in air[16].

There has been a renewed focus on the applicability of UV technology for inactivating coronaviruses, and specifically the SARS-CoV-2. An earlier study detailed the use of 254 nm UV source for the inactivation of the SARS-CoV-1 virus in culture with complete inactivation after 7 minutes of exposure[13]. Since the beginning of the pandemic, there have been a few studies regarding SARS-CoV-2 susceptibility to UV. In one study, pulsed

xenon UV technology was shown to be effective in inactivating the SARS-CoV-2 virus inoculated on N95 masks by greater than 4 logs, after 5 minutes of exposure[16]. Another study reported 6 log reduction in SARS-CoV-2 in suspension by UVC with a 1 J/cm^2 dose[17]. UV-C has been utilized by a few groups for efficacy testing against SARS-CoV-2[18,19]. For UV-LED, a 3-log reduction was reported at 280 nm wavelength after 3mJ/cm^2 dose[20].

However, a 2021 review shows that most of the studies for determining the efficacy of UV and light emitting systems against coronaviruses utilize the virus in suspension and do not consider real world modalities of transmission, especially aerosol transmission[21]. One of the few studies of such nature that have been conducted, indicates a strong effect of UV, especially 222nm UV-C against coronaviruses[22]. Apart from the UV, short wavelength visible light with a spectrum from 380 to 500 nm that includes violet, indigo, blue, and some blue-green light systems, have also been used for disinfection purposes. More specifically, short wavelength visible light at 405 nm has been shown to inactivate pathogens such as *Pseudomonas aeruginosa* and Staphylococcus aureus, achieving as much as 95.1% and nearly 90% inactivation, respectively, with the microbes inoculated onto agar[23]. An LED light array producing 405 nm was used to inactivate *E. coli* in solution, resulting in 0.4 log reduction by a dose of 117 J/cm^2 [24]. However, there is a sparsity of research on the application of blue light technology for specifically antiviral purposes. To this effect, the present study was carried out, to assess the efficacy of four commercially available UV and blue light-based devices, for inactivating a surrogate of SARS-CoV-2 coronavirus on surfaces and in air. The specifications of the devices are detailed in the methods section. As the first tier of evaluation of device efficacy, all four

devices were tested and their ability to inactivate SARS-CoV-2 surrogate inoculated on a surface was assessed.

Having thus established the inactivation potential of the devices, as the second step, the ceiling mounted devices that were efficient in inactivating the virus on surfaces were assessed in terms of air disinfection. The surrogate of SARS-CoV-2 used in this study was human coronavirus 229E (HCoV-229E)[25]. Although an alphacoronavirus and not a beta coronavirus like SARS-CoV-2, HCoV-229E is one of the other coronaviruses known to cause disease in humans and has been one of the most extensively utilized as a surrogate for study of disinfection[26–28]. The virus was challenged with UV and light-based technologies on surfaces and in air, with the results being interpreted as validating the applicability of the tested devices.

5.3 Materials and Methods:

5.3.1 Description of Devices Tested:

The description of devices tested in this study is summarized in Table 1.

Device A: This is a rectangular device, handheld device intended for surface sterilization. The device contains a linear UV source of 53.5 cm length, with the low-pressure mercury lamp producing UV-C light with a peak at 254 nm. The device has a wattage rating of 55W. The device has a handle with which it can be maneuvered over a surface.

Device B: This is also a handheld device. At the center of the device, there are 12 LED sources, placed in a linear fashion. The device has a wattage rating of 30W, producing UV-C light with a peak at 275 nm. A handle is utilized to guide the device over surfaces.

Device C: This is a disc shaped device with 7.2 inches diameter, with a 2 inch by 2-inch

krypton chloride (KrCl) excimer lamp. The device is rated 15W with a 12-volt DC input. The UV unit produces UVC with a peak at 222nm wavelength. This is a ceiling-mounted device, intended to be installed at a height of 8-11 feet. The major application of this device is for air disinfection,

Device D: This is a ceiling-mounted LED blue light-based device. It has a 6-inch diameter light, producing light in dual modality (Blue/White). Here, in this study, the blue light, produced at a peak wavelength of 405 nm was used. The power consumption of the device is 38W.

5.3.2 Viral Strain:

Human coronavirus 229E (HCoV-229E) was used in the inactivation experiments. HCoV-229E is a member of the genus *Alphacoronavirus* and is one of the globally prevalent coronaviruses, a group that includes SARS-CoV-2, which is a beta coronavirus. HCoV-229E was acquired from ATCC (Strain no. VR-740, American type culture collection, Manassas VA). Viral aliquots of 10^7 pfu/mL were made and stored at -80°C. A HCoV-229E viral plaque assay was developed for the quantification of the virus in experimental samples.

5.3.3 HCoV-229E Plaque Assay:

The Huh 7.5 cell line (provided courtesy of B. Lindenbach, Yale School of Medicine, New Haven, CT) was used in the viral quantification plaque assay[29]. The Huh 7.5 cells were plated in 12-well plates and incubated overnight at 37°C (5% CO2). The following day, i.e., the day of the experiment, after aspirating the media from each well, 100 µL of virus treatment and control samples were added to each well. The plates were incubated for 1 h at 37°C 5% CO_2 with gentle rocking every 10 minutes. Following incubation, a mixture

of 2X DMEM (Dulbecco's Modified Eagle Medium) and 2.4% Avicel (microcrystalline cellulose powder) was overlain on the cells to avoid any air bubbles. The cells were then incubated at 33°C (5% CO2) for 4 days. For visualizing plaques after the incubation, cells were fixed with 5% formaldehyde for 1 hour at room temperature. After removing the formaldehyde, the cells were stained with a 2% crystal violet solution. The plaques were counted, and the pfu/mL was calculated using the following formula: Plaque count X virus dilution factor X 10 = pfu/mL sample.

5.3.4 Experimental Setup for Inactivation of HCoV-229E on Surface:

Figure 1 shows the experimental setup used in the study. The entire experiment was conducted inside a class II A2 biosafety cabinet. The device being evaluated was held above the surface of the cabinet floor, at a predetermined height. For the two handheld devices, this was one inch, which is the expected distance at which these devices would be operated in their intended operation. For the ceiling-based devices, ideally the devices would be installed at a height of 8-11 feet. However, due to the necessity of these experiments needing to be conducted inside a biosafety cabinet, a height of eight inches was chosen as the height at which device could feasibly be held above the surface of the cabinet floor.

As shown in Figure 1, each individual device was held above the virus-inoculated surface (circular stainless-steel coupon, 1.82 cm diameter). The device was turned on and the appropriate UV/light meter was placed directly underneath the location of the exposure coupons. For all four devices, the measurement of intensity was performed at the peak wavelength of the device. For UV measurement, an X1-5 optometer (Gigahertz-Optik, Amesbury MA) was utilized. For the measurement of blue light, the CSS-45 remote

spectral detector (Gigahertz-Optik, Amesbury MA) was used. The UV/blue light irradiance measurement was conducted in triplicate and averaged. The measurement devices utilized were calibrated by the manufacturer against the appropriate standards and verified before operation. A treatment coupon was then placed at the treatment spot, and treatment was conducted for the specific timepoint. The treatment timepoints were chosen according to the intended application of the devices being assessed. For the two handheld devices, device A and device B, short time points of 1, 3, and 10 seconds were selected. For the celling-based device C, intermediate timepoints were chosen, 30 seconds, 1 minute and 5 minutes. For the blue light-based device D, the longer time points chosen were 1,5 and 60 minutes.

5.3.5 Surface Inoculation and Recovery of HCoV-229E:

10 µL of the 229E of the concentration 10^7 pfu/mL, was added to the center of a stainless-steel coupon (1.82 cm diameter) as the inoculum (10^5 pfu on each coupon) and spread gently across the face of the coupon, as shown in Figure 1. The coupons were allowed to dry and then utilized for either UV treatment or held as control untreated samples. Post treatment, each coupon was added to a petri dish. 100 µL DMEM was gently pipetted onto the surface of the coupon. Once the layer of DMEM covered the entire coupon surface, gentle pipetting action was performed to remove the solution from the coupon, thus recovering the viral inoculum.

5.3.6 Experimental Setup for Inactivation of HCoV-229E in Air:

A ‘single-pass’ experimental chamber was utilized to determine the efficacy of UV and blue light-based technologies on aerosolized virus; this apparatus has been used in earlier inactivation studies of various airborne microorganisms[30–32]. The body of the chamber is constructed with stainless steel and consists of three parts: 1) the head (165x165x343 mm), 2) the main body (63x305x381 mm), and 3) the tail (42x305x25 mm). The head part of the chamber consisted of ports for the injection of viral bioaerosol and supplemental HEPA-filtered air (see below for details). In the main body section of the chamber, there is a fused quartz UV exposure window (279x254 mm). The device to be evaluated was installed directly above this window at a height of 8 inches from the upper surface of the quartz window. Sampling of the UV-exposed bioaerosol and untreated control bioaerosol was performed through a sampling assembly connected at the end of the tail part. A schematic of the experimental setup is shown in Figure 2. The entire experimental setup including the chamber and sampling apparatus was placed inside a biosafety cabinet. UV intensity measurement was performed by placing the UV sensor at a single 29 mm diameter circular section on the bottom of the exposure window directly underneath the UV device prior to sampling. Three measurements were recorded and averaged. The total UV exposure dose (mJ/cm^2) for bioaerosol inactivation was calculated as UV intensity (mW/cm^2) multiplied by time of treatment (seconds).

5.3.7 Generation of HCoV-229E Bioaerosols:

Briefly, a single-jet Collison nebulizer (CH Technologies, NJ) containing 1×10^7 pfu/mL HCoV-229E in PBSA (Phosphate Buffered Saline + 0.1% Bovine Serum Albumin) was operated at 40 psig (pound-force per square inch) input pressure. The output of the nebulizer, producing viral bioaerosols at 3.3 lpm (liters per minute) was connected to an

input port at the bottom of the head section of the chamber. Supplemental HEPA-filtered air (25 lpm) was injected through the second input port to ensure mixing of the bioaerosol with air in the chamber. The total input airflow into the chamber was 28.3 lpm which is equivalent to 1cfm (1cubic feet per minute). The UV exposure time, which was the residence time of the bioaerosol in the exposure window, was calculated to be 7.6 seconds.

5.3.7.1 Bioaerosol Sampling:

An SKC Bio sampler (SKC Inc., Eighty-Four, PA) was utilized for sampling of the UV exposed bioaerosol and the untreated bioaerosol (baseline). The bio sampler had an operational flowrate of 12.5 lpm. To balance the 28.3 lpm flow rate of the chamber, a bypass pump operating at 15.8 lpm was connected to the sampling assembly. 20 mL of viral sampling fluid was added to the bio sampler. Sampling was performed for 20 min for each sample (baseline and UV- treated). Triplicate samples were first collected for the control baseline, followed by the UV- treated samples in triplicate.

5.3.7.2 Environmental Parameters:

The temperature and relative humidity were measured during experiments with a HOBO data logger (Grainger, Lake Forest IL). Ozone levels were measured with an Aeroqual series 200 ozone monitor (Gas Sensing, Inwood IA).

5.3.8 Statistical Analysis:

The inactivation experiments were performed in triplicates and the log reduction values at each timepoint were calculated, as detailed in earlier publications from this group[7,9,33]. In summary, accounting for the natural decay of the microorganisms at time t, the log

reduction was calculated according to the following equation where, CExp (0) is the microorganism concentration of the treatment coupon at time '0' while CExp (t) is the concentration of the exposed microorganisms at time 't'. The log reduction (LR) is defined as:

$Cexp\ (0)\ LR = Log10\ (Cexp(t))$ (Equation 1)

The aerosol inactivation results were used to determine the Z-value of the UV exposure. By definition, the Z-value is equivalent to the slope for the relationship between UV dose and logarithm of % survival[32]. The higher the Z-value, the more susceptible the organism. This is calculated as:

$Z = \ln (No)/D$ (Equation 2)

Where, No= baseline viral concentration averaged across the triplicate sampling runs, Nuv =UV-exposed viral concentration averaged across the triplicate sampling runs and D = effective UV dose (mJ/cm^2), i.e., Intensity measured (mW/cm^2) X time of exposure (seconds). For the aerosol inactivation results, a logarithmic fit of the survival fraction (N_{UV}/N_0) of the virus was plotted against the UV exposure dose.

5.4 Results and Discussion:

Figure 3 shows the summary of results of the tier one inactivation testing, performed on stainless steel surfaces inoculated with the virus. For device A (254 nm), the UV intensity measured at the treatment surface was 8.07 mW/cm^2. The corresponding doses for the different treatment timepoints were calculated to be 8.07, 24.2 and 80.67 mJ/cm^2 (for 1, 3 and 10 seconds respectively). The temperature measured near the surface of treatment was approximately 71° F. Relative humidity was 43.4%. There was no significant difference

between these values and environmental measurements, taken away from the UV device. Ozone levels were below the limit of detection of 0.01 ppm. The control (baseline) samples did not show significant reduction in the viral concentration for the entire time course of the treatment. For control samples held for 1, 3 and 10 seconds, the concentration of the virus recovered was 8.83×10^4 ($\pm$ 4.71×10^3) pfu/mL, 8.83×10^4 ($\pm$ 1.43×10^4) pfu/mL, and 6×10^4 ($\pm 1.08 \times 10^4$) pfu/mL, respectively. The insignificant reduction in the control concentration of the virus can be attributed to the fact that HCoV-229E has been shown to be extremely resilient in its survivability on various surface materials[34] (Bonny et al., 2018). In the case of the UV treatment, complete inactivation was observed for all three time points, as shown in Figure 3(A). No viable virus was recovered from the treatment coupons. This would translate to 4.94, 4.94 and 4.77 log reduction at UV doses of 8.07, 24.2 and 80.67 mJ/cm^2 (for 1, 3 and 10 seconds of UV exposure respectively). Thus, it can be inferred that only momentary contact with the UV produced by this device (254 nm) can be effective in inactivating HCoV-229E on stainless steel surfaces. These HCoV-229E inactivation results are in line with published data on UV 254 nm with other microorganisms. As it is well known, the 254 nm light damages the viral deoxyribonucleic acid (DNA) or ribonucleic acid (RNA) so that the virus cannot replicate[15,24,35]. The susceptibility of HCoV-229E to UV radiation, especially 254nm, has been well studied and one study reported a dose of 1.8 mJ/cm^2 leading to one log reduction[36]. As the doses delivered in the present study are magnitude higher, the higher inactivation observed is coherent. For SARS-CoV-2 itself, there are few studies assessing its susceptibility with 254nm handheld devices. A recent study reported a 6-log inactivation of SARS-CoV-2 in liquid suspension exposed with a mercury UVC lamp (254 nm) at 5 cm (2 inches) distance with a 1048 mJ/cm^2 dose[17].

Another study of note utilized handheld 254-nm UV devices evaluated against SARS-CoV-2 at a 5 cm (2 inches) distance. Results in that study indicate a complete inactivation (6 log reduction) after a UV dose of 800 mJ/cm^2 [37]. The highly efficient results presented in the current study further indicate that device A will be an effective handheld surface sterilization device against SARS-CoV-2. For the handheld device B (275 nm), the UV intensity measured at the treatment surface was 20.61 mW/cm^2. The corresponding dose for each treatment timepoint was calculated to be 20.61, 61.83 and 206.1 mJ/cm^2 (for 1, 3 and 10 seconds respectively). The temperature measured near the surface of treatment was 70.1° F and the relative humidity was 43.2%. Here, it is to be noted that, although there was no significant increase in the temperature in the surrounding area, the device itself became extremely hot to the touch. Ozone levels were below the limit of detection of 0.01 ppm.

Figure 3(B) summarizes the inactivation as a function of exposure time for device B. Here, similar values were observed for control, as the earlier handheld device with 8.83×10^4 ($\pm$ 4.71×10^3) pfu/mL for 1 second, 8.83×10^4 ($\pm$ 1.43×10^4) pfu/mL at 3 seconds, and 6×10^4 ($\pm 1.08 \times 10^4$) pfu/mL at 10 seconds. For the UV exposed surface, a complete inactivation was observed for all three time points. No viable virus was recovered from the treatment coupons. This would translate to 4.94, 4.94 and 4.77 log reduction at for doses of 20.61, 61.83 and 206.1 mJ/cm^2 (for 1, 3 and 10 seconds respectively). The inactivation results are identical to the 254 nm device A. However, the dose values reported here for the 275 nm device B are three (3) times greater due to its higher intensity than the 254 nm device.

LED UV-C disinfection is an emerging field in the application of UV for disinfection purposes, and there are few studies of the inactivation of coronaviruses at LED

wavelengths. There has, however, been renewed interest due to the current pandemic. A recent study discovered that across the UV-C LED wavelength spectrum, 267 nm, which is similar to the 275 nm operation of this device, was the most effective wavelength in inactivating another surrogate of SARS-CoV-2, the HCoV-OC43[37]. In another study, a UV LED instrument was used to treat a clinical isolate of SARS-CoV-2 at 2 cm, which is like the distance utilized in the current study. Here a dose of 37.5 mJ/cm^2 led to a 99.9% (3 log) inactivation[38]. Thus, from the results obtained against HCoV-229E in this study, it can be inferred that the 275-nm device B is also likely well-suited to inactivate coronaviruses in relatively short contact times, validating its handheld operation.

Device C is intended for a ceiling-based operation. As this device is a 222 nm UV-C device, it is considered to be safer for human exposure, as compared to 254 nm[39,40]. Here, the UV intensity was significantly lower than the other two UV based devices evaluated in this study. The UV intensity measured at the treatment surface was 0.02 mW/cm^2. During the treatment, the temperature gradually increased near the treatment zone compared to surrounding one, with the initial temperature being 75.2° F and the final temperature measured at the end of the 5-minute treatment elevated to 80.2° F. Relative humidity remained constant and same as initial pretreatment levels, at 45.4%. Ozone levels were below the limit of detection of 0.01 ppm.

Figure 3(C) summarizes the surface inactivation results as a function of exposure time. Here, a gradual time course of inactivation was observed for the timepoints evaluated. The three timepoints utilized for treatment were 30 seconds, 1 minute and 5 minutes. The calculated UV dose for the three treatment timepoints was 0.6, 1.2 and 6 mJ/cm^2, respectively. For the untreated controls, the concentrations of virus recovered were 8x10^4

(± 4.08x10^3) pfu/mL, 4.33x104 (±4.71x10^3) pfu/mL and 5x104 (± 4.08x10^3) pfu/mL, respectively. For the UV treatment, 6.66x10^4 (± 1.01x10^4) pfu/mL were recovered after 30 seconds and 1.5x10^4 (± 1.08x10^3) pfu/mL after 1 minute. The highest level of inactivation was observed after 5 minutes of treatment with 8.5x10^2 (± 1.08x10^2) pfu/mL recovered. This constitutes a 1.77 log reduction (6 mJ/cm^2 UV dose). Linear Curve fitting analysis for the inactivation time course led to a log reduction rate of 0.34 logs/minute (R^2 = 0.738). Far-UVC light (207–222 nm) is very strongly absorbed by proteins through peptide bonds, as well as by other biomolecules, leading to intracellular damage. However, the ability of far-UVC to penetrate biological materials is limited compared with conventional germicidal UV light (254 nm or greater), which can reach and damage internal nucleic acids[41,42]. Fewer studies of the efficacy of 222nm UV against coronaviruses exist, as opposed to the more prevalent 254 nm. But recent studies have indeed pointed towards the applicability of 222 nm UV for inactivating coronaviruses. One study reported an inactivation of 99.95% (3.3 log reduction) after a 19.42 mJ/cm^2 dose[43]. Another study utilized a 222nm source placed 24 cm above a coupon inoculated with SARS-CoV-2, with a 2.35 log reduction at a dose of 3 mJ/cm^2 [44]. The results from the current study are congruous with these data.

For blue light-based device D, the light intensity measured at the treatment surface was 21.67 mW/cm^2. When the device was operated for the longest timepoint of treatment, i.e., 1 hour, the temperature of the treatment zone increased from 75.1°F to 82.3°F. The relative humidity also decreased from 40% to 28.2%. Ozone levels were below the limit of detection of 0.01 ppm. Figure 3(D) summarizes the inactivation produced by a light-based device D as a function of exposure time. Here, no significant inactivation for the shorter

timepoints tested was observed, namely 1 and 5 minutes. At 1- and 5-minute treatment, the controls at these timepoints were $4.33x10^4$ ($\pm$ $4.71x10^3$) pfu/mL for 1-minute and $5x10^4$ ($\pm$ $4.08x10^3$) pfu/mL for the 5 minutes. For the UV exposed samples, $5x10^4$ ($\pm$ $4.08x10^3$) pfu/mL were recovered for 1 minute of treatment and $6x10^4$ ($\pm$ $1.78x10^3$) pfu/mL for the 5-minute treatment. Hence, the treatment time was increased significantly, to 60 minutes. For this 60-minute treatment, the control samples contained $8.33x10^4$ ($\pm$ $6.23x10^3$) pfu/mL. The light treated samples contained $9.166x10^3$ ($\pm$ $6.23x10^2$) pfu/mL. This indicates an 89% (0.958 logs) reduction. The calculated light dose for the 1-, 5- and 60-minute timepoints was 1.3, 6.5 and 78 J/cm^2. This product was advertised to disinfect over an extended period of exposure which resulted in the extended testing durations chosen here.

There are only a few studies in the literature regarding the use of blue light technology against viruses, especially coronaviruses. A recent study analyzed various wavelengths for their efficacy against HCoV-229E and it was observed that for 405 nm pulsed blue light, there was 44% reduction after a 130 J/cm^2 dose[45]. Blue light was also recently evaluated in the context of SARS-CoV-2, with the results indicating that at the lowest tested irradiation dose of 0.035 mW/cm^2, a reduction of 55.08% was seen after 4 hours of treatment, and the reduction after 24 hours was 90.17%[46]. Comparatively, device D has shown higher inactivation potential in this study. However, it should be noted that the increase in the temperature and substantial reduction in the relative humidity may have also contributed to the inactivation observed here. Given the notable enhancement in viral reduction observed here as a function of time compared to previous work, future investigation of the influence of temperature and humidity on this type of treatment would be valuable. Further, since a 1-h long exposure was required to produce 1 log reduction, it

was surmised that studying inactivation of airborne HCoV-229E for this device with the current single-pass aerosol chamber setup, which has an exposure residence time of 7.6 seconds, would be infeasible as the delivered dose would be too small to lead to meaningful inactivation. For device D, a larger, room-sized chamber with longer residence and contact time would be more appropriate for evaluating the potential antiviral effect.

As the second tier of evaluation, we investigated the efficacy of device C in inactivating airborne HCoV-229E. As detailed in the methods section, the aerosolized virus was exposed to UV light at 222 nm from device C and inactivation was determined. Figure 4 denotes survival fraction of the HCoV-229E plotted against the UV dose. Here, the concentration of the virus sampled in the bio sampling fluid during control runs (no UV exposure) was 9×10^3 ($\pm$ 2.58×10^3) pfu/mL. After 222 nm UV exposure, the concentration of the surviving virus was 8.17x 102 ($\pm$ 1.34 x 102) pfu/mL, representing a 90.9% reduction (~1 log) in the concentration of aerosolized HCoV-229E. The intensity of UV that the airborne virus was exposed to was measured to be 7.32 $\mu W/cm^2$. The effective UV dose delivered to the airborne viruses was calculated by multiplying this intensity with the residence time of the bioaerosol in the exposure zone of the chamber, which was 7.6 seconds. This came out to 55.63 $\mu J/cm^2$. During the experiment, the relative humidity and temperature inside the chamber were monitored. During control runs, this was 50% RH and 70°F and during the UV exposure runs, 54.33% RH and 70°F. Ozone levels were below the limit of detection of 0.01 ppm. The z value, as described in the methods section, was calculated, and found to be $0.043 cm^2/\mu J$ ($4.31\ cm^2/\mu J$).

Only a few studies exist regarding the use of the 222 nm UV technology against airborne coronaviruses. In a recent study, a 222 nm UV device was utilized for inactivating

airborne HCoV-229E and HCoV-OC43 with a chamber like the one utilized in present study. They report a k-value, which is calculated with the same formula as the z-value, of 0.41 mJ/cm^2. This is significantly lower than the 4.31 mJ/cm^2 value reported in this study[22]. It is worth noting though that the exposure time utilized by them was significantly higher (approximately 20 seconds Vs 7.6 seconds) which makes it difficult to compare z values across studies given that the devices were different as well.

Furthermore, in another study by our group utilizing the same experimental setup and protocol using vaccinia virus, a surrogate of influenza virus, the reported Z-value was 2.54 mJ/cm^2 for a 254 nm UV device, which is lower than the Z-value for the case of the coronavirus inactivation from device C. The higher Z-value reported here is indicative of the higher potential to inactivate coronavirus compared to influenza virus[32]. It is worth noting that device C is to be installed in the ceiling of a room. Therefore, it was important to evaluate the inactivation of airborne coronavirus that this device will produce under real-world settings and dose. The region where there is the greatest chance of viral transmission in a room is where the human occupants of the room are breathing, coughing, sneezing etc., commonly referred to as the breathing zone. This zone is 6 feet from the floor per ASHRAE standard[46]. For a 10 ft ceiling height and a breathing zone of 6 ft above floor, we measured the UVC 222 nm intensity from Device C at the breathing zone and found it to be 0.771 μW/cm^2 (below the occupational safety regulatory exposure limit of ~0.8 μW/cm^2)[22]. At this intensity and assuming the logarithmic fit of survival fraction as a function of exposure dose (Figure 17; Z-value = 0.0431cm^2/μJ), we calculated that it would take Device C approximately 1.2 min to inactivate 90% of airborne coronavirus in the breathing zone, ~1.5 min for 95%, ~2.3 min for 99%, and ~3.5 min for 99.9% reduction,

assuming no mixing of room air and absence of other sinks for the virus such as ventilation and air filtration units.

In conclusion, the results presented here affirm the efficacy of the 254nm and 275nm handheld devices in terms of their intended ability to inactivate viruses on surfaces, as well as demonstrating the efficacy of a ceiling based 22nm UVC device for the inactivation of airborne viruses. These results indicate the promise of UV based technologies for the inactivation of viruses and should be considered as additional intervention tools for reducing the risk of infectious disease transmission especially in public and food industry settings. Future studies to assess the efficacy of the UV based technologies in countering foodborne virus contamination are currently being planned. Such studies are important not only for this, but future pandemic crises caused by viral disease transmission.

5.5 Figures and Tables:

Table 6. Details of devices tested in this study.

Device	Type of Device	Peak Wavelength	Power rating	Intended use
A	Handheld, low-pressure mercury lamp	254 nm	55W	Surface Disinfection
B	Handheld, LED array	275 nm	30W	Surface Disinfection

C	Ceiling based, Krypton lamp	222 nm	15W	Air Disinfection
D	Ceiling based, can LED light	405 nm	38W	Air Disinfection

Fig 14. Schematic of the surface inactivation efficacy testing of chosen UV/light-based intervention technologies against an inoculated SARS-CoV-2 surrogate.

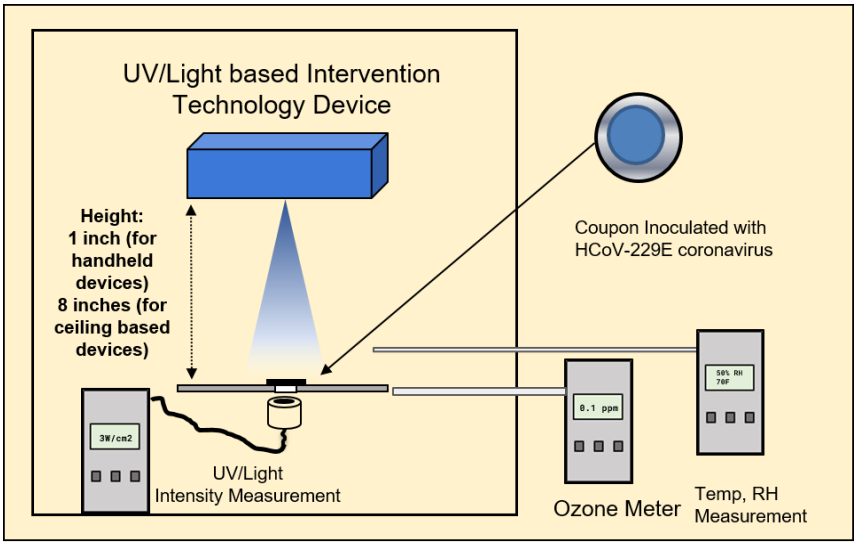

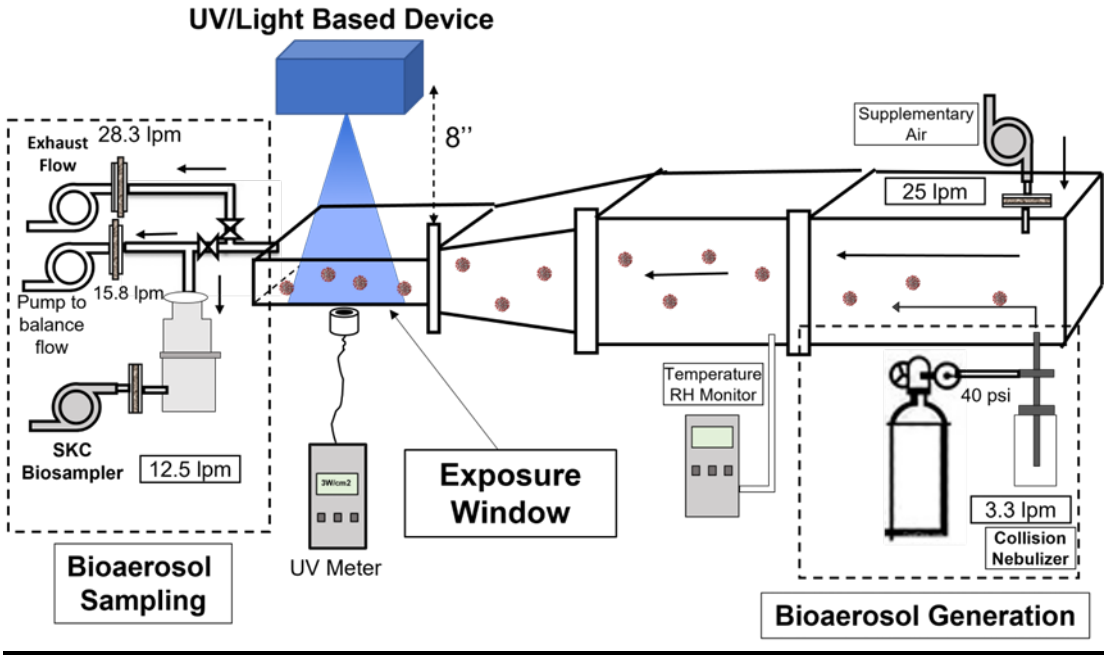

Figure 15: Schematic of the air disinfection efficacy testing of UV based device C. The 'single-pass' experimental chamber is shown, along with experimental airflows.

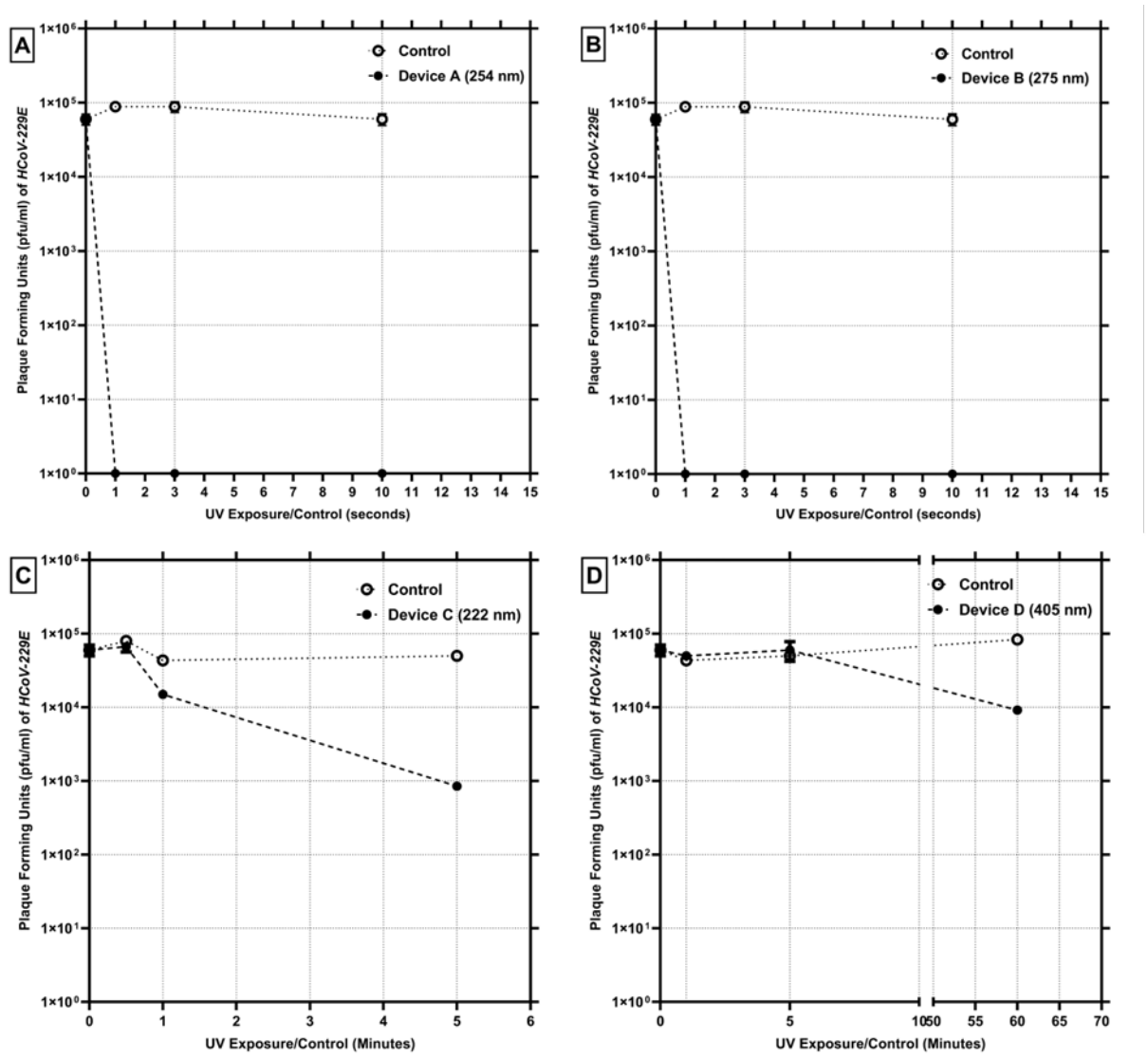

Figure 16: Summary of the surface inactivation efficacy testing of UV/light-based devices. The control (○) and treatment (●) concentration values (PFU/mL) of HCoV-229E are shown as a function of exposure time. The values are averages of triplicate runs and error bars are one standard deviation.

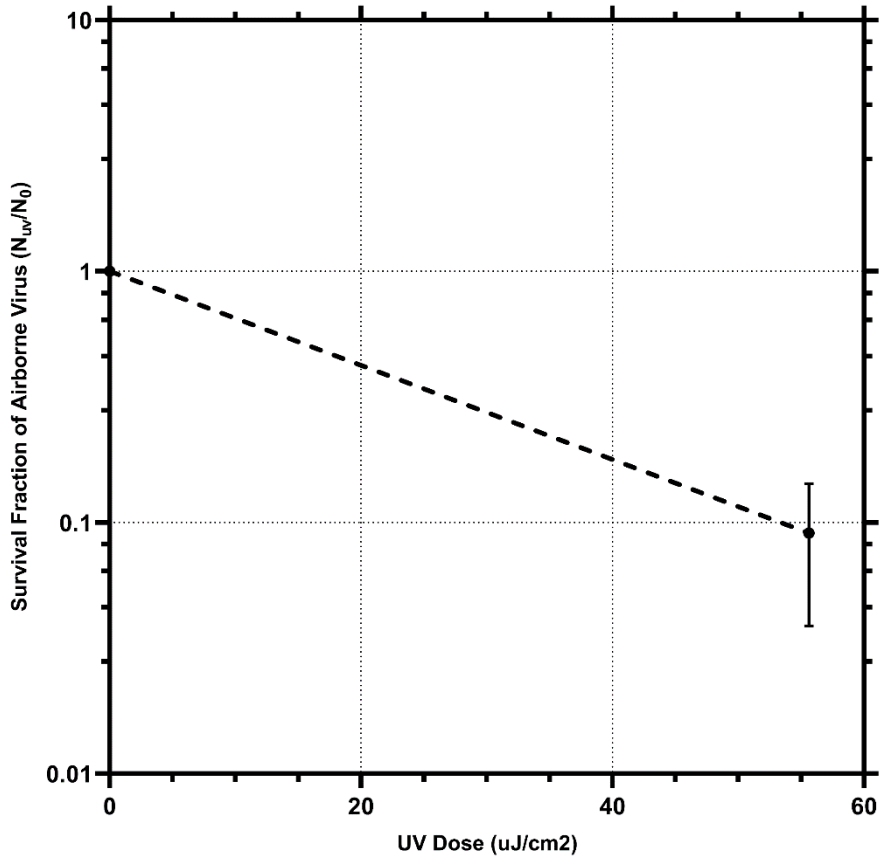

Figure 17: Inactivation of aerosolized HCoV-229E by device C as a function of UV exposure dose (uJ/cm^2). The values are averages of triplicate runs and error bars represent one standard deviation. A logarithmic fit was performed assuming a survival fraction of 1 at the UV exposure dose of 0 uJ/cm^2.

5.6 References:

1. CDC. COVID Data Tracker. *Centers for Disease Control and Prevention* https://covid.cdc.gov/covid-data-tracker (2020).
2. Moschovis, P. P. *et al.* Aerosol transmission of SARS-CoV-2 by children and adults during the COVID-19 pandemic. *Pediatr. Pulmonol.* **56**, 1389–1394 (2021).

3. Yasmin, F., Ali, S. H. & Ullah, I. Norovirus outbreak amid COVID-19 in the United Kingdom; priorities for achieving control. *J. Med. Virol.* **94**, 1232–1235 (2022).
4. Lu, Y. *et al.* The Rise in Norovirus-Related Acute Gastroenteritis During the Fight Against the COVID-19 Pandemic in Southern China. *Front. Public Health* **9**, (2022).
5. National norovirus and rotavirus bulletin week 40: data to week 38 (25 September 2022). *GOV.UK* https://www.gov.uk/government/statistics/national-norovirus-and-rotavirus-surveillance-reports-2022-to-2023-season/national-norovirus-and-rotavirus-bulletin-week-40-data-to-week-38-25-september-2022.
6. Mahase, E. Covid-19: What new variants are emerging and how are they being investigated? *BMJ* **372**, n158 (2021).
7. Huang, R. *et al.* Inactivation of Hand Hygiene-Related Pathogens Using Engineered Water Nanostructures. *ACS Sustain. Chem. Eng.* **7**, 19761–19769 (2019).
8. Vaze, N. *et al.* An integrated electrolysis – electrospray – ionization antimicrobial platform using Engineered Water Nanostructures (EWNS) for food safety applications. *Food Control* **85**, 151–160 (2018).
9. Huang, R. *et al.* A novel antimicrobial technology to enhance food safety and quality of leafy vegetables using engineered water nanostructures. *Environ. Sci. Nano* **8**, 514–526 (2021).
10. Pyrgiotakis, G. *et al.* Optimization of a nanotechnology based antimicrobial platform for food safety applications using Engineered Water Nanostructures (EWNS). *Sci. Rep.* **6**, 21073 (2016).

11. Vaze, N., Soorneedi, A. R., Moore, M. D. & Demokritou, P. Inactivating SARS-CoV-2 Surrogates on Surfaces Using Engineered Water Nanostructures Incorporated with Nature Derived Antimicrobials. *Nanomaterials* **12**, 1735 (2022).
12. Stein, B., Rahmsdorf, H. J., Steffen, A., Litfin, M. & Herrlich, P. UV-induced DNA damage is an intermediate step in UV-induced expression of human immunodeficiency virus type 1, collagenase, c-fos, and metallothionein. *Mol. Cell. Biol.* **9**, 5169–5181 (1989).
13. Darnell, M. E. R., Subbarao, K., Feinstone, S. M. & Taylor, D. R. Inactivation of the coronavirus that induces severe acute respiratory syndrome, SARS-CoV. *J. Virol. Methods* **121**, 85–91 (2004).
14. Reshi, M. L., Su, Y.-C. & Hong, J.-R. RNA Viruses: ROS-Mediated Cell Death. *Int. J. Cell Biol.* **2014**, 467452 (2014).
15. Mackenzie, D. Ultraviolet Light Fights New Virus. *Eng. Beijing China* **6**, 851–853 (2020).
16. Simmons, S. E. *et al.* Deactivation of SARS-CoV-2 with pulsed-xenon ultraviolet light: Implications for environmental COVID-19 control. *Infect. Control Hosp. Epidemiol.* 1–4 doi:10.1017/ice.2020.399.
17. Heilingloh, C. S. *et al.* Susceptibility of SARS-CoV-2 to UV irradiation. *Am. J. Infect. Control* **48**, 1273–1275 (2020).
18. Storm, N. *et al.* Rapid and complete inactivation of SARS-CoV-2 by ultraviolet-C irradiation. *Sci. Rep.* **10**, 22421 (2020).
19. Biasin, M. *et al.* UV-C irradiation is highly effective in inactivating SARS-CoV-2 replication. *Sci. Rep.* **11**, 6260 (2021).

20. Minamikawa, T. *et al.* Quantitative evaluation of SARS-CoV-2 inactivation using a deep ultraviolet light-emitting diode. *Sci. Rep.* **11**, 5070 (2021).
21. Chiappa, F. *et al.* The efficacy of ultraviolet light-emitting technology against coronaviruses: a systematic review. *J. Hosp. Infect.* **114**, 63–78 (2021).
22. Buonanno, M., Welch, D., Shuryak, I. & Brenner, D. J. Far-UVC light (222 nm) efficiently and safely inactivates airborne human coronaviruses. *Sci. Rep.* **10**, 10285 (2020).
23. Guffey, J. S. & Wilborn, J. In vitro bactericidal effects of 405-nm and 470-nm blue light. *Photomed. Laser Surg.* **24**, 684–688 (2006).
24. McKenzie, K. *et al.* The effects of 405 nm light on bacterial membrane integrity determined by salt and bile tolerance assays, leakage of UV-absorbing material and SYTOX green labelling. *Microbiol. Read. Engl.* **162**, 1680–1688 (2016).
25. Malik, Y. A. Properties of Coronavirus and SARS-CoV-2. *Malays. J. Pathol.* **42**, 3–11 (2020).
26. Meyers, C. *et al.* Lowering the transmission and spread of human coronavirus. *J. Med. Virol.* **93**, 1605–1612 (2021).
27. Carraturo, F. *et al.* Persistence of SARS-CoV-2 in the environment and COVID-19 transmission risk from environmental matrices and surfaces. *Environ. Pollut.* **265**, 115010 (2020).
28. Cimolai, N. Environmental and decontamination issues for human coronaviruses and their potential surrogates. *J. Med. Virol.* **92**, 2498–2510 (2020).
29. Huh-7: A human “hemochromatotic” cell line - Vecchi - 2010 - Hepatology - Wiley Online Library. https://aasldpubs.onlinelibrary.wiley.com/doi/10.1002/hep.23410.

30. Ko, G., First, M. W. & Burge, H. A. Influence of relative humidity on particle size and UV sensitivity of Serratia marcescens and Mycobacterium bovis BCG aerosols. *Tuber. Lung Dis. Off. J. Int. Union Tuberc. Lung Dis.* **80**, 217–228 (2000).
31. McDevitt, J. J., Rudnick, S. N. & Radonovich, L. J. Aerosol Susceptibility of Influenza Virus to UV-C Light. *Appl. Environ. Microbiol.* **78**, 1666–1669 (2012).
32. McDevitt, J. J. *et al.* Characterization of UVC Light Sensitivity of Vaccinia Virus. *Appl. Environ. Microbiol.* **73**, 5760–5766 (2007).
33. Vaze, N. *et al.* A nano-carrier platform for the targeted delivery of nature-inspired antimicrobials using Engineered Water Nanostructures for food safety applications. *Food Control* **96**, 365–374 (2019).
34. Bonny, T. S., Yezli, S. & Lednicky, J. A. Isolation and identification of human coronavirus 229E from frequently touched environmental surfaces of a university classroom that is cleaned daily. *Am. J. Infect. Control* **46**, 105–107 (2018).
35. Beck, S. E. *et al.* Comparison of UV-Induced Inactivation and RNA Damage in MS2 Phage across the Germicidal UV Spectrum. *Appl. Environ. Microbiol.* **82**, 1468–1474 (2016).
36. Boegel, S. J. *et al.* Robust Evaluation of Ultraviolet-C Sensitivity for SARS-CoV-2 and Surrogate Coronaviruses. *Microbiol. Spectr.* **9**, e0053721 (2021).
37. Gerchman, Y., Mamane, H., Friedman, N. & Mandelboim, M. UV-LED disinfection of Coronavirus: Wavelength effect. *J. Photochem. Photobiol. B* **212**, 112044 (2020).
38. Inagaki, H., Saito, A., Sugiyama, H., Okabayashi, T. & Fujimoto, S. Rapid inactivation of SARS-CoV-2 with deep-UV LED irradiation. *Emerg. Microbes Infect.* **9**, 1744–1747 (2020).

39. Buonanno, M. *et al.* Germicidal Efficacy and Mammalian Skin Safety of 222-nm UV Light. *Radiat. Res.* **187**, 483–491 (2017).

40. Freeman, S. *et al.* Systematic evaluating and modeling of SARS-CoV-2 UVC disinfection. *Sci. Rep.* **12**, 5869 (2022).

41. Goldfarb, A. R., Saidel, L. J. & Mosovich, E. The ultraviolet absorption spectra of proteins. *J. Biol. Chem.* **193**, 397–404 (1951).

42. Coohill, T. P. Virus-cell interactions as probes for vacuum-ultraviolet radiation damage and repair. *Photochem. Photobiol.* **44**, 359–363 (1986).

43. Jones, J. P. & Norton, K. 222-nm ultraviolet light inactivates dried inocula of human rhinovirus and human coronavirus on a glass carrier. *J. Hosp. Infect.* **117**, 190–191 (2021).

44. Kitagawa, H. *et al.* Effectiveness of 222-nm ultraviolet light on disinfecting SARS-CoV-2 surface contamination. *Am. J. Infect. Control* **49**, 299–301 (2021).

45. Enwemeka, C. S., Bumah, V. V. & Mokili, J. L. Pulsed blue light inactivates two strains of human coronavirus. *J. Photochem. Photobiol. B* **222**, 112282 (2021).

Conclusion:

Environmentally transmissible viruses have a significant impact on human and animal health along with economic impacts. The recent CoVID-19 pandemic underscored the importance of environmentally transmissible viruses and the significance of ways to combat such outbreaks. Conventional methods for detection and control of the environmentally transmissible viruses suffer from limitations that need to be improved for better detection and control. Since these viruses are usually found in small numbers in a matrix of large organic material, it becomes imperative to concentrate the virus particles before detection. Control of such viruses also requires novel disinfection strategies where conventional methods would fail. Human noroviruses are one of the major environmentally transmissible viruses that are responsible for most of the non-bacterial foodborne illnesses across the world. Since noroviruses are usually found in food and environmental samples, concentrating the virus prior to detection is crucial for their detection. While conventional concentration methods that rely on charge/physical properties as in the case of non-specific methods and specific magnetic bead-based methods that rely on viral surface proteins can concentrate virus particles from samples, their efficiency is quite low. Moreover, the tradeoffs with the non-specific and specific concentration methods such as co-concentration of inhibitory substances and higher cost restrict large scale deployment of these concentration methods. The bacterial concentration method we propose involves the use of engineered bacterial clones that express specific peptides targeting human norovirus. The advantage of using such a system is that it can be used for scaling up the concentration methods. Moreover, this method of concentration is very easy to handle and does not require special equipment or

expertise, making it an ideal choice for resource limited settings. Conventional concentration methods using native bacterial strains can display dramatically different capture efficiency based on culture conditions and any major manipulation of the culture media can have a detrimental effect on capture efficiency. While we still must test the capture efficiency of the engineered *E. coli* under different culture conditions, we are hopeful that manipulating the culture conditions would not have as much of an effect on the capture efficiencies of these clones because display of norovirus capture peptides is inducibly expressed. While focusing on the concentration methods, we also wanted to test the efficacy of *C. elegans* as a model for norovirus replication. Previous studies in our lab have shown that human norovirus is internalized by *C. elegans* worms, and this has been confirmed with both RT-qPCR and microscopy. We then tested whether the *C. elegans* worms can promote replication of murine norovirus (MNV) which is often used as a surrogate for human norovirus. Mutant worms that express a known MNV receptor CD300If have been tested to see if they support MNV replication. Surprisingly enough, the wild type worms we tested have shown similar replication efficiencies as their mutant counterparts, with about 1-2 log increase in genomic copies after 72 hours; a similar increase as has been observed with other norovirus models. While we are unsure of the mechanisms of the wild type worms' propensity to support MNV replication, we hypothesize that the *E. coli* worms that are used as a feed to support MNV growth in vitro could promote the binding of the virus to the intestinal tract of *C. elegans* worms.

As mentioned above, control of environmentally transmissible viruses is very important for reducing outbreaks. Conventional methods for controlling environmentally transmissible viruses involve the indiscriminate use of disinfectants that can lead to

potential human health hazards and accumulation of said disinfectants in the environment. Moreover, some pathogens can develop resistance due to indiscriminate use of such disinfectants. Thus, there is an immediate need for novel disinfection methods that do not involve the use of large amounts of disinfectants to achieve desired disinfection rates. We tested the efficacy of one such novel disinfection method that utilizes engineered water nanoparticles for encapsulating active ingredients, that can be sprayed on surfaces of food and other surfaces. We demonstrated that this novel method of disinfection can be used to target surrogates of foodborne and airborne viruses such as human norovirus and SARS-CoV-2. While the surface disinfection efficacy of this novel method against norovirus and SARS-CoV-2 surrogates was appreciable, the air disinfection capability of this technique is currently being tested. It must be noted that using a targeted and precise delivery of active ingredients without leaving a residue is of significant value in a food industry setting. We demonstrated that the EWNS system was able to achieve ~3.5 log reduction in viral load with only 258 pg/cm^2 of active ingredient, which is well below the EPA recommended levels for foods and food contact surfaces.

We also tested the claims of commercially available light-based disinfection devices for their efficacy in disinfecting surfaces and airborne viruses. Out of the four devices tested, two handheld devices were able to efficiently disinfect surfaces inoculated with a SARS-CoV-2 surrogate while the other two were not very effective in reducing the viral load even after prolonged exposure. The fact that these devices are currently commercially available and are utilized by institutions has significance, as this work suggests that these devices likely have a negligible effect in mitigating the risk of viral transmission. While the testing was performed under strict experimental conditions, the results obtained in our

experiments cannot be completely extrapolated to real life scenario as there are several factors that could potentially interfere with the performance of such UV-C based lights. However, it should be noted that our experimental setup placed the ceiling mounted light closer to the virus, which would presumably enhance its efficacy. Regardless, the results of our work suggest that the degree to which utilization of light-based devices reduces the risk of viral transmission warrants further scrutiny. In summary, this work emphasizes the importance of sample concentration prior to detection especially when complex matrices like food and environmentally transmissible viruses are involved. It also underscores the importance of new models (*C. elegans*) for studying infectivity and replication of foodborne viruses like the human norovirus. The EWNS and UV based disinfection methods discussed here are novel methods that not only address virus transmission but also prioritize environmental sustainability.